An Investigation into the Development and Implementation of Multidimensional Gas Chromatography

A thesis submitted in fulfilment of the requirements
for the degree of Doctorate of Philosophy

Michael S. Dunn

Bachelor of Applied Science

October 2011

School of Applied Science
RMIT University

DECLARATION

I certify that except where due acknowledgement has been made, the work is that of the author alone; the work has not been submitted previously, in whole or in part, to qualify for any other academic award; the content of the thesis is the result of work which has been carried out since the official commencement date of the approved research program; any editorial work, paid or unpaid, carried out by a third party is acknowledged; and, ethics procedures and guidelines have been followed.

_____

Michael S. Dunn

ACKNOWLEDGEMENTS

I would like to take this opportunity to thank my primary supervisors Prof. Philip Marriott and Prof. Mike Adams for initiating and continuing this project respectively.

I would also like to express my sincere gratitude to my secondary supervisor Dr. Robert Shellie. Though we have not had much contact over the duration of my candidature you have certainly made the biggest impact.

A big thanks goes to my pseudo supervisor and now close friend Paul Morrison. If you were not there to stop my day dreaming and hassle me out of the laboratory then I would probably still be there and never finish. It has been a pleasure to work with you both in the laboratory and on the bike in the hills.

To all of the friends I have made at RMIT and Ensign Laboratories both past and present. Your friendship and encouragement helped me endure some tough times during my candidature.

A special mention should be given to Dr. David Beale who since a road trip to Sydney for a drunken conference in 2003, has become and continues to be a close friend.

To my family though you have no idea what I have been doing the past five years your constant love and support has always been there to help me through.

Last but not least, a very special thank you goes to my beautiful wife Charlotte. Though we have had our ups and downs over the past 7 years we have always managed to persevere and come out on top. Your love, support, kindness and patience have provided me with the strength I needed to get through this. This body of work is as much yours as it is mine.

TABLE OF CONTENTS

TABLE OF FIGURES

TABLE OF TABLES

PRESENTED WORKS

Publications

M. Dunn, N. Vulic, R. Shellie, P. Morrison, S. Whitehead, P.J. Marriott, Semi-fast targeted multidimensional gas chromatography for the quantitative analysis of allergens in fragrance products, J. Chromatogr. A 1130 (2006) 122-129

M. Dunn, R. Shellie, P. Morrison, P. Marriott, Statistical model of overlap theory in two-dimensional chromatography, *manuscript in preparation*

M. Dunn, R. Shellie, P. Morrison, P. Marriott, A theoretical approach to retention time locked multidimensional gas chromatography (RTL-MDGC), *manuscript in preparation*

M. Dunn, R. Shellie, P. Morrison, P. Marriott, Studies towards retention time locked targeted multidimensional gas chromatography (RTL-tMDGC), *manuscript in preparation*

M. Dunn, R. Shellie, P. Morrison, P. Marriott, Studies towards retention time locked comprehensive two dimensional gas chromatography (RTL-GC×GC). Application to GC×GC, *manuscript in preparation*

Posters

M. Dunn, R. Shellie, P. Morrison, P. Marriott, (2008) Retention time locking for comprehensive two dimensional chromatography, Presented at the ACROSS Symposium on Advances in Separation Science, Tasmania, Australia

Presentations

M. Dunn, R. Shellie, P. Morrison, P. Marriott, S. Whitehead, (2006) Semi fast targeted multidimensional gas chromatography for the analysis of allergens, Presented at the 9th symposium on hyphenated techniques in chromatography, York, United Kingdom

M. Dunn, R. Shellie, P. Morrison, P. Marriott, S., (2006) Multidimensional gas chromatography using capillary etched pneumatic switching and cryogenic focusing for the quantitative analysis of suspected allergens in fragrance, Presented at the 16th RACI Research and Development Conference, University of Wollongong, Australia

CHAPTER 1

EXECUTIVE SUMMARY

For almost half a century the technique of Multidimensional Gas Chromatography (MDGC) has been utilised by chromatographers who have sought greater levels of separation than that offered by conventional single column technology. Its origin begins with the Targeted MDGC (tMDGC) approach which involves the direct transfer of selected portions of a primary separation to a secondary column for further analysis. In the mid 1990's with the invention of a device known as a modulator, tMDGC was joined by the Comprehensive Two Dimensional Gas Chromatography (GC×GC) technique which applies a secondary separation to the entire primary separation. In their infancy both tMDGC and GC×GC were weighed down by technical and practical shortcomings that essentially limited their use to specialised research laboratories. However, as time progressed so too did the technology which had managed to overcome a large number of its shortcomings and expand its user base significantly but still within the confines of research laboratories. This body of work aims to further develop MDGC towards a commercially viable product so that it may become a more attractive analytical technique for commercial laboratories.

Using a modified Statistical Model of Overlap for MDGC, theoretical models and experimental results were used to assess the benefits, flaws and boundaries of MDGC. The data was then used to directly compare between the two MDGC techniques of tMDGC and GC×GC. The results suggested that the choice of what MDGC technique to apply is critical to the analyses being undertaken. The argument that the more modern and popular GC×GC technique has succeeded tMDGC has no grounds. In fact, GC×GC and tMDGC appeared to be complimentary techniques with tMDGC proving to be more suited for assays requiring quantification and GC×GC more suitable assays requiring qualification.

During the comparisons between tMDGC and GC×GC, it was found that the auxiliary pressure supplied to a Deans switch located at the union of the ^{1}D and ^{2}D could alter the retention times of both the ^{1}D and ^{2}D dimensions simultaneously. An increase in the Deans switching pressure would slow the flow of carrier gas on the ^{1}D while increasing the flow of carrier gas on the ^{2}D and *vice versa*. This then led to the notion that for every combination of retention times on the ^{1}D and ^{2}D there will be a unique combination of the ^{1}D inlet pressure and the Deans switching pressure.

A pressure tuning procedure was developed that once performed can accurately calculate the required ^{1}D inlet and Deans switching pressures required to achieve a specified ^{1}D and ^{2}D retention times. In conventional single column gas chromatography, the adjustment of the pressure drop to accurately reproduce retention times between individual separations is known as Retention Time Locking (RTL). The benefit of RTL is that when a separation is locked to a previous analysis it is possible to identify unknown peaks by cross referencing the retention times. Extensive retention time libraries for a standard method can be used to identify unknown peaks from a locked separation. By successfully applying the pressure tuning procedure to a MDGC system, independent RTL of both columns is achieved.

Described here is a pressure tuning procedure that once performed can accurately calculate the required ^{1}D inlet and Deans switching pressures required to for a specified ^{1}D and ^{2}D retention times. In conventional single column gas chromatography, adjustment of the pressure drop across a column to ensure identical retention times between individual separations is known as Retention Time Locking (RTL). The benefit of RTL is that when a separation is locked to a previous analysis, it is possible to identify peaks by cross referencing the retention times. The then allows for the creation of retention libraries for a standard method that can always be locked too for future identifications. By applying the novel pressure tuning procedure to a MDGC separation, it is possible to independently RTL both columns in a MDGC system and apply the benefits of to RTL to MDGC. This thesis investigates the application of RTL to both the tMDGC and GC×GC techniques.

CHAPTER 2

GENERAL INTRODUCTION

2.1 A BRIEF HISTORY

The birth of chromatography occurred around the turn of the 20th century with the pioneering work of Michael Tswett, who successfully separated plant pigments by a continuous adsorption/desorption process between a flowing hydrocarbon solvent and an open tube filled with inulin powder (a carbohydrate) [1]. Tswett described the process he observed and coined the term chromatography from the Greek words *chromatos* and *graphia* meaning colour and writing. For these reasons Michael Tswett is considered by many to be the father of chromatography [2].

Soon after the initial work by Tswett, chromatography became a well-recognized technique used among natural product researchers for the separation of plant pigments [2]. With the seminal work of Martin and Synge in 1941, chromatography was revolutionised with the invention of counter current liquid-liquid partition chromatography [3]. The importance of this work was recognised throughout the scientific community and was awarded the 1952 Nobel Prize in chemistry. Martin and Synge also predicted the likelihood that a gas could also be used as the moving phase in partition chromatography [3]. Their comments however, fell on deaf ears and nobody thought to experimentally test their predictions, until 1951 when Martin himself and James, a former co-worker of Synge, successfully developed the novel technique of gas-liquid partition chromatography and gave birth to the modern technique of gas chromatography [4, 5].

In 1958 Golay, in an exceptional piece of inductive reasoning, demonstrated that a labyrinthine trail through the originally employed packed bed could be replaced by a much straighter path through a narrow open tubular capillary column yielding much greater efficiencies [6]. Initially, capillary columns were constructed of either steel or glass and remarkable separations were achieved but due to practical limitations encountered with the technology commercial columns were essentially unavailable and their use was limited to a small minority of applications.

In 1979 it was first realised that fused silica could be applied to make robust and less problematic capillary columns for gas chromatography [7]. Inert fused silica tubing material could readily produce columns with adequate strength, flexibility and high

temperature stability capabilities dramatically changing the way gas chromatography was practised. In 1997 fused silica capillary columns amounted to approximately 95% of all columns sold throughout the world [8].

In a very short time gas chromatography has become the leading technique for the separation and analysis of volatile inorganic/organic compounds and is the most widely used analytical technique in the world [5]. Gas chromatography is a mature technique that is well understood and characterised, however new innovations in development are still being introduced, further extending its analytical capabilities.

2.2 LIMITATIONS OF LINEAR GAS CHROMATOGRAPHY

2.2.1 Lack of Peak Capacity

Even with high efficiency narrow bore capillary columns, the modern analyst is still at the mercy of complex samples [9]. The overall resolving power of a linear column can be interpreted in terms of its peak capacity n_c. The peak capacity is defined as the number of single peaks that can be positioned side by side in the separation space at a given resolution between neighbouring peaks. A sample with m components could theoretically be resolved if m was to equal $n_{c,}$ however, to achieve this in practice the separated peaks must be evenly spaced at the highest allowed density. Unfortunately, for almost all complex samples the distribution of peaks within the separation space is not even. Rather, they are scattered disproportionately across the chromatogram causing multiple component overlap. Even in cases where the separation space is considerably larger than that required theoretically ($n_c >> m$), peak overlap still occurs. The overlap of peaks poses a serious problem for the analysis of complex samples, to the extent that it is impossible to eliminate peak overlap in such samples and therefore must be tolerated [10].

In a study undertaken by Berger, a 400 meter capillary column consisting of 1.3×10^6 effective plates and a peak capacity of 1000 was used in the analysis of a petroleum sample [11]. The efficiency achieved in this analysis is somewhat close to the upper limitations of linear capillary gas chromatography and yet there is still a considerable amount of peak overlap [9]. As explained below, for the analysis of samples similar in complexity to petroleum, linear capillary gas chromatography is inadequate as it does not possess the resolving power required for complete/near complete separation of the numerous components present.

2.2.2 Statistical Model of Overlap Theory (SMO)

Statistical Model of Overlap (SMO) theory is a mathematical tool developed by Giddings et al. to quantitatively describe the consequence of statistical events in a chromatographic process [12-14]. Even though its mathematical treatment is quite

complex, it serves as a convenient tool to explain the fundamental causes of peak overlap, and propose solutions. To avoid unnecessary complications only selected key equations from SMO theory will be discussed here to delineate the magnitude of the component overlap conundrum.

SMO theory assumes that the retention of all components within a sample is statistically controlled and the distribution of peaks within the separation space random. Provided that the value of n_c is in accordance with the critical resolution, the total number of distinguishable peaks *p* can be approximated by:

$$p = me^{-m/n_c} = me^{-\alpha}$$

Equation 2.1

Where α is known as the saturation and is defined as the ratio between the number of components in the sample and the peak capacity at critical resolution. As discussed above, if all peaks were uniformly spaced with α equal to 1, the total number of visible peaks *p* would be equal to *m*. In practice observed peaks are anything but uniform and instead are disproportionately scattered throughout the separation space according to their chemical characteristics causing many to coalesce.

SMO theory states that in practice no more than 37% of the peak capacity is utilised to generate peak resolution i.e. $p(max) = 0.37\ n_c$ demonstrating the limitations of linear chromatography [13]. Exacerbating this problem is the fact that many of the peaks observed represent the combination of two or more components indicating that the total number of peaks representing single components *s* must be smaller than *p* and is given by:

$$s = me^{-2m/n_c} = me^{-2\alpha}$$

Equation 2.2

Equation 2.2 is the most important of the equations shown as it describes the relationship of *s* in terms of n_c and *m*. It also informs us of the total number of components isolated and hence subject to analytical measurement. The ratio *s*/*m* is defined as the fraction of all components isolated as single components; this ratio can

be thought of as the probability P_1 that any given component in the sample may be an isolated component:

$$P_1 = {}^{s}/_{m} = e^{-2\alpha}$$

Equation 2.3

It is important to note that according to SMO theory, the value of *s* can never exceed 18% of the total peak capacity, i.e. for a column with a n_c of 100, a maximum of 18 components will be separated[13]. This implies that greater values of n_c are required for increasing values of *m* if P_1 is to remain constant after *s* = 18% of n_c. From **Equation 2.3**, α is the governing value in determining the probability of a peak consisting of one component. Being that α is the ratio of m/n_c and for a given sample *m* is a constant, the peak capacity is the only experimental variable that the analyst can use to alter the separation quality.

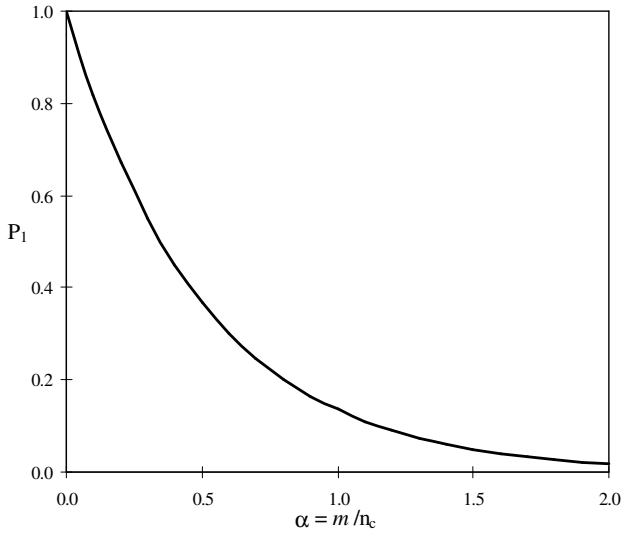

Figure 2.1 Probability of isolating a single component against varying degrees of saturation.

As displayed in **Figure 2.1**, if α was assigned a value of 1, there would be a 13.5% probability that a single component in the mixture could become resolved from its nearest neighbours by a value equal to or greater than the level of resolution specified. If the saturation is halved to 0.5, the probability of resolving the same component becomes 37% and if halved again to 0.25, the probability is still disappointingly low

at 61%. Likewise, for a 90% probability that a component could be separated, a peak capacity of 19.23 times the size of *m* would be required and 200 times greater than *m* for a 99% probability of isolating any component [9].

By way of example consider a sample of 50 components (*m*=50). By varying α, P_1 and the corresponding peak capacity required to produce the appropriate value of α can be calculated. **Figure 2.2** displays a plot of the peak capacity against the probability of isolating a single component, while **Table 2.1** presents the probability found for certain values of α and the respective values of n_c for a 50 component sample [9].

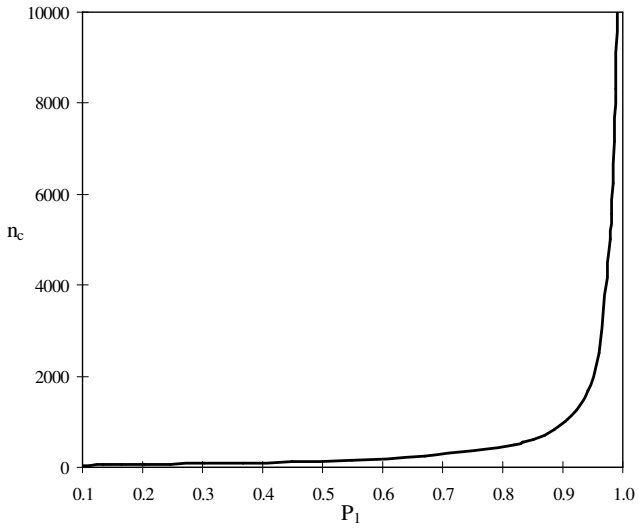

Figure 2.2 A plot of the peak capacity n_c against the probability of isolating a single component P_1 for a sample of 50 components.

Table 2.1 Probability of finding an isolated component for certain values of α, with the required n_c to achieve the corresponding value of α for a 50 component sample.

n_c	α	P_1
50	1.00	0.14
100	0.50	0.37
200	0.25	0.61
500	0.10	0.82
1000	0.05	0.90
10000	0.005	0.99

It is very discouraging to observe the large peak capacities required for high probabilities of peak resolution (purity) for a sample of only 50 components. The chromatographer's only option to improve the probability of separation is to lower α by increasing the peak capacity. Unfortunately the limited gains made in peak capacity by altering the length (increasing) or internal diameter (decreasing) of capillary columns, are insufficient to achieve adequate separation of a 50 component sample [9]. Although single capillary columns can have extremely high peak capacities, complex samples such as petroleum can contain 10^5 to 10^6 components and are effectively impossible to resolve [10]. **Figure 2.3** summarises the relation between n_c and resolution quality for various sample complexities. Clearly, an alternative approach is required for enhanced separation to be achieved for mildly complex samples.

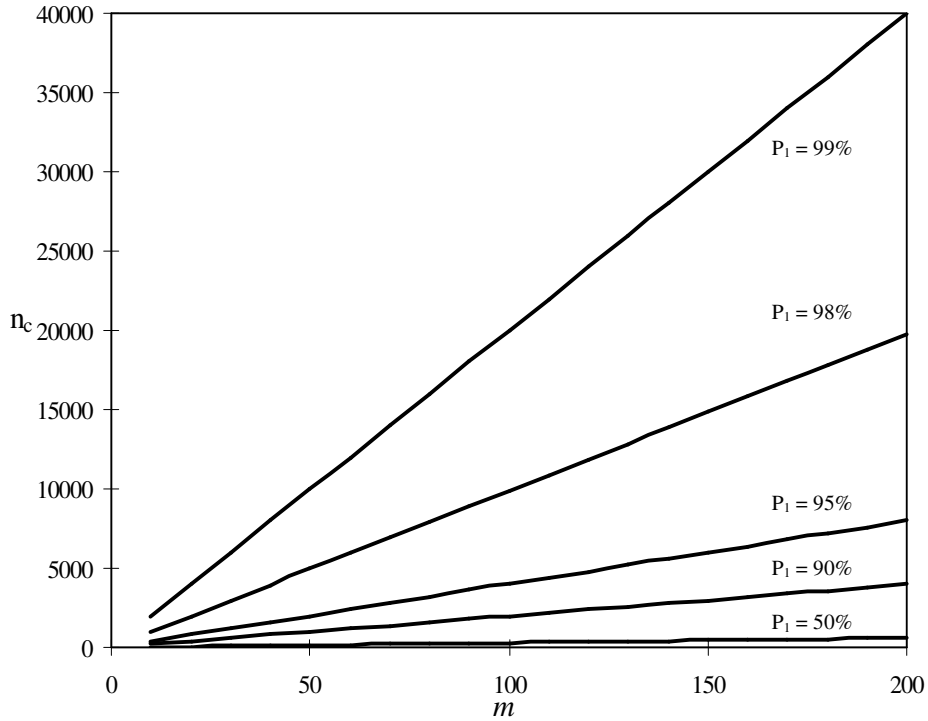

Figure 2.3 A plot of the peak capacity n_c required to obtain certain probabilities (P_1) against varying sample complexity (*m*).

2.3 MULTIDIMENSIONAL GAS CHROMATOGRAPHY

2.3.1 What is Multidimensional Gas Chromatography?

Multidimensional Gas Chromatography (MDGC) requires the transfer of selected fractions from a primary separation column to a mutually independent secondary separation column [15]. Commonly referred to as "heart cutting," MDGC is generally employed for the separation and isolation of target analytes of complex samples where linear GC has proven to be unsuccessful [16, 17]. The aim of a typical MDGC system is to either increase the peak capacity of a separation system or increase the speed of analysis [18]. The increase in speed of analysis is very important in industrial applications where the routine analysis of complex samples is common but it is the increase in peak capacity that is more imperative. To increase the peak capacity using linear GC the analyst can choose to lengthen and/or decrease the internal diameter of a column, however these gains in peak capacity are very limited due to practical/technical problems.

2.3.2 Benefits of Multidimensional Gas Chromatography

As depicted in **Figure 2.4**, by reanalysing selected fractions of the effluent from a primary separation the peak capacity for the targeted fractions is expanded. Each fraction collected will contain m_f amount of components and when subjected to a secondary separation step will generate a chromatogram independent from the primary separation. The components within the selected fractions are therefore subjected to a significantly increased peak capacity. The theoretical peak capacity of a MDGC system is simply the sum of the peak capacities for each of the individual columns or stages [9]. If several heart-cuts are transferred then the contribution from each repetition needs to be considered. The overall peak capacity $n_{c(tot)}$ for a heart-cut system is therefore given by.

$$n_{c\ (total)} = \sum \overline{n_c}$$

Equation 2.4

Where $\overline{n}_c$ is the average peak capacity of the columns in the MDGC system. We must also note that the entire sample is not subjected to the enhanced peak capacity, but only the fractions which are heart-cut and transferred to the second separation.

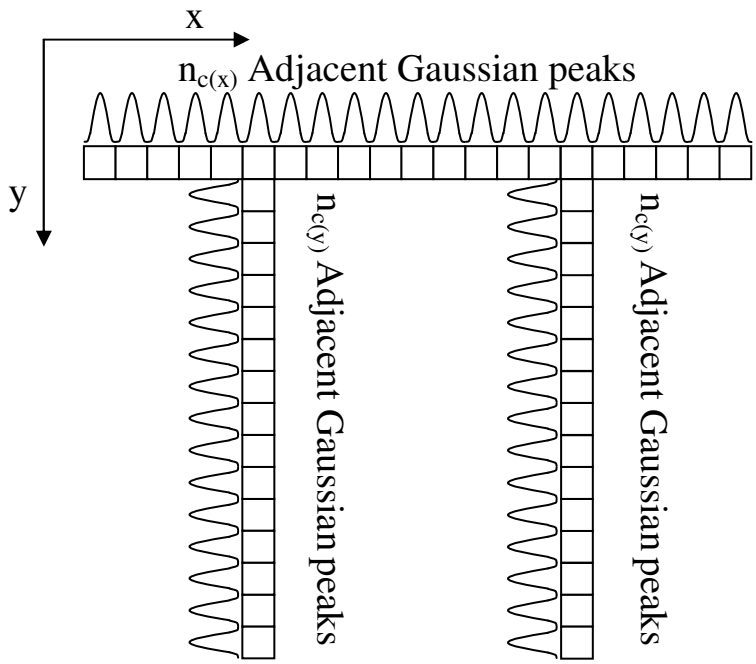

Figure 2.4 Illustration of peak capacities for the independent reanalysis of two heart-cuts [9].

Thus MDGC may be thought of as not just the increase in peak capacity to which a selected fraction is subjected to, but instead a method which allows the reanalysis of targeted fractions consisting of a significantly smaller amount of components (m_f) than the original sample (m). As a result the saturation value α for the separation of m_f is dramatically lowered by the increase in n_c and the decrease in m, this effect is illustrated in **Figure 2.3**. Therefore a typical MDGC experiment consists of two stages, the separation of the selected fractions consisting of a reduced number of components and the reanalysis of the fractions by subjecting them to a more selective secondary analysis.

The degree to which a MDGC separation produces enhancement in peak capacity is governed by the orthogonality of the two separating stages employed [10]. In other words, there is no point in transferring a selected fraction to an identical column; there will be little change in the separation of the components and hence a very small enhancement of the peak capacity. The effect of complementary selectivity has been

described by Deans who failed to separate toluene from naptha (a cut from crude oil) on a linear GC system exhibiting over 10,000 plates [16]. The analysis was then attempted on a two-dimensional system with just over 5,000 plates providing more than adequate separation.

2.3.3 Basic Instrumental Arrangements

In a MDGC system the coupling of the two or more columns can be classified as either offline or online. An offline coupling system requires the manual collection of effluent from the primary column followed by manual re-injection into the secondary column. Clearly this is not a feasible approach as many problems arise due to poor reproducibility and the inconsistent handling of samples. A direct online method is more commonly used where the automated collection and transfer of effluent occurs within a sealed analytical system. In practise a direct online system usually consists of a mechanical or pressure driven switching device allowing the automatic diverting of flows between columns [19, 20].

2.3.3.1 Transfer Valves and Vents

Mechanical rotary switching valves were the instrument of choice for early MDGC systems given their easy installation and operation [21-24]. Still, technical disadvantages such as dead volume, adsorption effects, limited maximum operating temperatures, potential gas leakage or flow path plugging, and limited flexibility restricted the use of MDGC to a very limited number of applications. In 1968 Deans introduced pressure driven switching enabling the non-intrusive diversion of flows using pressure balancing at specific junctions [25]. The main advantage of pressure driven switches is that they do not require any moving parts in the flow path of the system or in the higher temperature zone of an oven, thereby removing the problems found for early mechanical switches and allowing MDGC to be used extensively for many applications [26, 27]. Nevertheless, as time went on the technology for the manufacturing of mechanical valves improved and in 1985 a study by Gordon et al. compared the effectiveness of the two switching techniques, concluding that neither technique was superior [28].

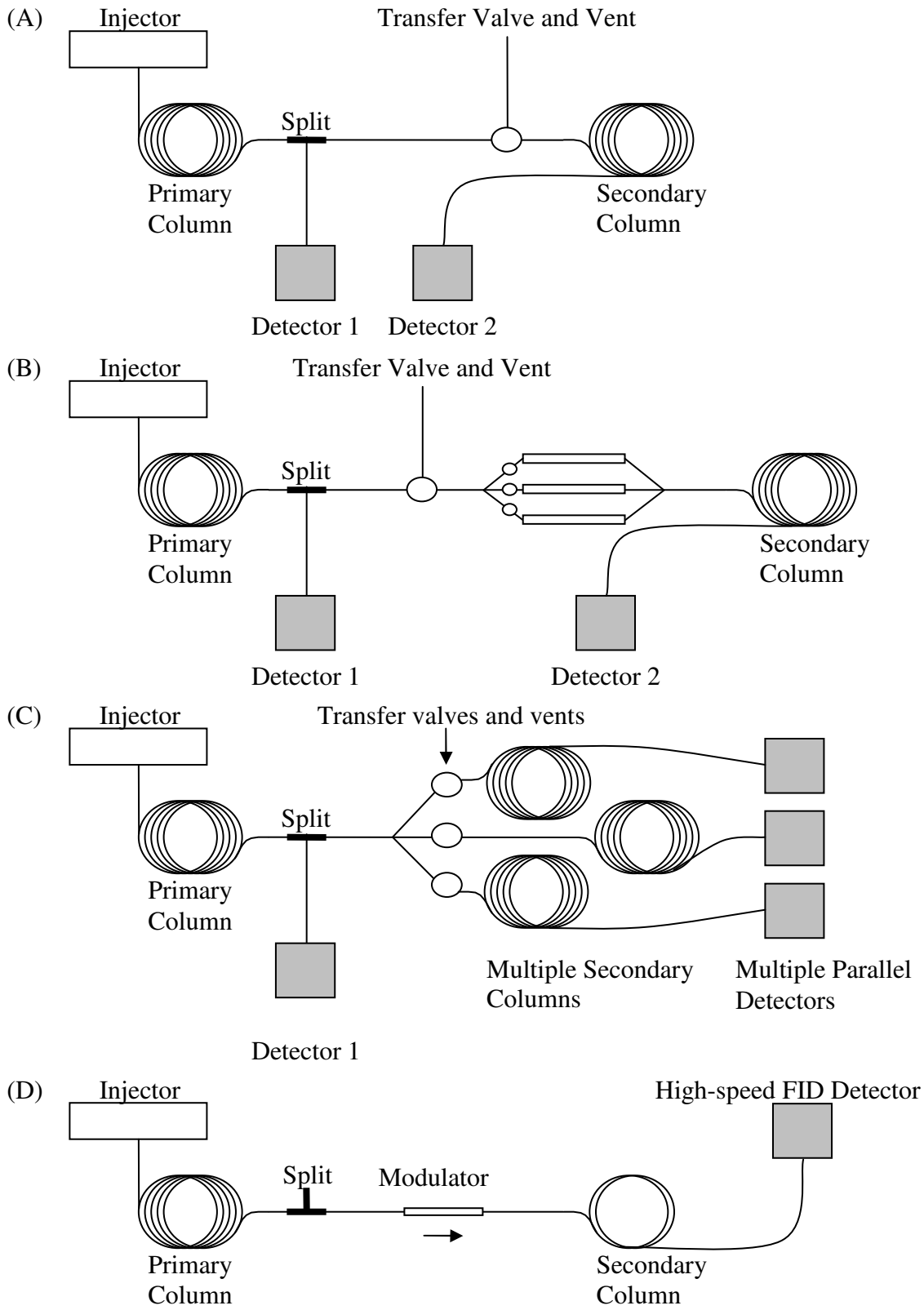

Figure 2.5 MDGC instrumental configurations: (a) direct transfer heart-cut configuration; (b) multiple parallel trap configuration; (c) multiple parallel column configuration; (d) comprehensive MDGC configuration [10].

Figure 2.5 displays the most common configurations employed for MDGC. For simplicity further operational parameters are not illustrated. For example; both columns could be contained in separate ovens allowing the optimal temperature to be separately employed for each column and providing the determination of accurate retention indices or a refocusing device could be installed at the beginning of the second column to compensate for the peak dispersion of compounds being heart-cut from the first column [26, 29-31].

Figure 2.5 (A) represents the most simplistic configuration of all four systems where both the primary and secondary columns are simply coupled together through a flow transferring device allowing discrete fractions to be diverted. A fundamental drawback of this system is that components from different heart-cuts may intermingle in the second column. The use of a refocusing device can assist in holding heart-cuts until the second column is available but is ineffective when several short heart-cuts are to be taken sequentially. The application of multiple parallel traps or multiple columns as shown in **Figure 2.5** (B) and (C) overcome this problem. Parallel trap act as a storage device holding single heart-cuts until their secondary analysis is required, while multiple secondary columns allow each successive heart-cut to be sent to individual columns of different phases.

2.3.3.2 Modulation

Extending beyond the multiple trap, column and detector arrangements in **Figure 2.5** (A) to (C), the question arises as to how an entire sample might be analysed in a multidimensional fashion, rather than just targeted portions of the effluent leaving the primary column? Ideally, a dedicated secondary column or trap must be available for each heart-cut. For a truly complex sample one would require very small heart-cuts, so as not to introduce a large value of m_f on to the secondary column, therefore requiring an impractical large number of traps or secondary columns. For a sample of little complexity this may be achievable but it is a grossly inefficient use of the technology.

In 1991 Phillips et al. performed MDGC in a completely novel manner using a device he invented called a modulator [32]. The modulator is positioned around the outside of a column and enables the collection and focusing of the passing effluent which can

then be rapidly reinjected. The MDGC system arrangement is illustrated in **Figure 2.5** (D) with the columns being directly coupled and the modulator being positioned at the union. In this arrangement the modulator will collect and focus the passing primary separation and then rapidly reinject it onto a short high speed secondary column in the form of a narrow pulse. Illustrated in **Figure 2.6** the process is repeated at a pre-set frequency (usually 4-8 sec) throughout the entire analysis and effectively breaks the primary separation into a large number of small secondary separations. This style of MDGC is commonly referred to as comprehensive two-dimensional gas chromatography or GC×GC and since its first report in 1991 has attracted much interest with the body of literature still growing rapidly [33-46].

Figure 2.6 clearly shows how the modulator with a fast ^{2}D capillary column can continually sample and analyse the ^{1}D separation (upper chromatogram) with a number of fast ^{2}D separations (lower chromatograms). If performed at a rate fast enough then it is possible to reconstruct the original ^{1}D separation and ensure that original separation is preserved – a requirement of performing MDGC. As the output of a GC×GC experiment is merely the collection of a large number of fast ^{2}D chromatograms it becomes very difficult to visually monitor the ^{1}D separation. To overcome this, the many fast ^{2}D separations are arranged side by side spaced according to their injection time as shown in **Figure 2.6**. This creates a 3D chromatogram made up of a 2D separation space combined with the detector response. Commonly this 3D GC×GC chromatogram is either represented by either a contour or heat map style of plot. This enables the analyst to recognise and asses both the ^{1}D and ^{2}D separations visually.

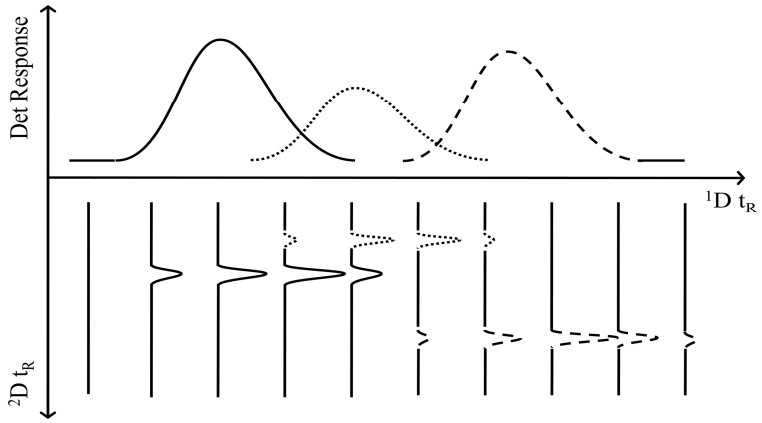

Figure 2.6 The modulator has repeatedly sampled the ^{1}D separation on the above axis and fractioned it into a number of fast ^{2}D chromatograms on the bottom axis. If the modulator samples at a rate fast enough then the ^{1}D separation has not been destroyed as it is possible to reconstruct it from the ^{2}D.

The total peak capacity produced when performing GC×GC is approximately the product of the peak capacities of the two individual columns and is written as [9].

$$n_{c\,(total)} = n_{c\,(^1D)} \times n_{c\,(^2D)}$$

Figure 2.7 illustrates the increased peak capacity for a GC×GC system. The potential peak capacity for a GC×GC arrangement as shown in **Figure 2.5** (D) is clearly much larger than any other conventional MDGC arrangement.

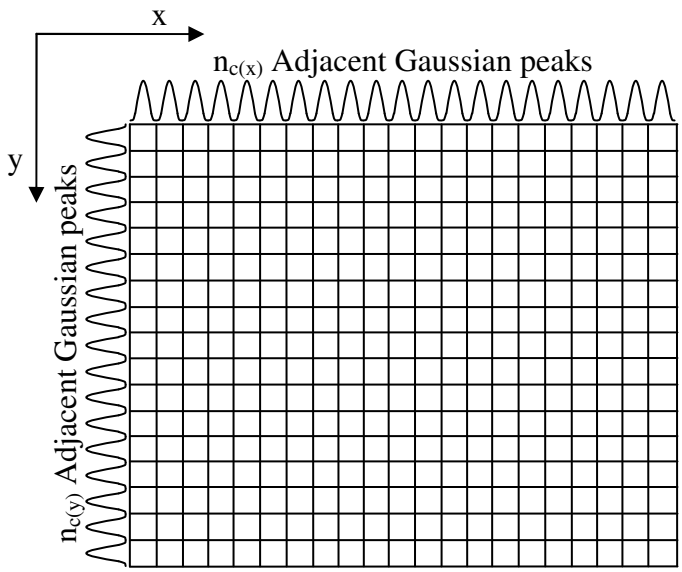

Figure 2.7 Illustration of peak capacities for a comprehensive GC×GC system [9].

2.3.3.3 Cryogenic Modulation

Most modulators today are of the cryogenic type where the collection, trapping and reinjection are performed by cooling narrow bands across the surface of a capillary column to increase a solutes retention to the point it is considered trapped. These modulators were pioneered by Marriott et al. who demonstrated the cryogenic approach in 1994 with the development of the Longitudinal Modulated Cryogenic System (LMCS) [47, 48].

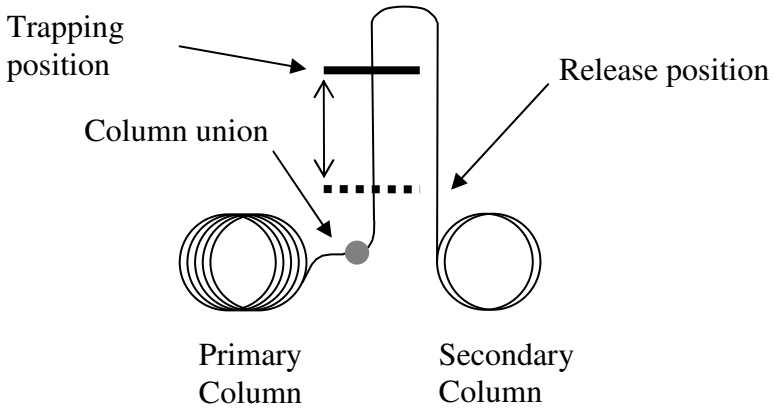

Figure 2.8 Schematic diagram of the longitudinal modulated cryogenic trapping operation employed in this study.

Figure 2.8 illustrates the working mechanisms of a LMCS unit. Using a stream of rapidly expanding CO_2 it chills a narrow band in the upper trapping position. Passing solute becomes trapped and focused within this narrow band until the stream of CO_2 is quickly shifted to the lower release position. The formerly chilled upper band quickly heats within the GC oven and rapidly remobilises the trapped solutes. While the formerly trapped solutes remobilise and continue through the secondary column, the stream of CO_2 is now chilling the lower band halting any proceeding solute from entering the secondary column. The stream of CO_2 then returns to the trapping position tacking with it any halted solute held at the lower release position. Although other cryogenic modulators with differing mechanics exist, they all operate around the premise of the trap and release position shown in **Figure 2.8**.

2.4 MODES OF MULTIDIMENSIONAL GAS CHROMATOGRAPHY

2.4.1 Targeted Multidimensional Gas Chromatography (tMDGC)

2.4.1.1 Switching tMDGC

Referred to as targeted MDGC (tMDGC), it is the most widely recognised application of MDGC. It allows the transfer of a specific region of the ^{1}D separation to the start of the ^{2}D for further separation. The mechanism by which solute(s) is (are) passed to the ^{2}D is by directing carrier flow from the ^{1}D with a mechanical valve or pneumatic switching device. At some time subsequent to this heart-cut process, normal displacement separation of the transferred cuts on ^{2}D is permitted. Within this general operation, it is possible to include a second oven (which houses the ^{2}D), a cryotrap to focus and reinject the heart-cut fractions, and various detection options including effluent splitting to more than one detector. In an advanced operational mode multiple parallel cryotraps were employed, which means that from a single injection of sample into ^{1}D, a series of sequential heart-cuts may be made into separate cryotraps [49].

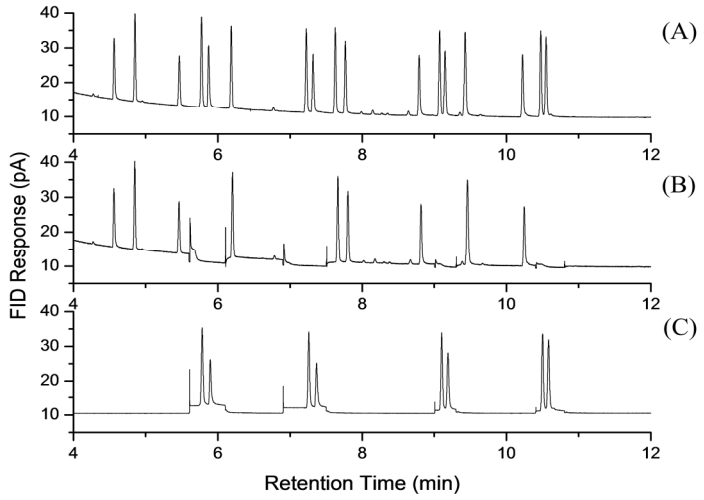

Figure 2.9 Four heart-cuts are taken from the ^{1}D separation shown in (A) with the resulting ^{1}D and ^{2}D separations shown in (B) and (C) respectfully [50].

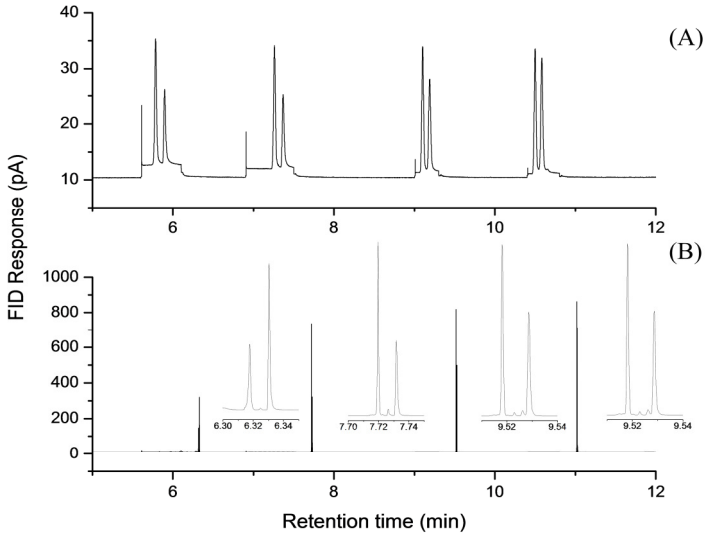

Figure 2.10 The same ^{2}D heart-cuts from **Figure 2.9** when cryofocusing and rapid reinjection with a cryogenic modulator is applied [50].

An application of extreme complexity which testifies to the lengths to which some analysts must go to adequately characterize their samples was the multiple heart-cutting method of Gordon et al. who, for a flue-cured tobacco essential oil, employed 23 heart-cuts of a few minutes duration across the entire primary separation. Due to instrumental limitations only one heart-cut could be performed per injection thus resulting in a 48 hour run time. Regardless, the tMDGC approach managed to separate hundreds of compounds with many being identified for the first time in such a sample [51]. Clearly, this demonstrates that separation is a noble goal, which justifies the efforts required to achieve analytical resolution. **Figure 2.11** presents just two of the heart-cut analyses from this sample and clearly illustrates the complexity of the sample and the complete lack of separation on the primary column.

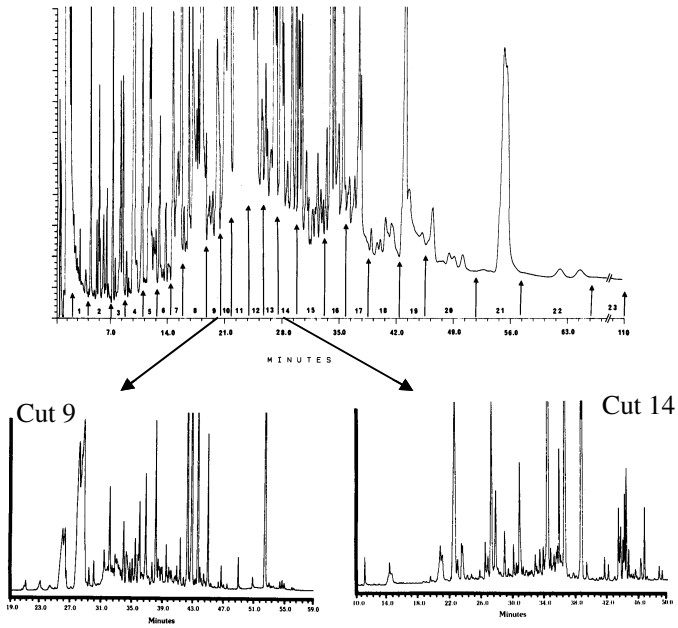

Figure 2.11 Multidimensional gas chromatography analysis of tobacco essential oil. Only two of the 23 heart-cut fractions are shown in expanded format [51].

2.4.1.2 Selective Zone Cryogenic Focusing

Using a modulator like that described in **Figure 2.8** it is also possible to perform a tMDGC separation using a technique known as Selective Zone Cryogenic Focusing (SZCF). SZCF uses a GC×GC arrangement where the entire ^{1}D separation must pass through a cryogenic modulator before reaching the ^{2}D. However, rather than continually operate the modulator throughout the entire ^{1}D separation, SZCF only operates the modulator at specified times that target desired portions of the ^{1}D separation. Unlike tMDGC or GC×GC, SZCF destroys the entire ^{1}D separation leaving only the targeted ^{2}D separation of the heart-cut region.

2.4.1.3 Preparative tMDGC

tMDGC has also been used to obtain preparative amounts of very pure chemicals [52, 53]. Following one or more heart-cuts, each from a unique and orthogonal separation column, the final heart-cut is collected in a cryogenic trap where it can be released and collected post analyses. Because capillary GC analyses sample volumes of typically 0.2 to 10 µL scale, the amount collected following numerous heart-cuts is very low. Therefore the analysis is performed a number of times until a preparative

amount of the isolated substance is collected in the cryogenic trap. This requires that the cryogenic trap is operated over the entire experiment and not just during the actual analysis.

2.4.1.4 Flow Reversal (Back-Flushing)

For a number of flow switching devices an auxiliary flow at the device is required to provide a separate carrier flow to the flow path the switch is not facing. If this auxiliary flow is sufficiently large to counter the carrier forward direction flow along ^{1}D then it is possible to switch the valve device at a given time to reverse the carrier flow and back-flush any retained solutes still on the ^{1}D. Back-flushing is of use when volatile solutes are to be analysed in a sample that contains heavier solutes that are not of analytical interest. By not passing these undesired components through the whole separation system, shorter analysis times and lower temperatures operation will result. **Figure 2.12** shows the value of such a mode where the heart-cut of pyroglutamic acid enantiomers onto an enantio-selective separation column means that the total sample need not enter the chiral ^{2}D column, and the backflushing process means that higher temperature need not be used to force the less volatile matrix components to be eluted through the column in the forward direction [54].

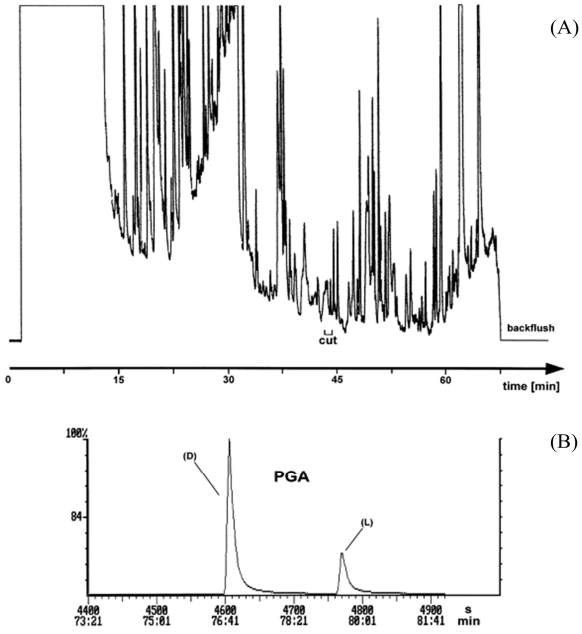

Figure 2.12 tMDGC analysis of enantiomeric urinary compounds, with enantiomeric pyroglutamic acid resolved on a chiral column, using MS detection [54].

2.4.1.5 Packed to Capillary Switching

Apart from the obvious performance advantages (efficiency) of capillary columns, sample capacity can impose limitations on the amounts of injected sample introduced into the column. Major components can become severely overloaded if a minor or trace component of interest requires that more sample be injected. If the minor component is poorly resolved from a major component there are few easy strategies that allow greater injected amounts to increase detectivity of the trace compound. By using a first packed column, more sample can be injected, and if a heart-cut event is able to exclude most of the interfering component from entering 2D, whilst allowing full transfer of the target compound, then the second (capillary) column will most likely now provide good resolution and the required trace analysis will be successful. Several companies offer conventional switching or valve approaches to tMDGC. Thus, Siemens, Gerstel and SGE report commercial systems that permit a variety of modes of operations, with simple heart-cutting and backflushing commonly supported. As switching valves may be used, valve suppliers such as VICI (Valco Instruments Co. Inc.) offer consumables that can be used for these functions. For specific advanced applications and a 'systems solutions approach,' Analytical Controls have off-the-shelf systems designed for target applications in the petrochemical industry. These are not trivial systems, and are designed to satisfy the needs of the petroleum industry for precise chemical class measurements in complex feedstock and refined products. This is represented by the PIONA (Paraffins-Isoparaffins-Olefins-Naphthenes- Aromatics) analysis task. The nature of the task requires a variety of column types, such as polar and non-polar capillary columns, molecular sieve packed traps, a hydrogenator unit, and so forth. Dallüge et. al. reviewed the application of MDGC to the oil industry, including the PIONA system [55]. Various backflushing steps are also included, with the final goal being the complete class fractionation of the analysed material into the desired molecular types. Operation up to compounds of boiling point 270 °C is achieved. The PIONA system was extended to include separation of oxygenates and termed the Reformulyser system, because these are now included in petrochemical formulations. Figure 2.13 is a representation of the latter system, demonstrating the complexity of analysis and the extent to which the analyst had to devise a system to provide the necessary analytical

data to adequately characterize the sample. The system separates the following fractions in order of elution: isomerates – saturates – alkylates – olefins – benzene – toluene – ethanol – C9 aromatics – C8 aromatics. Clearly, this is not a system that can be set up without considerable effort.

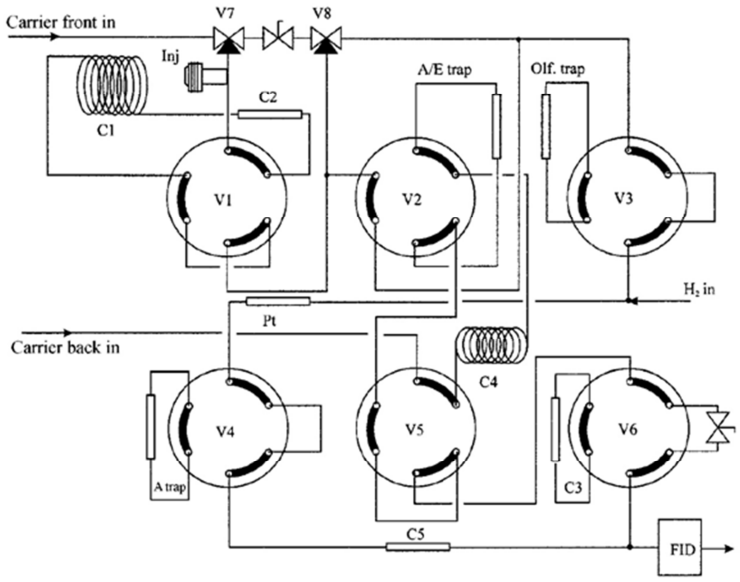

Figure 2.13 A sketch of the reformulyser multidimensional GC system used for oil product analysis, taken from the published work of Beens [55]. C1 and C2: polar and non-polar capillary GC separation columns respectively; C3: packed column (alcohol retention); C4: Tenax aromatics trap; C5: olefin hydrogenator; C6: olefin trap to retain olefins; C7: alkane trap to retain alkanes; C8: packed Porapak column for oxygenate separation; C9: packed 13X column. Note that various valves are omitted for clarity.

2.4.2 Comprehensive 2D GC (GC×GC)

Phillips and Beens summarised the principles of GC×GC, in particular how it is capable of generating higher peak capacity [56]. Compounds that coelute on ^{1}D may be separated on ^{2}D provided that the selectivity of the ^{2}D differs from that of the ^{1}D (i.e. different/ orthogonal stationary phases are used), and that peak widths are small peak identity because the patterns in the 2D space are relatively well reproduced. This means that the chemical nature of the compound will determine its location in the 2D plot, and so this pictorial presentation style is a major new feature in gas chromatographic analysis, offered by the GC×GC technique.

Applications are quickly expanding in number and breadth, as investigators are extending the technique to new studies - both for different chemical types and for fundamental aspects of the GC×GC technique. There is no reason why any volatile compound could not be suitably qualified/quantified by using GC×GC. The only requirements are that the modulation process must be appropriate for the compounds to be analysed, and that a suitable column set is available for the specific separation demanded. However, it is in the area of complex samples that GC×GC excels. The most component-rich complex samples that have been presented in the literature include cigarette smoke [55, 57, 58], petrochemicals [59-64], essential oils [65-70] and atmospheric organics [71-73]. The nature of the separation, often attributed to its orthogonality, which allows enhanced sample characterisation, is the fact that the 2D plot presents different chemical classes in different, distinct regions of the separation space. As the ^{1}D may separate by a mechanism based largely on boiling point, and the ^{2}D is selected to provide a complementary separation mechanism (such as polarity), then the space can be construed as showing a trend in separation from low to high boiling point in ^{1}D retention time, and low to high polarity in ^{2}D retention time. Indeed, within classes of compounds very specific separation bands may be identified that assist greatly in identification within particular groups simply by recognizing the factors that give the structure observed.

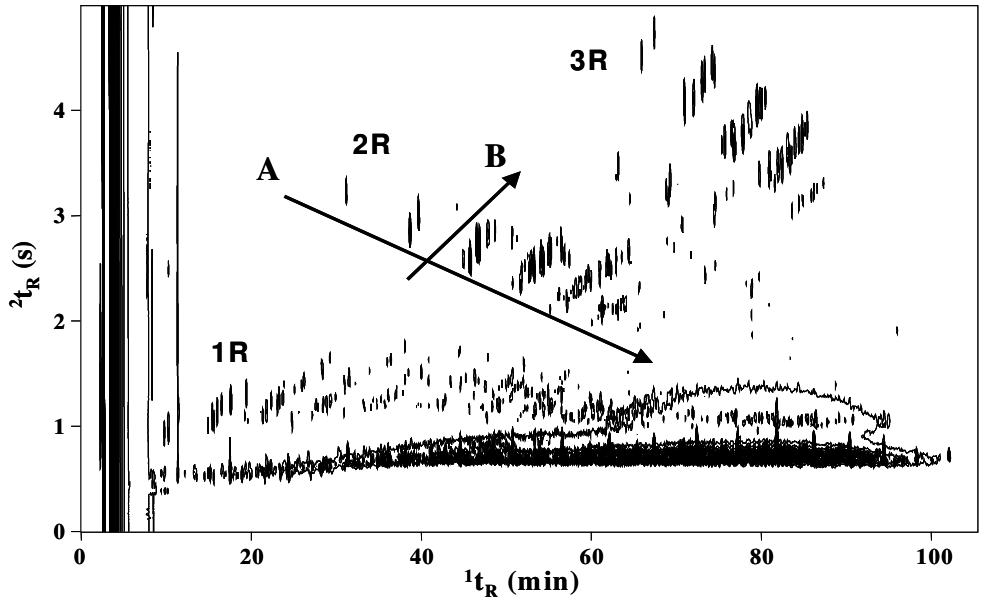

Figure 2.14 GC×GC analysis of diesel oil sample. Different regions showing various classes of aromatic compounds are highlighted [74].

Figure 2.14 is a GC×GC 2D chromatogram of a diesel sample, using a column set of 5% phenyl methyl polysilphenylene siloxane (non-polar) and polyethylene glycol (polar) for the ^{1}D and ^{2}D, respectively. The important features to highlight are the well resolved aromatic regions, with benzenes (1R), naphthalenes (2R) and anthracenes/ phenanthrenes (3R) indicated. With respect to alkyl naphthalenes, as the number of alkylsubstituents increase, members of the 'group' elute later in ^{1}D, but have a shorter ^{2}D retention time ($^{2}t_{R}$) - see line (A) in **Figure 2.14**. This suggests that the component boiling point increases, but individual compound polarity is relatively unaffected. Note that the oven temperature increases in the temperature programmed analysis. However, within a group of geometrical isomers, for example, of the same number of alkyl carbons on the aromatic ring structure (such as C3 naphthalenes), there is an evident trend to increasing retention (see line (B) in **Figure 2.14**). Thus, there will be a polarity difference within this group of isomers that must be related to the structural arrangement of groups around the aromatic ring. This observation seems to hold true across each of the aromatic classes. The intricate and unique chemical signatures of each class of compound presented in this pictorial manner makes for facile comparison of, for example, the variation in aromatic content of samples, without recourse to means such as spectroscopic detectors (mass spectrometry). Such an approach has been employed by researchers at Shell Amsterdam for the quantification of the aromatic content of oils, showing good agreement with classic methods of measurement [59].

2.5 OBJECTIVES

The main objective of this work was to understand the limitations and flaws of the MDGC techniques in their current states and determine which are more likely to impact the uptake of the technology by industry. MDGC has been researched for over 50 years with only a small number of industrial laboratories adopting the technique. It appears that the bulk of the research conducted is focused on expanding the technology and not refining it for general use. Though many researchers see their achievements in separation as motivation enough for industry to adopt the technology, they could not be further from reality. Industry is focused on making money by selling their products, period. Analytical laboratories are viewed as a very costly yet necessary evil in assuring and controlling the quality of product purchased, made or sold. Because the cost of quality assurance is so great it is typically balanced against the financial risk associated. Unless a new analytical technology can service a new niche for the right price or an old one for a cheaper price then it has next to no chance of being accepted.

Rather than focusing on expanding or exploring the separating power of MDGC techniques, this work will focus on refining the technique so that it may be more appealing for industry to adopt in the future.

2.5.1 Specific Objectives

2.5.1.1 Chapter 3

Investigate the benefits and limitations of tMDGC and GC×GC through the use of a probability model based on the already existing SMO theory. Use the model to compare the two techniques to develop a greater understanding of their unique capabilities.

2.5.1.2 Chapter 4

Further the investigation in Chapter 3 with laboratory experiments to assess the modified SMO theory probability model.

2.5.1.3 Chapter 5

MDGC techniques can generate some amazing separations but in most cases fails to match the retention time precision found with regular GC. Chapter 5 aims to develop and model a retention time locking technique that will ensure robust and reproducible retention times for both separations in a MDGC system.

2.5.1.4 Chapter 6

Develop a tMDGC system configuration that can perform the retention time locking approach outlined in Chapter 5 and investigate the newly developed technique.

2.5.1.5 Chapter 7

Develop a GC×GC system configuration that can perform the retention time locking approach outlined in Chapter 5 and investigate the newly developed technique.

2.6 SIGNIFICANCE OF RESEARCH

An assessment and comparison of the tMDGC and GC×GC techniques using SMO theory models and experimental results has never been performed. Such an assessment will clearly outline the flaws, benefits and limitations of the two techniques and provide chromatographers with a better perspective on how to use and develop the technology.

The development of a retention time locking technique for tMDGC and GC×GC is a significant step for the refinement of the MDGC technologies. When it comes to chromatography, separation is just as important as identification. The ^{2}D separation of two or more overlapping peaks on the ^{1}D is an impressive feat but it is not of much use if you cannot identify your analyte to the same precision as that found for conventional GC. Analysts using MDGC technologies are still confined to using only the ^{1}D retention time or relative retention time/retention indices. The development of independent retention time locking for both the ^{1}D and ^{2}D will enable accurate identifications to be made using a suitable library and not the comparison of recently run standards.

The research presented within this thesis has much significance within the field of MDGC and has the potential to take MDGC a step closer to routine use within an industrial environment.

CHAPTER 3

APPLICATION OF STATISTICAL MODEL OF OVERLAP THEORY TO MULTIDIMENSIONAL GAS CHROMATOGRAPHY

3.1 SUMMARY

The original work by Davis and Giddings on the development of a statistical model of overlap (SMO) theory for chromatography has been adapted for targeted multidimensional chromatography (tMDC). Although many advancements of this early SMO approach have been made to help better model the chromatographic phenomenon, the original theory can still be applied as a simple tool to approximate the performance of a chromatographic system. This present study adapts the original SMO theory to tMDC in an effort to develop an equivalent tool to approximate the performance and understand the advantages of multidimensional separation systems, which has recently gained new impetus.

With the total peak capacity of the tMDC system, the sample size and the length of the heart-cut, the number of observable peaks and the probability of isolating any one component being separated have been calculated for both the primary and secondary dimensions of a tMDC separation. It is predicted that a tMDC system with a total peak capacity of 200 (100 per column) can be subjected to a sample of 850 components and have a 60% chance of isolating any one component contained within a heart-cut. While a single dimensional chromatographic system with a peak capacity of 200 cannot analyse a sample of greater than 50 components if it is to maintain a 60% chance of separation.

3.2 INTRODUCTION

One area of study that has played an important role in the growth of chromatography is the development of probabilistic models to determine the likelihood of peak overlap. The overall aim of such mathematical models is to inform the separation science community where the technology/approach fares in regards to total or acceptable levels of separation. Klein and Tyler, considered by many to be the pioneers of the Statistical Overlap Theories (SOT), developed the first model in 1965 [75]. Unfortunately the study went largely unnoticed and the field remained relatively silent for almost 20 years. In the early 1980s, statistical theories in chromatography were revisited resulting in the development of a number of SOTs but none as well known as the Davis and Giddings model termed statistical model of overlap (SMO) [12]. SMO theory predicted that the extent of peak overlap in chromatography is far greater than originally anticipated for complex samples and that the chromatography of the time could not provide enough separating power to achieve adequate separation.

Soon after the development of SMO many studies were conducted to determine the accuracy of its discouraging predictions [76-81]. Tests and comparisons of SMO against detailed computer simulations and experimental results for both LC and GC separations revealed that SMO, for all its simplicity provided a good representation of practical results but much more refinement was needed [82-86]. More complicated variants soon appeared, attempting to resolve the discrimination between previous models and experiment [87-89]. These newer more complicated models dealt with parameters that the first SMO theory did not, such as non-homogeneous peak distributions and varying peak widths / heights and delivered more precise predictions when tested against both experimental and simulated chromatograms [90-92]. Although, more refined and accurate these new and advanced models of SMO had become significantly more complex and far beyond the knowledge of the typical chromatographer. The considerable gains in complexity of the models yielded only small improvements in the predictions over that of the original SMO theory. Though not precise in its predictions the original SMO theory for all its simplicity and limitations did have accuracy and gave the chromatography community a wealth of information. It is for this reason that the original SMO theory is commonly used as a

simple yet informative tool to not only illustrate but provide a qualitative metric for the performance and limitations of chromatography. As a testament to its value the original published work has been cited well over 300 times and partly reproduced in many books and reviews. If the reader wishes to learn more about the development of SMO and other SOT models the author suggests a comprehensive review by Davis [93].

In general, SMO theory brought to the separation science community the message that vast improvements in chromatography were required. Many chromatographers, directed by the theoretical work of Giddings, moved towards Multidimensional Chromatographic (MDC) systems as a means to alleviate the apparent lack of separating power [14]. The earliest approach to MDC was Targeted Multidimensional Chromatography (tMDC), where a targeted portion of a primary separation was collected and transferred to a secondary separation for further analysis. Termed as heart-cutting the transfer can be done in stages or in real-time with the use of mechanical or pneumatic switches. Unfortunately, in the past tMDC was plagued by many technical issues involving the heart-cut operation leading to dead volume, reproducibility and activity. Another more recent development in MDC is Comprehensive Multidimensional Chromatography (cMDC). Rather than transferring targeted portions of the primary separation to the secondary, cMDC requires the transfer of the entire primary separation in many small heart-cuts to a very fast secondary separation. The end result is many small secondary chromatograms sampled from the primary separation that when aligned vertically and in order can be viewed as a two-dimensional separation space. Most importantly, cMDC was not limited by the technical issues that threatened tMDC and quickly grew in popularity.

Following the arrival of cMDC techniques [32], Davis and co-workers further developed SMO to model and predict the cMDC approach [94, 95]. The predictions faired favourably when compared with subsequent computer simulations and experimental 2D separations [96, 97]. Some refinements over the years have been made to better represent the approach [98, 99]. To date, no SMO or SOT model has been developed to predict the performance of a tMDC system. This may be due to the technical difficulties this approach had in the past which prevented its wider use, or perhaps the overwhelming popularity of cMDC simply dwarfed it. Regardless, with

recent development and commercialisation of new state of the art flow switches it is now possible to achieve true tMDC and finally realise its full potential. Chromatographers are also finding a unique role for tMDC where extra separation is required for very complex regions of interest [25, 100-103].

The body of work presented here aims to adapt the original SMO theory to a tMDC system to deliver a simple yet effective tool to illustrate the separation power of a tMDC system. Focus will be given to targeted multidimensional gas chromatography (tMDGC) for discussion, though the principles hold true for all tMDC approaches.

3.3 THEORY

The theory is largely adapted from the early work of Davis and Giddings [12], with adaptations for a tMDC approach. The authors recognise that advancements of this early approach have been made elsewhere but choose this approach as a simple yet effective tool to help chromatographers understand how close tMDC is to complete or adequate separation.

The saturation of an analytical separation (α) can be defined as the ratio between the number of components contained within a sample (m) and the peak capacity (n_c).

$$\alpha = \frac{m}{n_c}$$

Equation 3.1

When performing multidimensional chromatography with heart-cutting each separation dimension will have its own value of α as illustrated in **Figure 3.1** and expressed in **Equation 3.3**.

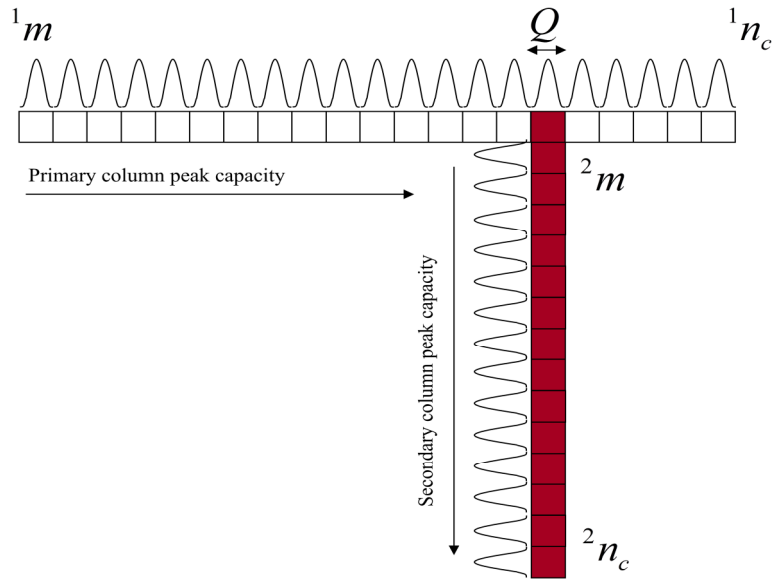

Figure 3.1 Schematic illustration of a primary and secondary separation following a heart-cut of length Q.

For the first analytical dimension $^1\alpha$ is identical to what is expected for a single column system in the absence of a heart-cut event. For $^2\alpha$, the calculation is very

different as the number of compounds allowed to enter the second dimension (^2m) is dependent on the variables ^1m, ^1n_c and the length of a heart-cut (Q), where Q is derived from the peak capacity and given as the number of peaks contained within the heart-cut event. Hence, Q = 2 represents a heart-cut with a length that spans the distance represented by two neighbouring peaks, in peak capacity units.

$$^1\alpha = \frac{^1m}{^1n_c}$$

Equation 3.2

$$^2\alpha = \frac{^2m}{^2n_c}$$

Equation 3.3

Assuming a constant distribution of peaks, the primary separation $^1\alpha$ represents the number of compounds located within every peak zone of the ^1n_c. The number of compounds entering the second dimension can therefore be expressed as the product of $^1\alpha$ and the length of the heart-cut event Q.

$$^2m = \left(\frac{^1m}{^1n_c}\right) \times Q$$

Equation 3.4

Substituting **Equation 3.4** into **Equation 3.3**, $^2\alpha$ now becomes.

$$^2\alpha = \frac{\left(\frac{^1m}{^1n_c}\right) \times Q}{^2n_c}$$

Equation 3.5

Using the original SMO theory Davis and Giddings provides **Equation 3.6** and **Equation 3.7** which predict the number of distinguishable peaks (p) and the probability of isolating any one component (P_1) respectively.

$$p = m \times e^{-m/n_c}$$

Equation 3.6

$$P_1 = \frac{s}{m} = e^{-2\alpha}$$

Equation 3.7

Where S is the predicted number of singlet peaks. Substituting ${}^1\alpha$ and ${}^2\alpha$ into **Equation 3.6** and **Equation 3.7** will allow p and P_1 to be predicted for both the ^{1}D and ^{2}D separations when performing heart-cutting experiments.

Both separation columns will differ in their ability to separate components and therefore have their own unique value of p denoted as ${}^1p$ and ${}^2p$ for the ^{1}D and ^{2}D columns and calculated using **Equation 3.8** and **Equation 3.9** respectively. For the calculation of ${}^1p$ in **Equation 3.8**, adjustments have been made to represent the loss of peak capacity and number of components due to the heart-cut. The sum of ${}^1p$ and ${}^2p$ denoted as ${}^tp$ in **Equation 3.10** represents the total number of distinguishable peaks for the multidimensional experiment.

$${}^1p = \left({}^1m - {}^2m\right) \times e^{-\left({}^1m - {}^2m\right)/\left({}^1n_c - Q\right)}$$

Equation 3.8

$${}^2p = {}^2m \times e^{-{}^2m/{}^2n_c}$$

Equation 3.9

$${}^tp = {}^1p + {}^2p$$

Equation 3.10

Just as shown for p, two values of P_1 are calculated for each dimension and denoted as ${}^1P_1$ and ${}^2P_2$ for the primary and secondary separations respectively.

$${}^1P_1 = \frac{{}^1s}{{}^1m} = e^{-2{}^1\alpha}$$

Equation 3.11

$${}^2P_1 = \frac{{}^2s}{{}^2m} = e^{-2{}^2\alpha}$$

Equation 3.12

Note that the equations presented here do not explicitly recognise a 'measure of difference' for the differing separation mechanisms between the columns. The elution of compounds through both columns is statistically random and is simply considered on the basis of probabilities. This implies that the separation mechanisms of both columns are independent of the other and are assumed to be orthogonal.

Please note that P_1 will be written as $\underline{P}_1$ in all figures to aid the reader in defining it from p.

3.4 RESULTS AND DISCUSSION

3.4.1 Number of Distinguishable Peaks

Using **Equation 3.8** and **Equation 3.9**, the peak number i.e. the total number of distinguishable peaks including singlet, doublets, triplets, etc. can be calculated for both dimensions. Expressed as a function of the ${}^1n_c$ fraction, i.e. the ratio of ${}^1n_c$ to ${}^tn_c$, values of p can be generated for varying ratios of primary and secondary n_c whilst maintaining a constant total peak capacity (${}^tn_c$). **Figure 3.2** depicts the effect of increasing the number of components m on a system, whilst maintaining constant ${}^tn_c$ and Q values of 200 and 3 respectively. The values of ${}^tn_c$ and Q were chosen as to represent a typical multidimensional system with a relatively narrow heart-cut. The combination of two chromatographic dimensions to yield a ${}^tn_c$ of 200 using any ${}^1n_c$ fraction is a trivial task while a heart-cut equivalent to a width of 3 peaks in the first dimension (Q = 3) is also somewhat standard. Provided the chromatography on the ^{1}D shows good retention reproducibility, the intended region to be transferred can be reliably heart-cut.

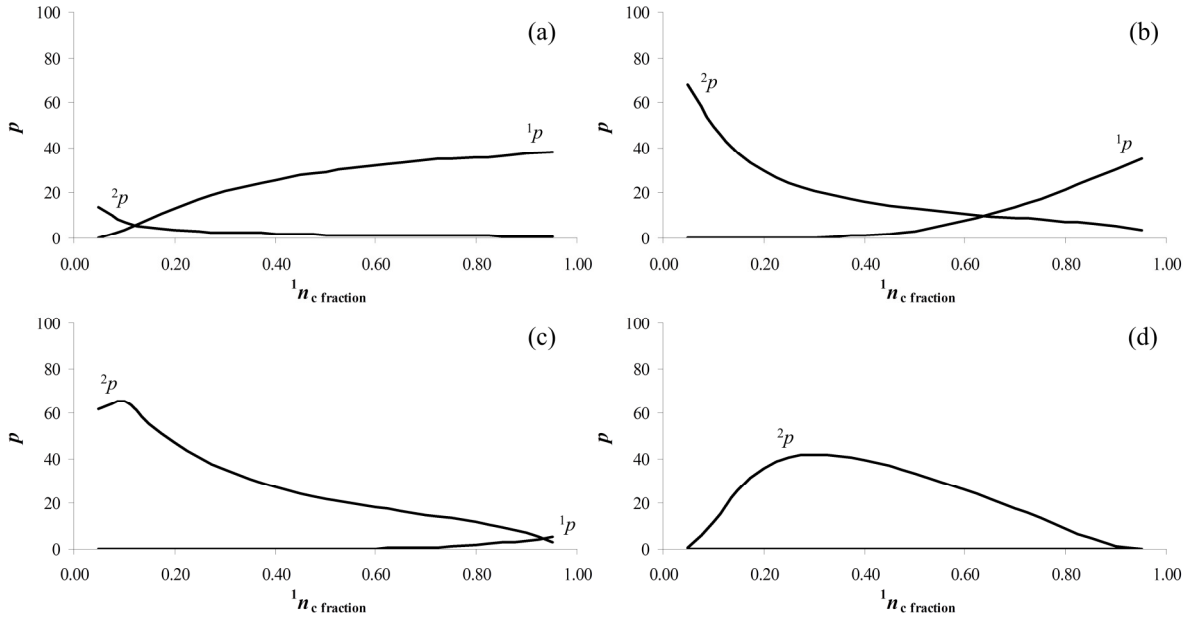

Figure 3.2 The number of predicted singlet peaks as a function of the ${}^1n_c$ fraction for Q = 3, ${}^tn_c$ = 200 and m = 50 (a), 500 (b), 1000 (c) and 5000 (d).

Figure 3.2 (a) illustrates the calculated ${}^1p$ and ${}^2p$ for a sample containing 50 components. Not surprisingly the ${}^2p$ curve almost mirrors a ^{1}D system where the ${}^1p$ is

plotted against increasing n_c. One impact the ^{2}D does have is at low ^1n_c fraction where $^1\alpha$ is at its highest value i.e. maximum saturation. A heart-cut of Q = 3 captures approximately 15% to 30% of ^1n_c and will therefore transfer a greater number of components (as m increases) to the ^{2}D consequently increasing ^2p and lowering ^1p.

As m is increased to 500 in **Figure 3.2** (b) the role of the ^{2}D at lower ^1n_c values has drastically changed, shown by a significant increase in ^2p. In the previous example where m = 50, the $^2\alpha$ showed an excess of ^2n_c for the separation of the small number of transferred peaks. Now with m = 500 a heart cut of Q = 3 transfers a greater number of components to the ^{2}D lowering $^2\alpha$ to a more efficient value. In this example, as the ^1n_c fraction increases (more of the total separation capacity resides in the ^{1}D column) $^1\alpha$ will decrease, making a heart-cut of Q = 3 less effective in passing many compounds to the ^{2}D. Coupled with the deterioration in separating power on the ^{2}D, ^2p falls quickly as ^1p rises to approach the approximate values determined in **Figure 3.2** (a).

As expected, a sample containing 1000 components causes a much higher saturation on the ^{1}D. $^1\alpha$ is so high that even as the ^1n_c fraction approaches 1.0, ^1p still remains small. For this case, heart-cutting to the ^{2}D has little effect as the ^2n_c at this point is too small to have any significant effect for the large number of components taken within a heart-cut event. At a low ^1n_c fraction however, we see that **Figure 3.2** (c) resembles **Figure 3.2** (b) with a ^{2}D column of high separation power, complementing a ^{1}D column of lower effective separation. Differing from **Figure 3.2** (b), is the decline in ^2p as the ^1n_c fraction approaches 0.0. Simply, the cause of this fall in ^2p is that the heart-cut has transferred such a great number of components to the ^{2}D that its full potential has been exceeded and as such its separating capabilities are compromised. Although the ^{1}D at this point appears to provide nothing regarding ^1p (i.e. very few peaks are distinguishable single peaks), it is apparent that its contribution is still essential as it does provide some fractionation of the sample prior to a heart-cut. If there is little prior fractionation gained from the ^{1}D column, one can find that the ^{2}D may become excessively saturated beyond optimal performance. In summary, too much fractionation on the ^{1}D may lead to too few components being

transferred to the ^{2}D resulting in an excess of separating power, i.e. a waste of separating power for too few components.

In **Figure 3.2** (d) *m* has been increased to 5000 components. The saturation on the ^{1}D is so high that no single peaks are predicted to occur. This implies that the chromatogram observed would consist of an increased base line containing an overlapped band of 5000 unresolved peaks. As *m* increases, the ability of the ^{1}D to fractionate the complex mixture becomes more limited and therefore requires a larger amount of $^{1}n_{c}$. Because of this, the apex of ^{2}p described previously becomes more pronounced and continues to move to the right. The maximum ^{2}p value has also decreased from 65 with 1000 components, to 41 for 5000 components. This indicates that though the maximum ^{2}p apex has shifted to the right allowing for greater ^{1}D fractionation the number of components entering the ^{2}D via a Q = 3 heart-cut exceeds its separation capabilities.

The above results suggest that the role of the ^{2}D is largely dependent upon the length of the heart-cut. **Figure 3.3** illustrates the effect of wider (Q = 10) and narrower (Q = 1) heart-cuts in regards to ^{1}p and ^{2}p (same conditions as that used in **Figure 3.2** (c)). As anticipated the effect on the ^{1}D is minimal with no significant changes noted. The ^{2}D however, differs greatly with Q especially with complex samples with large *m*. The large heart-cut can easily transfer too many compounds, causing high saturation of ^{2}D, while a smaller heart-cut can transfer too few components and "waste" the available separation capacity.

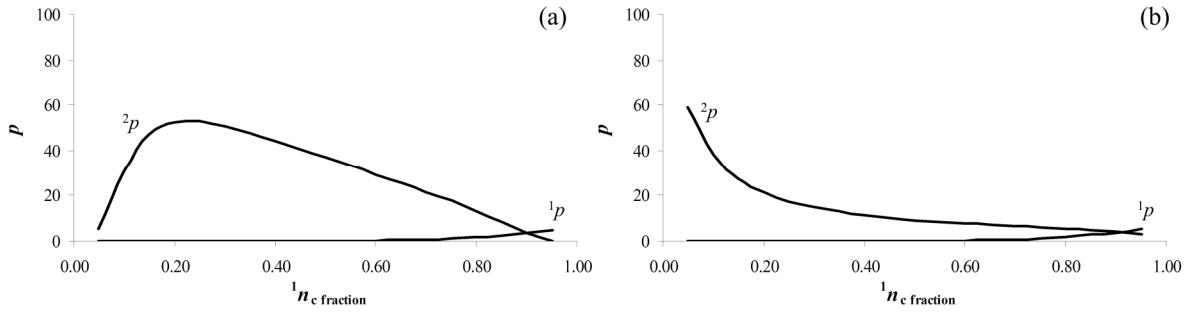

Figure 3.3 The number of predicted singlet peaks as a function of the $^{1}n_{c}$ fraction for, $^{t}n_{c}$ = 200, m = 1000, Q = 10 (a) and 1 (b).

It is possible to use this probabilistic model to generate information relating to comprehensive MDC, such as a typical comprehensive two dimensional gas chromatographic system (GC×GC), the basic concepts of which may be referred to elsewhere [104]. Ideally for a GC×GC experiment heart-cut lengths are typically determined as a quarter of the typical ^{1}D peak width. By using a heart-cut length of Q = 0.25 the model will determine the ^1p and ^2p values for a GC×GC system for only one heart-cut/modulation cycle. **Figure 3.4** (a) demonstrates a system of 200 $^t n_c$ used to separate a sample of m = 5000 with a heart-cut of Q = 0.25. Note that a typical GC×GC system can provide a greater total peak capacity then 200. For this example a value of 200 $^t n_c$ has been chosen to equal the prior examples and therefore assist in the comparison of the techniques and further illustrate the benefits of GC×GC.

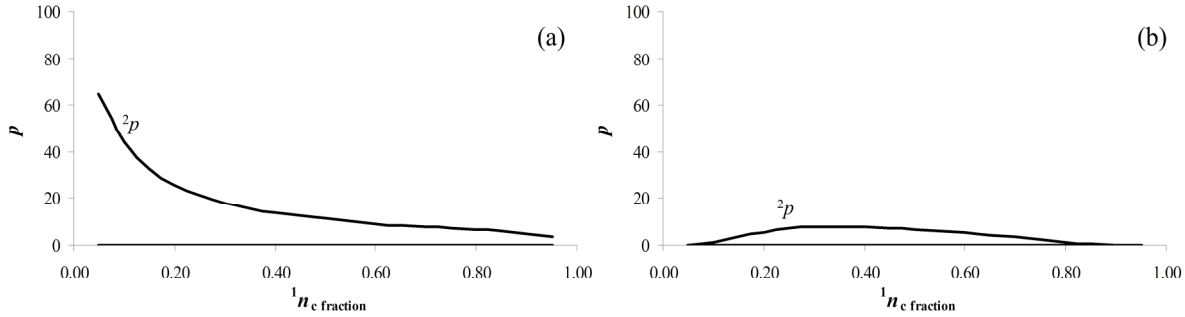

Figure 3.4 The number of predicted singlet peaks for a GC×GC approach as a function of the $^1 n_c$ fraction for, Q = 0.25, m = 5000, $^t n_c$ = 200 (a) and 50 (b).

To generate a value of p for not just one heart-cut but the many that that occur sequentially in a GC×GC experiment, an analysis time of 1 hr and a modulation cycle of 5 s are assumed, therefore generating a total of 720 individual ^{2}D chromatograms. Using a $^1 n_c$ fraction of 0.9 to represent a GC×GC system, it is found that a total of 3528 peaks are predicted. Because we have heart-cut and modulated at ¼ of a ^{1}D peak width at base, a single component will be spread between 4 consecutive ^{2}D separations. Therefore, of the 3528 peaks predicted there are approximately 3528/4 ≈ 882 resulting distinguishable peaks arising from the 5000 components injected. To apply the same procedure to other $^1 n_c$ fractions, adjustments must be made to the ^{1}D analysis time, modulation cycle and Q. For instance at low $^1 n_c$ values the ^{1}D peak width will decrease with the shorter analysis time, requiring that Q and the modulation period change accordingly. For an identical GC×GC system run at $^1 n_c$

fractions of 0.5 (30 min, 2 s, Q = 0.1) and 0.1 (6 min, 0.5 s, Q = 0.025), p values of 1058 and 1080 are generated respectively. From this it appears that as the ${}^{1}n_c$ fraction is lowered p will increase. However, it is very unlikely that this increase will ever justify the development of new GC×GC systems that can operate at low ${}^{1}n_c$ fractions; the conventional thinking is that the second dimension in GC×GC has a much lower peak capacity with fast sampling turn-around for each heart-cut fraction. How the experiment might swap to permit a higher capacity second dimension is unclear.

One factor that may encourage GC×GC users to move towards lower ${}^{1}n_c$ fractions is time savings. Separations involving complex samples can be very time consuming and as such may be costly. Shown in **Figure 3.4** (b) is a system of 50 ${}^{t}n_c$ attempting an identical separation to that in **Figure 3.2** (a). A comparison of **Figure 3.4** (a) and (b) suggests that it is possible to generate equal values of p on a system employing one quarter of the ${}^{t}n_c$ and operating at a lower than normal ${}^{1}n_c$ fraction. This would ensure a much shorter separation time without compromising the separating power.

3.4.2 Probability of Isolating a Single Peak

Figure 3.5 (a) is a representation of the original Giddings and Davis model showing the deterioration in P_1 as the sample complexity is increased. For a peak capacity of 200 it is questionable to see how rapidly P_1 falls giving very little chance of separation of any peak as a single component, for samples greater than m = 300.

Using **Equation 3.10** and **Equation 3.11**, the probability of isolating any one component P_1 can be calculated for both the primary and secondary separations. Expressed as a function of the ${}^{1}n_c$ fraction, values of P can be generated for varying ratios of primary and secondary n_c whilst maintaining a constant total peak capacity (${}^{t}n_c$). **Figure 3.5** (b) displays the ${}^{1}P_1$ and ${}^{2}P_1$ for a model consisting of ${}^{t}n_c$ = 200, m = 50 and Q = 3. Indicated by the dashed lines in **Figure 3.5** (b) is the ${}^{1}P_1$ when the ${}^{1}n_c$ fraction approaches 1.0 (200 n_c). Compared to the model in **Figure 3.5** (a) at m = 50 both P_1 values agree with only a slight difference caused by the removal of ${}^{1}n_c$ during the heart-cut process or event.

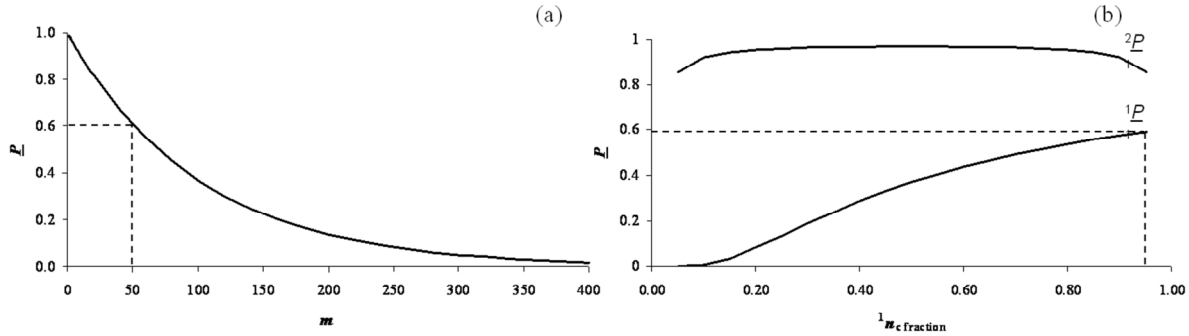

Figure 3.5 (a) Adopted from the original SMO work published. A system of only one dimension with a n_c of 200, the probability of isolating any one component as a function of the sample size. (b) The predicted probability of isolating any one component for the primary and secondary dimensions as a function of the ^1n_c fraction for $^tn_c = 200$, $m = 50$ and $Q = 3$. As the ^1n_c approaches 200 i.e. a ^1n_c fraction of 1.0, the probability of isolating any one component on the ^{1}D approaches 6.0, mirroring the value obtained from the corresponding single column system shown in (a).

By cutting any one component across to the second dimension, the probability of its separation dramatically increases, as depicted in **Figure 3.5** (b) and so the remarkable capability of the MDC process to provide increased separation is validated. $^2P_1$ values of 0.9 and above are calculated for most ^1n_c fractions except at the extremes where the $^2P_1$ tapers off slightly. This is caused by an increase in $^2\alpha$ made by the transfer of too many compounds to the ^{2}D at low ^1n_c fraction, and a lack of ^2n_c at high ^1n_c fractions. This result implies that for any individual compound contained within a sample containing 49 other components, there will be a 90% or greater chance of separation if it is heart-cut to the ^{2}D.

Another advantage of tMDC is the analysis time savings. If a 0.6 P_1 chance of isolation of any one compound is acceptable for a system of $n_c = 200$ and a sample of $m = 50$ as indicated in **Figure 3.5** (a), then it is possible to provide the same probability with a multidimensional system employing ^tn_c of only 50. This equates to a 75% reduction of the separation space which can potentially be reflected in the shortening of the analysis time. The ability to significantly reduce the time taken for an analysis is extremely beneficial to industry, especially those who require routine analysis.

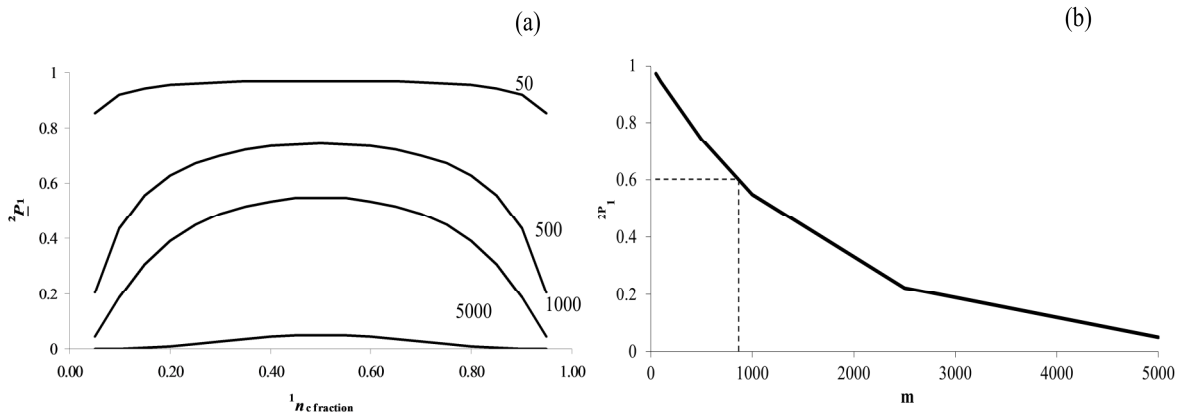

Figure 3.6 (a) The predicted probability of isolating any one component within a sample on the ^{2}D following a heart-cut, as a function of the ^1n_c fraction when, Q = 3, $^t n_c$ = 200, m = 50, 500, 1000 and 5000. (b) *M*aintaining a ^1n_c fraction of 0.5 i.e. both dimensions have the same peak capacity, the probability of isolating any one component is plotted against the sample size. With a $^t n_c$ of 200 a predicted probability of 0.6 is achieved for a sample size of approximately 900, compared to 50 for a single column system in **Figure 3.5** (a).

Increasing the sample complexity to 500, 1000 and 5000 components has a considerable effect on the $^2P_1$ curve as shown in **Figure 3.6** (a). It appears that the increase in $^2\alpha$ noted on the high and low ^1n_c fractions previously for **Figure 3.5** (b) has become more pronounced with increasing m and has caused the probability to rapidly fall. This in turn has caused the $^2P_1$ curve to take on a more pronounced shape with the highest $^2P_1$ value at a ^1n_c fraction of 0.5. This evidence implies that for extremely complex samples it is best to choose primary and secondary columns that will provide equal n_c to increase separation performance.

By maintaining a constant ^1n_c fraction such as 0.5 it is possible to plot the $^2P_2$ against an increasing sample complexity (m) as shown in **Figure 3.6** (b). Not surprisingly the curve appears to mirror the shape of the identical single dimensional plot in **Figure 3.5** (a). In comparison the range of m is far greater for the $^2P_1$ plot with reasonable separation probabilities being generated up to m = 4000. Both the single and multidimensional systems shown in **Figure 3.5** (a) and **Figure 3.6** (b) respectively employ capacities (n_c) of 200, however, the multidimensional system can provide an equivalent probability for a much larger sample size. Indicated by the dashed lines, a 60% chance of isolating any one component can be achieved with a sample size of

approximately 900 and 50 for a heart-cutting and single column system respectively. This represents an 18 fold increase in the isolation capabilities of a tMDGC system in comparison to a system containing only one column.

3.5 CONCLUSION

It is evident that SMO and its adaption to MDC presented here cannot be viewed as more than a simple tool for the generation of numerical values relating to the probable separating power of a multidimensional system. As with SMO the adaption of SMO for MDC also suffers from the same shortcomings and does not account for many factors that would affect a separation or the apparent quality of a separation such as varying peak heights, column overloading, column bleed, tailing and varying distributions of peaks within a separation space.

The adaptation of SMO theory to MDC is essentially the separate application of SMO theory to both the primary and secondary separations. The individual SMO predictions for the ^{1}D and ^{2}D are related by the number of components transferred to the secondary separation which is derived using the heart-cut length Q and the resulting distribution of peaks following a separation on the ^{1}D. This implies that the predicted separations of the ^{1}D and ^{2}D are both statistically random and completely independent/orthogonal of one another, a feat that cannot be achieved in a practical sense in MDC. It is therefore important to note that the results presented throughout this chapter will be more promising than those determined experimentally. How much the predicted results differ from those obtained experimentally is still yet to be determined. This further emphasises the point that this adaptation of SMO to MDC can only be viewed as a simple yet useful tool to predict, compare and reference the apparent strengths of a separation.

Another shortcoming lies in the determining of ^2m. Equation 3 assumes a constant distribution of peaks on the primary separation. Therefore a heart-cut of length Q taken at two locations of the ^{1}D separation will transfer the same number of components to the ^{2}D. Experimentally this scenario is unrealistic, as the 'local' value of $^1\alpha$ can vary immensely throughout a separation. In practice peaks eluting from a column will generally gather randomly in local clusters of varying distributions.

Regardless of its shortcomings, the overall objective of creating a simple tool to measure the potential separating power of a MDC system was successfully met. It was determined that for a given n_c, a ^1n_c fraction of 0.5 (i.e. equal separating power on

both the ^{1}D and ^{2}D) proved to be the optimal. Unfortunately, for comprehensive MDC systems that continually sample and heart-cut the entire ^{1}D to the ^{2}D at a given frequency, a fast ^{2}D that ensures each separation is complete before the next begins is essential. For a typical comprehensive MDC system the majority of the separating power lies in the ^{1}D. This limitation of comprehensive MDC does not allow for the application of the optimal $^{1}n_c$ fraction of 0.5, in fact, this limitation causes comprehensive MDC to operate close to the most non-optimal $^{1}n_c$ fraction. However, because the total separating power of a comprehensive MDC system is the product of the ^{1}D and ^{2}D, the inherent inefficiency in the ^{1}D and ^{2}D arrangement is overcompensated by the enormous gains made by operating the two columns in a comprehensive MDC fashion. This is true when looking at the entire comprehensive MDC chromatogram but not when focusing on a targeted area such as a single peak or heart-cut. When qualifying or quantifying specific components within a sample you are only interested in the separating power being delivered to your components of interest and not the entire sample. Therefore, when employing MDC for the targeted analysis of specific analytes, comprehensive MDC would not be the most suitable approach.

For targeted tMDC, only select portions of the ^{1}D are sampled, heart-cut and transferred to the ^{2}D for further analysis. This means that the operational restrictions that limit the column arrangements in comprehensive MDC are not an issue for tMDC. A tMDC system has the freedom to easily alter its $^{t}n_c$ to best suit the analysis and operate at the optimal $^{1}n_c$ fraction of 0.5. A comparison between a single column system and a MDC system (0.5 $^{1}n_c$) both having a total of 200 $^{t}n_c$ found that for a 60% chance of isolating a single component, the MDC system can manage a sample of approximately 900 components compared to 50 for the single column system.

Being that the majority of separations are performed to qualify or quantify a specific analyte it does raise the question as to why comprehensive MDC is vastly popular over tMDC. When in fact, if the correct technique was employed it should be the other way around.

It is important to note that the modifications of SMO theory described here are applicable to any chromatographic separation that can be performed in a multidimensional fashion.

CHAPTER 4

TARGETED MULTIDIMENSIONAL GAS CHROMATOGRAPHY FOR THE ANALYSIS OF ALLERGENS IN FRAGRANCE PRODUCTS

4.1 SUMMARY

Two approaches are described and compared for the qualitative and quantitative analysis of allergens in fragrance products, which are defined by the Scientific Committee of Cosmetics and Non-Food Products. The first consists of a comprehensive two-dimensional gas chromatography (GC×GC) experiment using both a "conventional" non-polar/polar column combination and an "inverse" polar/non-polar column set. The second approach uses a targeted multidimensional gas chromatography (MDGC) system employing a Deans type pneumatic switch and a longitudinally modulated cryogenic system (LMCS).

It was found that the conventional and inverse column sets complement each other well. Compounds well retained on the second dimension of one column set were the first to be eluted from the other. This provides flexibility in regards to relative sensitivity, wrap around and selectivity on the second column. In some instances allergens co-eluting with matrix components on the second dimension for a given column set were clearly resolved on the other.

Adopting a non-polar/polar column set, the targeted MDGC system successfully separated all allergens. The instrument is set up in a similar fashion to a GC×GC system with the addition of a pneumatic switch coupling both columns and a cryogenic trap at the beginning of a longer second dimension (^{2}D) column. The data are easier to process than for a GC×GC experiment being almost identical to that of a single column system. The targeted MDGC method described here has the capacity to deliver far greater efficiency to targeted regions of a primary separation than a GC×GC experiment, whilst still maintaining overall run times similar to those of a conventional 1D GC experiment. A LMCS positioned at the beginning of the ^{2}D column delivers enhanced sensitivity, accurate ^{2}D retention times and narrower peak widths; in consequence, these are responsible for an impressive resolution obtained from the fast, relatively short (~ 5 m) ^{2}D column.

The two column set GC×GC analysis provided a quick and effective means to qualitatively determine the presence of six allergens in a commercially available air

freshener, however all were not adequately resolved from matrix components. In contrast, quantitation was straightforward using the targeted MDGC method.

4.2 INTRODUCTION

A list of 26 raw fragrance materials have been identified by the Scientific Committee on Cosmetic Products and Non-Food Products (SCCNFP) as likely to cause contact allergies when applied to the skin. Following the 7th Amendment of the European Cosmetic Directive 76/768/EEC in 2003, cosmetic products which contain any of these 26 raw materials, above a prescribed level, must be declared on the product's packaging. Of the 26 allergens listed by the SCCNFP, 24 can be determined by gas chromatography, however the quantitative determination of these compounds presents a significant challenge owing to the chemical complexity of fragrance products and the low threshold levels set by the European Cosmetic Directive. These difficulties have provided impetus for the development of improved methods for the quantitative analysis of allergens in raw fragrance materials and products containing fragrance ingredients.

Due to their inherent complexity, most fragrance mixtures cannot be quantitatively analysed by simply using just one analytical dimension. Thus GC/MS has been a common approach, for the analysis of allergenic fragrance ingredients [105-110]. In GC/MS, the compounds separated on the first dimension are further analysed by the mass spectrometer which acts as a second dimension. Rastogi used GC/MS to identify 11 of the defined allergens from commercial cosmetic products followed by FID for quantitation [109]. Neglecting the increase in analysis time, this approach is clearly hindered by inaccuracies generated when co-eluting peaks interfere with the FID quantitation. To avoid this Ellendt and co-workers operated the mass spectrometer in SIM mode, monitoring two individual ions for each compound [110]. However the quantitation procedure followed in this study is thought to be unacceptable on the basis of analysis time, choice of internal standard and breakdown of standard solutions [111]. A thorough study utilising selected ion GC/MS was conducted by Chaintreau *et al* who successfully managed to quantitatively analyse all 24 of the volatile allergens, but still required the mass spectrometer to be operated in scan mode to verify the occurrence of compounds [108]. Another approach, also utilising GC/MS used two separate injectors that each fed different analytical columns [112]. The effluent from the two columns was combined immediately prior to the MS interface, and the chromatograms from each column were collected sequentially.

Two analyses were performed for each sample, with the GC/MS operated in full-scan mode, leading to two numerical results for each allergen which helped to minimise false-negative and false-positive results. The major disadvantage of this approach (and those like it) is the doubled analysis time. Surprisingly, this recently reported method appears to be based on commonly used approaches in GC (dual parallel column operation), and prompts one to question why the previous researchers either overlooked such a straightforward approach, or found such an approach not to be useful for allergens analysis. The use of fast GC/MS analysis increases the throughput of allergens analyses [113] but this does not address the problems caused by related overlapping compounds commonly found in fragrance separations. Although a great deal of attention has been made in prior studies to minimise false negatives and false positives, the analysis of allergenic fragrance ingredients is still problematic using linear separations. An alternative hyphenated technique is two-dimensional GC (GC-GC), where the compounds separated on the first dimension are subsequently analysed on an additional chromatographic dimension. Coupling GC-GC to a third MS dimension provides additional separation of the target analytes, delivering improved quantitative results.

Comprehensive two-dimensional gas chromatography (GC×GC) is an advanced chemical separation technique in which the whole sample is subjected to two independent dimensions of separation (columns). GC×GC delivers superior separation and increased sensitivity to the whole sample within the same time as a conventional single column analysis. These advantages make GC×GC highly suited to the analysis of fragrances and fragrance ingredients such as essential oils [65]. A GC×GC chromatogram is typically displayed as a three-dimensional surface or a two-dimensional contour plot. For a complex sample the contour or surface plot can be viewed as a unique qualitative fingerprint for each individual sample. Suitably fast scan rates for GC×GC-MS analysis can be achieved by the use of a time-of-flight mass spectrometer [114] or by using a rapid scanning quadrupole mass spectrometer with a reduced mass scan window [115]. With inexpensive faster quadrupole mass spectrometers becoming readily available, the possibility to acquire data at 33 Hz in scan mode has enabled satisfactory conditions for allergens analysis [116].

A GC×GC system consists of column set coupled together through a device called a modulator. In order to obtain maximum peak capacity in a GC×GC experiment, any correlation in the stationary phases of the two separation steps must be minimised to encourage multiple and independent separation mechanisms. In some cases however, maximum orthogonality sometimes results in long retention times on the short second column. Much of the GC×GC literature to date employs a non-polar primary column coupled to a polar secondary column (conventional column set), though recently more interest in the usage of a polar/non-polar column set (inverse column set) has arisen. Adahchour and co-workers found that for the analysis of diesel oil the use of both a conventional and an inverse column set gave complementary results aiding in the identification of target compounds and unknowns [117]. This approach was also adopted by Ryan *et al.* for the analysis of coffee [118]. Although a very challenging/varied matrix, the analysis benefited greatly from the extra selectivity provided by the combination of the two column sets.

In this chapter GC×GC analysis is shown to also complement a novel heart-cutting two-dimensional GC system. Heart-cut multidimensional gas chromatography (MDGC) is a powerful approach to improve the separation of selected regions of a ^{1}D separation. Heart-cutting is the process of transferring selected portions of the primary separation to a secondary column for further analysis. Unlike GC×GC, a classical heart-cutting approach only applies further separation to selected regions of the primary separation, rather than the whole sample. MDGC can provide greater peak capacity for the selected regions as it is not restricted to the short second column used in GC×GC methods. The use of a longer ^{2}D column also alleviates some detection issues because it will result in wider peaks, which are more compatible with full-scan qMS detection. Unfortunately in the past MDGC suffered from many technical issues such as surface activity, dead volume, peak broadening, instrument complexity and the destruction of the separation proceeding a heart-cut[20, 28, 51, 119]. Recently the use of MDGC employing mechanical switching and cryofocusing for rapid release of heart-cuts, has been shown to generate a powerful and versatile technique [50, 120]. In addition the effectiveness of an alternative approach to heart-cutting termed "selective zone compression pulsing" (SZCP) has been investigated [121]. SZCP works by simply coupling two columns together with a cryotrapping modulator positioned between them (identical to a GC×GC system). The modulator

operates throughout the whole run and is moved between the trap and release positions at specific times. The major benefit of SZCP is the simplicity of the system. The instrument is operated no differently to a single column experiment, there is no obstruction to the primary column flow and the system can still perform in a GC×GC fashion if needed. This paper investigates the suitability of both a conventional column set arrangement and an inverse polarity column set GC×GC analysis, contrasted with the new MDGC approach which employs a fast second dimension column for the determination and quantitation of allergens in a commercial air freshener.

4.3 EXPERIMENTAL

4.3.1 Gas Chromatography System:

All analyses were performed using an Agilent Technologies 6890 model gas chromatograph equipped with two flame ionisation detectors (100 Hz), 7683 series auto sampler, two injection modules, and Chemstation software. The GC was retrofitted with an Everest model longitudinally modulated cryogenic system (Chromatography Concepts, Doncaster, Australia). The GC was equipped with a split / splitless injector, operated at 250^{o}C with an injection volume of 1.0 µL. A pneumatic Deans switching system (model G2855B, Agilent Technologies, Burwood, Australia) was installed inside the GC oven to enable multiple sequential heart-cuts of the primary column effluent.

4.3.2 Separation Columns:

For the GC×GC experiments two complementary column sets were used. The first was a non-polar/polar (conventional) column set consisting of a ^{1}D fused silica capillary column of 95% methyl - 5% phenyl polysilphenylene-siloxane (BPX5) phase (0.25 µm d_f) with dimensions 30 m x 0.25 mm i.d., connected to a ^{2}D separation column of polyethylene glycol (BP20) phase (0.10 µm d_f) with dimensions 1.5 m x 0.10 mm i.d. The 2nd was a polar/non-polar (termed herein as an inverse phase) column set consisting of a ^{1}D fused silica capillary column of polyethylene glycol (SolGel Wax) phase (0.25 µm d_f) with dimensions 30 m x 0.25 mm i.d., connected to a ^{2}D separation column of 100% polydimethyl siloxane (BP1) phase (0.10 µm d_f) with dimensions 1.0 m x 0.10 mm i.d. The generic GC×GC instrumental arrangement is shown in **Figure 4.1 (**A).

The targeted MDGC column set comprised of a ^{1}D fused silica capillary column of 95% methyl - 5% phenyl polysilphenylene-siloxane (BPX5) phase (0.25 µm d_f) with dimensions 30 m x 0.25 mm i.d., connected as the input line to the Deans switch which had two balanced downstream columns - a ^{2}D separation column of polyethylene glycol (BP20) phase (0.10 µm d_f) with dimensions 5 m x 0.10 mm i.d. and a balance flow line deactivated capillary tubing (5 m x 0.10 mm). The GC×GC arrangement shown in **Figure 4.1** (A) is modified as in **Figure 4.1** (B) to provide the

two balanced downstream columns (^{2}D and UT) connected through the Deans switch valve (V) to the primary column ^{1}D.

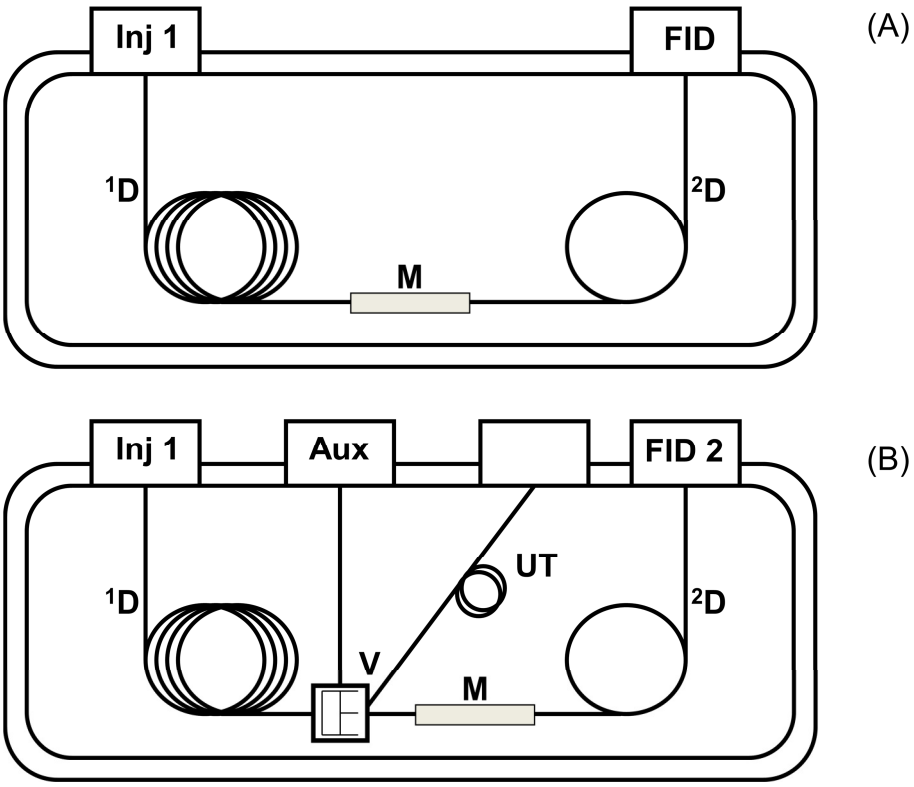

Figure 4.1 (A) Schematic diagram of a GC system incorporating the longitudinal multidimensional cryogenic system (LMCS) positioned at the coupling of the two columns. (B) This system is retrofitted with a Deans type pneumatic switching valve (V) at the end of the primary column allowing heart-cuts to be taken. The primary flow can be switched between an uncoated tubing (UT) and a second separation column (^{2}D). A cryogenic modulator (M) is positioned at the beginning of the ^{2}D for trapping and focusing of heart-cut regions.

4.3.3 GC Conditions:

All non-polar/polar column experiments reported had a split ratio of 50:1 with an initial temperature of 50°C which was increased to 100°C at a rate of 15°C/min after an initial hold time of 3 min. The temperature was then increased to 240°C at a rate of 3°C/min. The LMCS was moved longitudinally back-and-forth along the column every 4 s at -5°C. All polar/non-polar column experiments reported had a split ratio of 30:1 with an initial temperature of 65°C which was increased to 245°C at a rate of

3°C/min after an initial hold time of 1 min. The LMCS modulation period was 5 s at -40°C.

All targeted MDGC experiments employed a spilt ratio of 50:1 with an initial oven temperature of 60°C. Following an initial hold time of 1 min the oven temperature was programmed to increase at a rate of 5°C/min until a final temperature of 260°C.

4.3.4 Pneumatic Deans Switch:

Figure 4.2 illustrates the mechanics of the switching valve (V) located within the GC oven. The switching valve works by guiding the effluent exiting the ^{1}D column to either the UT or ^{2}D. This is achieved by matching the pressure at the midpoint junction (p_m) between the ^{1}D column and the switching valve with the Aux flow. ^{1}D effluent can be transferred to either the UT or ^{2}D by altering the path the Aux input flow approaches the ^{1}D-V union. The monitoring position is used to monitor the ^{1}D separation by transferring the ^{1}D separation to the UT and FID 2. When a heart-cut zone is to be transferred to the ^{2}D, the Aux input flow is switched as shown to switch effluent to ^{2}D.

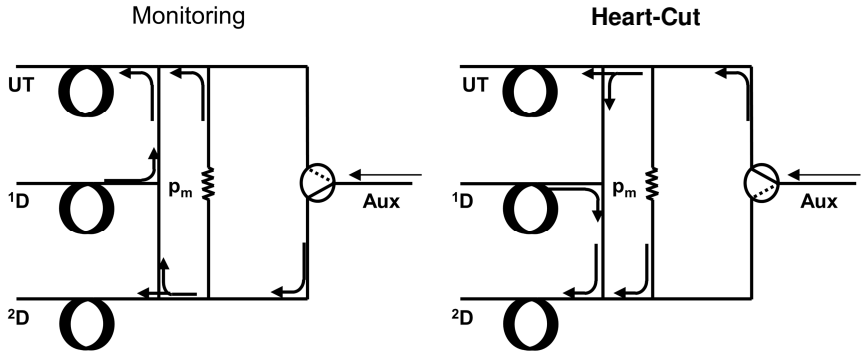

Figure 4.2 By changing the direction of the Aux flow within the switching valve the effluent exiting the ^{1}D is guided to either the UT or ^{2}D. The valve begins in the "waiting position" and switches to the "heart-cut" position as a targeted region of the ^{1}D separation approaches.

To determine the pressure to be applied to the front and back inlet a Deans Switch calculator provided by Agilent Technologies was employed. Because the Deans switch requires a pressure balance to be achieved at the midpoint, the GC carrier flow

must be operated under constant pressure. For the experiments conducted in this body of work a ^{1}D column flow of 1.5 mL/min and a ^{2}D column flow of 3.0 mL/min were desired. Substituting the desired flows into the Deans Switch calculator gave ^{1}D column and Aux pressures of 57.7 and 53.5 psig respectively. Applying these calculated pressures enabled multiple sequential heart-cuts to be taken successfully.

4.3.5 Samples:

All 24 allergens displayed in **Table 4.1** were purchased through commercial sources and were diluted in pesticide-residue grade hexane to give nominal standards of 2500 mg/L assuming 100% purity. Solutions containing all 24 allergens were then prepared at concentrations of 2, 5, 10, 20, 50 and 100 mg/L taking into account their original purity.

Table 4.1 Compounds listed as skin sensitising agents by the SCCNFP amenable to analysis by gas chromatography.

No.	Name	CAS-RN
1*	α-Isomethylionone	127-51-5
2	Amyl cinnamaldehyde	122-40-7
3	Amyl cinnamic alcohol	101-85-9
4	Anisyl alcohol	105-13-5
5	Benzyl alcohol	100-51-6
6	Benzyl benzoate	120-51-4
7	Benzyl cinnamate	103-41-3
8	Benzyl salicylate	118-58-1
9	Butylphenyl methylpropional	80-54-6
10	Cinnamaldehyde	104-55-2
11*	Cinnamic alcohol	104-54-1
12	Citral	5392-40-5
13	Citronellol	106-22-9
14	Coumarin	91-64-5
15	Eugenol	95-53-0

16	Farnesol	4602-84-0
17*	Geraniol	106-24-1
18	Hexylcinnamaldehyde	101-86-0
19*	Hydroxycitronellal	107-75-5
20	Hydroxyisohexyl-3-cyclohexene carboxaldehyde	31906-04-4
21*	Isoeugenol	97-54-1
22*	Limonene	5989-27-5
23	Linalool	78-70-6
24	Methyl-2-octynoate	111-12-6

* Compounds found in the air freshener analysed.

A commercially available air freshener was chosen as a real sample due to its known complexity, poorly resolved chromatography, and known presence of allergens. The presence of six allergens was indicated on the packaging of the product and are given in **Table 4.1**. The air freshener was diluted (1:10) with pesticide-residue grade hexane prior to analysis.

4.4 RESULTS AND DISCUSSION

4.4.1 Qualitative GC×GC Profile

To determine accurate ^{1}D and ^{2}D retention times for both the conventional and inverse column sets all 24 of the target compounds were analysed. **Figure 4.3** (A) and (B) illustrate the GC×GC two-dimensional contour plot for the allergen mix on both the conventional and inverse column sets respectively.

The allergens, being polar molecules, have relatively larger *k* values on the polar stationary phase and will therefore be more strongly retained. This causes problems for the conventional column set (polar ^{2}D) where the second dimension separation has a time restriction determined by the modulation period (it is preferred that retention time on the ^{2}D column be less than the modulation period). Thus the polar ^{2}D column affects the quality of the ^{2}D chromatogram for the analysis of allergens resulting in ^{2}D peak broadening and wrap around occurring for almost all compounds for the column set, dimensions and conditions given. Wrap around occurs when an analyte from a ^{2}D separation is not eluted within a single modulation cycle and is still present on the column when the next ^{2}D separation begins. The highly retained analyte is then interpreted as eluting with the following ^{2}D injection. Excessive broadening of peaks in the ^{2}D column for a GC×GC experiment is not favourable, reducing both sensitivity and peak capacity. In contrast, the inverse column set has a lesser tendency towards wraparound for the allergens under the conditions reported. They tend to be retained to greater elution temperature on the polar ^{1}D column, and when delivered to the ^{2}D column their polarity results in a relatively small $^{2}t_{R}$ on the non-polar ^{2}D phase.

Of course, this interpretation is only for the polar allergens, and in a complex matrix comprising both non-polar and polar compounds the situation is more complicated. This does not mean that as a general rule the inverse column set is the better of the two, as this clearly relies primarily on the nature of the matrix, and the ability of the column set to separate the allergens from matrix components. A specific column set may in fact separate target components from one another but if it cannot resolve them from the matrix, its effectiveness is compromised. So whilst the conventional column

set is therefore not necessarily a bad choice in comparison to the inverse column set, it does have a higher probability of matrix/allergen overlap.

Figure 4.3 GC×GC contour chromatograms of the 25 allergens on a (A) conventional non-polar/polar and a (B) inverse (polar/non-polar) column set.

Figure 4.4 GC×GC contour chromatograms of a commercially available air freshener on a (A) conventional non-polar/polar, and (B) a inverse polarity (polar/non-polar) column set. Resolved target allergens are indicted by circled numbers according to Table 1.

With the ^{1}D and ^{2}D retention times of the 24 compounds in the allergen mix established on the basis of the standard solution, the air freshener was analysed using identical experimental conditions. Allergens were identified by comparing their

GC×GC retention time coordinates against (resolved) compounds from the air freshener. **Figure 4.4** (A) and (B) present the GC×GC chromatograms of the air freshener on both the conventional and inverse column sets. The packaging of the air freshener reported the presence of six allergens (limonene, geraniol, hydroxycitronellol, cinnamic alcohol, α-isomethylionone and eugenol). The presence of the reported allergens was confirmed by the dual column set GC×GC analysis, with no other positive matches found for the 18 remaining compounds occurring on both columns.

Despite GC×GC offering a better result in comparison to a conventional single column analysis, two GC×GC analyses are still required as not all analytes can be resolved from matrix interferences due to the sample complexity, especially where a major matrix component occurs just prior to the target allergen. As individual GC×GC analyses, the overall chromatographic result for either of the column sets is not adequate for the task of reliable analysis of the allergens using GC×GC-FID. However, taking both sets of data together, the two sets of GC×GC retention time coordinates and a greater probability of achieving resolution does provide an acceptable result. The combination of the conventional and inverse column sets has therefore proven to be a useful tool for the identification of components within a complex matrix such as an air freshener employed here. The combined result of the conventional and inverse column sets managed to resolve all six allergens from the matrix - one compound from the conventional set, and the remaining five from the inverse set as indicated on **Figure 4.4** (A) and (B). This complementary result implies that in general more than one column arrangement may be required for a more complete analysis of a similarly complex sample. Choosing to employ only a single column set in this instance would mask the existence of one or more allergens within the matrix. It should also be noted that quantitation of the six allergens within the air freshener matrix was also achieved, using both the conventional and inverse column sets. The results of the GC×GC quantitation will not be discussed further here as it is not the primary focus of this study, where we wish to contrast the GC×GC approach with that of the targeted multidimensional gas chromatography method.

4.4.2 Quantitative tMDGC

A GC×GC system continually samples the ^{1}D column effluent at a given frequency, and in order to provide a number of sampling events for each ^{1}D peak a short ^{2}D column must be employed to ensure that each ^{2}D separation is completed before the beginning of the subsequent separation. However, if we choose to target only specific portions of a ^{1}D separation and selectively transfer (heart-cut) them to the ^{2}D the requirement for, and necessity to use, a short ^{2}D column is removed. By installing a switching device at the junction of the ^{1}D and ^{2}D columns the selective transfer of ^{1}D effluent on to a longer ^{2}D column than used for GC×GC is now possible. A GC×GC system may well provide a greater net peak capacity to the separation of the whole sample in comparison to a targeted MDGC system. The benefit of a targeted MDGC system is that it provides a greater amount of peak capacity to the targeted areas of interest at the expense of the remaining ^{1}D separation. For the analysis of selected compounds within a complex sample such as allergens in a fragrance, targeted MDGC becomes a more attractive technique of the two multidimensional techniques.

Figure 4.5 The single column analysis of a commercially available air freshener is shown in trace (A). The same analysis but with six heart-cuts (A, B_1, B_2, C, D and E). Trace (B) is the original separation minus the heart-cut areas while trace (C) shows the transfer of heart-cuts.

Displayed in **Figure 4.2** is the targeted MDGC system used for the selective heart-cut of ^{1}D effluent to the ^{2}D for further separation. The ^{1}D and ^{2}D columns are coupled using a Deans type pneumatic switching valve with a cryogenic trap positioned at the beginning of the ^{2}D for re-injection of the transferred effluent. To compare the effectiveness of GC×GC and MDGC, the same air freshener was analysed using the targeted MDGC system. It should be noted that the performance of the pneumatic switch was essentially flawless, allowing multiple, clean and quantitative heart-cuts to be taken within a single separation, and operated routinely and unattended for extended periods. Focusing and re-injection of these heart-cuts gave better separation than was observed for the GC×GC analysis, with an increase in sensitivity (peak response height) of at least 10 fold over conventional GC. **Figure 4.5** (A) is a chromatogram of the original air freshener analysis effectively a mono-dimensional 1-D GC conditions, which wholly passes through the uncoated tubing to FID 1 with

neither heart-cutting nor cryotrapping. The sample has many major and minor components, with the former displayed off scale to illustrate all peaks.

Precise heart-cut times of the six allergens in question were determined by injecting reference standards, ensuring that only the transfer of the target allergen and overlapping matrix components were delivered to the ^{2}D column. Allowing previously separated matrix components on the ^{1}D column to enter the ^{2}D column along with the allergen is first recognised as unnecessary, and secondly counteracts the advantage of having a simpler matrix for re-injection to the second column. **Figure 4.5** (B) shows the primary separation resulting from the transfer of the six precise heart-cuts to the ^{2}D column with no cryofocusing. Note in this case, the valve is held in the heartcut mode, and the target compounds are switched to the UT column. **Figure 4.5** (C) presents the FID 1 result and essentially displays what each of the six heart-cuts should resemble when entering the ^{2}D - the heart-cuts in this instance have not been transferred to the ^{2}D but to the UT instead. Plotting the heart-cuts in this manner does not indicate the final result, however it is useful in illustrating the precise ^{1}D fraction that enters the ^{2}D column. The arithmetic summation of both **Figure 4.5** (B) and (C) should be an approximate equivalent to **Figure 4.5** (A).

Figure 4.6 Second dimension chromatograms of the corresponding heart-cuts A-E following cryofocusing and rapid re-injection. The vertical scale has been expanded to show detail of smaller compounds.

The application of cryogen to the LMCS, and performing the trapping/mobilisation operation throughout the duration of all six heart-cuts as in **Figure 4.5** (C), is shown in **Figure 4.6** (A-E). Due to the reduced peak widths arising from the cryofocusing event, and the small elution time for each heart-cut zone, all six heart-cuts have been expanded and displayed separately. The limited number of timing events allowed within the software run table necessitated heart-cuts B_1 and B_2 be collected and re-injected together as shown in **Figure 4.6** (B). This is of little consequence as the targeted compounds naphthalene (internal standard) and geraniol are well resolved from each other, and also any previously co-eluting peaks, despite the collection of the two heart-cuts in the one cryotrap event.

Heart-cut C in **Figure 4.6** (C) is shown to contain the allergen hydroxycitronellal co-eluting with two major matrix components. Following the cryofocusing and re-injection of the heart-cut zone on the ^{2}D column, hydroxycitronellal is now completely separated from the very large matrix peaks. This example clearly demonstrates the advantages of a targeted MDGC approach over GC×GC. In **Figure 4.4** (A) the position of hydroxycitronellal has been indicated (peak 19, in dotted circle) and shows the target allergen hidden under (or overlapping) several overloaded matrix components. With a longer ^{2}D column (e.g. 5 m), the conventional GC×GC system may be able to achieve resolution identical to the targeted MDGC approach but at the expense of proper implementation of the GC×GC experiment; excessive wraparound would cause the GC×GC contour plot to become extremely complicated, if not useless. The MDGC instrument arrangement described here allows for multiple heart-cuts to be taken during a single experiment with no effect on the subsequent separation. Once taken, the heart-cuts are physically isolated from the primary separation and can be further separated on the ^{2}D column independent of the ^{1}D separation.

A limitation of having a longer ^{2}D column is that it becomes difficult to heart-cut closely eluting ^{1}D regions and separate them individually on the ^{2}D column. Rather than risk wrap around it becomes necessary to transfer both the desired regions together in one heart-cut, which spans the total elution window of both heart-cut zones. Thus, because of their close elution times on the ^{1}D column, α-

isomethylionone and isoeugenol were taken together in heart-cut E. With cryofocusing applied, **Figure 4.6 (**E**)** shows the separation of the two allergens from one another. However, the result is not as complete as might be desired, with α-isomethylionone not fully separated from a minor matrix component as indicated in **Figure 4.6** (E). A very small but still evident shoulder is noticed on the bottom right side of the peak. A possible way of further separating α-isomethylionone from the matrix in this instance may be to use a longer or different phase ^{2}D column, or incorporate another dimension of separation. By introducing a mass spectrometer as a third analytical dimension, complete separation or unique analysis of all six allergens should be achievable. For the described targeted MDGC system the scan rate of the quadrupole mass spectrometer should be more than adequate, due to broader peaks on the longer ^{2}D than obtained in the GC×GC experiment. The possibility of adopting a qMS as a third analytical dimension will be investigated in subsequent studies.

Table 4.2 reports the quantitation results of the six allergens limonene, geraniol, hydroxycitronellal, cinnamic alcohol, α-isomethyl ionone and eugenol in the air freshener by using targeted MDGC. The system proved to be very reproducible with relative standard deviations under 5% and R^2 values greater than 0.992 (peak area).

Table 4.2 Summary of calibration data using peak area for the 6 allergens found within a commercial air freshener. Five point calibration curves were used with each point in triplicate. The sample was run against the calibration curve in triplicate and averaged with the %RSD values listed.

Allergen	^{1}D t_R*	^{2}D t_R*	%RSD	R^2	Conc.†
Limonene	8.83	0.06	0.69	0.999	160
Geraniol	15.26	0.18	0.61	0.998	53
Hydroxy citronellal	16.52	0.21	0.89	0.999	33
Cinnamic alcohol	17.44	0.52	0.24	0.992	35
Isoeugenol	21.25	0.29	1.02	0.998	471
α-Isomethylionone	21.58	0.10	0.37	0.998	11

* Reported in minutes † Reported in mg/L

The overall limit of detection for all of the six allergens investigated was found to be 1 mg/L (split injection) but can vary depending on the length of the ^{2}D column and their $^{2}t_{R}$ values. A longer ^{2}D column implies further peak broadening thus lowering the sensitivity, but at the same time improving resolution and possible improving application of qMS. A balance between the ^{2}D phase choice and column length must be made depending on the requirements of the sample analysis.

CONCLUSION

The cryomodulation system positioned at the beginning of the ^{2}D column not only concentrates peaks for greater sensitivity but also delivers very precise sample introduction into ^{2}D and accurate ^{2}D retention times for further identification. Another benefit arising from the very narrow band introduction into the ^{2}D column is that the required length of the ^{2}D column is reduced. In the absence of cryotrapping and zone compression the peak widths entering the ^{2}D would be much larger, and would therefore require a longer column to achieve identical resolution. This would severely impact the overall analysis time, but more importantly the ^{2}D analysis time needed to achieve separation. If the ^{2}D separation becomes too long then compounds with low ^{2}D retention contained in a succeeding heart-cut may coelute or indeed pass the highly retained compounds from earlier heart-cuts and cause retention overlap or confound the data interpretation. The success of completing each heart-cut analysis before the next heart-cut is introduced to the ^{2}D column is important, because a truly targeted system should render the selected target region or compound independent from the remaining matrix.

Although slightly more complex than a GC×GC instrument which utilises one injector, a modulator and a detector, the MDGC system (Deans switch, UT and ^{2}D columns, and second carrier supply) has the advantage of simpler data processing. The handling of data for a GC×GC experiment is still relatively labour intensive, requiring more experience and processing time. However, data processing for the output of a MDGC experiment is almost identical to a single column analysis, allowing the same software packages and data interpretation to be used.

This work has displayed the benefits of a modern approach to MDGC with cryofocusing and essentially instantaneous re-injection and very fast ^{2}D analysis. Unlike GC×GC where the whole sample is subjected to a short length of ^{2}D, targeted MDGC only exposes selected portions of the primary separation to a length of ^{2}D column that can be considerably longer. By exploiting this, and adopting a longer, fast ^{2}D column, the targeted regions may be analysed on a column of much greater peak capacity than that available to a GC×GC experiment. The targeted fast MDGC

method described here has provided superior separation and quantitation for the analysis of allergens within a commercial air freshener.

CHAPTER 5

A NOVEL TECHNIQUE FOR THE APPLICATION OF RETENTION TIME LOCKING TO MULTIDIMENSIONAL GAS CHROMATOGRAPHY

5.1 SUMMARY

Retention Time Locking (RTL) in Gas Chromatography (GC) enables the duplication of chromatographic retention times for an analysis between laboratories, analysts, instruments and columns (of the same phase and phase ratio). A RTL reference library can be developed and used to identify separated peaks that result from a method locked to the reference method.

Using a combination of Poiseuille equations, the movement of carrier gas through a targeted multidimensional gas chromatographic (tMDGC) and comprehensive two dimensional gas chromatographic (GC×GC) systems were modelled. This enabled the void time and average linear velocity of the carrier gas to be determined for each individual capillary column of a multidimensional column set. The calculated void time derived from the Poiseuille models were then employed to investigate a novel concept in the application of RTL to both tMDGC and GC×GC. The concept involves the systematic variation of the union pressure between the coupled capillary columns to gain precise control of a compound's retention through both the primary and secondary columns. The results suggest that both RTL-tMDGC and RTL-GC×GC can be achieved with minimal system and procedural alterations. The novel RTL-tMDGC concept was then applied to a tMDGC system employing a Deans type pneumatic flow switching device. The auxiliary gas supplied to the Deans switch not only enabled the switching of the primary flow between the secondary columns, but also provided a source of supplementary carrier gas that allowed the systematic variation of the pressure at the union of the capillary columns.

5.2 INTRODUCTION

In gas chromatography the retention time is an absolute value resulting from the culmination of many parameters such as heat, carrier pressure/flow and column geometry. Any inconsistency in maintaining these parameters between experiments may result in irregular and unpredictable retention times. For this reason the retention time of an eluting peak has not been generally accepted as a unique value that can be exclusively related to the chromatography of a specific molecule.

Retention indices (RI) were introduced in order to normalise the experimental differences between separate GC experiments, generating a unique value that solely represents the chromatographic variables that control retention [122]. In 1998 a technique termed as retention time locking was developed that enabled the duplication of a chromatogram between systems [123-126]. By making precise adjustments to the pressure drop across a column it is possible to compensate/normalise for the net differences between experiments of the same method. Therefore, a method that is locked to a "standard" method can consistently duplicate the retention times of all eluting peaks. If an extensive retention time-locked library is created for a standard method, any new method locked to the standard method can utilise the library for identification purposes [127]. In this sense the retention time from a RTL experiment carries to the first approximation, the same weight as a RI for the identification of unknown peaks.

Peak identification made using RI or RTL on only a single separation column with a specific stationary phase, cannot be made with absolute confidence. For a more certain identification, RI or RTL are applied to two independent separations using differing (ideally orthogonal) stationary phases. With two separations, the possibility of a successful identification is significantly enhanced to a level that approaches mass spectroscopy (MS) [128]. A MDGC technique exposes select portions (tMDGC) or the entire sample (GC×GC) to two independent and ideally orthogonal separations in the one experiment [50, 65]. By applying RI or RTL to multidimensional GC (MDGC) techniques such as tMDGC and GC×GC, it should be possible to achieve an enhanced level of identification to accompany the improved separation within the one experiment. For more information regarding multidimensional GC the comprehensive

reviews by Bertsch [9, 35], Lewis [10], Tranchida [42] and Cortes [44] should be sought. The coupling of a support tool for peak identification such as RI and RTL to tMDGC or GC×GC would be most advantageous, with such a system combining improved separations with superior retention-based identification. The further hyphenation with MS detection would not only add a third dimension of spectral confirmation but increase the identification capability to a level not yet achieved in a single experiment.

The application of RI to tMDGC and GC×GC has been achieved with some limited success. For both MDGC techniques, the process of obtaining RI for the primary column (^{1}D) is very similar to conventional GC. The difficulty in combining RI to MDGC lies solely in the application of RI to the secondary column (^{2}D). Both RI-tMDGC and RI-GC×GC techniques have been successfully performed in the past, but they tend to be complex and may pose practical limitations in their implementation on a routine basis [129-131]. RTL on the other hand, does not require the peaks in both primary and secondary separations to be bracketed by reference compounds (e.g. alkanes) as is the case for RI calculation. Instead the elution of a single reference compound is adjusted (*via* pressure variation) to match that of a standard method which the analyst wishes to "lock" to. The successful development of RTL for MDGC methods may have the potential to overcome the perceived difficulties arising from the implementation of RI to MDGC techniques and provide a more effective approach to achieving identification over both the ^{1}D and ^{2}D separations.

By adjusting the pressure drop across the entire GC×GC column set, Shellie *et al.* attempted to combine RTL with GC×GC [132]. This approach proved to be successful for the RTL of both columns employing different carrier gases, detectors and instruments. However, as the pressure drop across both columns could not be independently adjusted, the technique was limited to the specific column set employed, or another set with identical geometry and stationary phase ratio. If for instance one or both of the columns in the GC×GC column set required maintenance (trimming) or replacing, it would be impossible to lock the system back to its original performance. To successfully apply RTL to MDGC, the ^{1}D and ^{2}D columns must be allowed to operate independently of the carrier flow through the total column set thus

allowing independent locking. This chapter documents a theoretical investigation into the application of RTL to both tMDGC and GC×GC.

5.3 THEORY

5.3.1 The RTL-MDGC Technique

5.3.1.1 RTL-MDGC System

The present work investigates the application of supplementary carrier gas to the coupling point of a MDGC column set. **Figure 5.1** depicts such an arrangement with three columns arranged in a T orientation. Not labelled in **Figure 5.1** is the ^{1}D outlet pressure ($^{1}p_o$), the T outlet pressure $^{T}p_o$) and the ^{2}D inlet pressure ($^{2}p_i$). This is due to the fact that when all three columns are coupled in such a T arrangement they effectively assume the same value, and henceforth are termed the midpoint pressure (p_m)

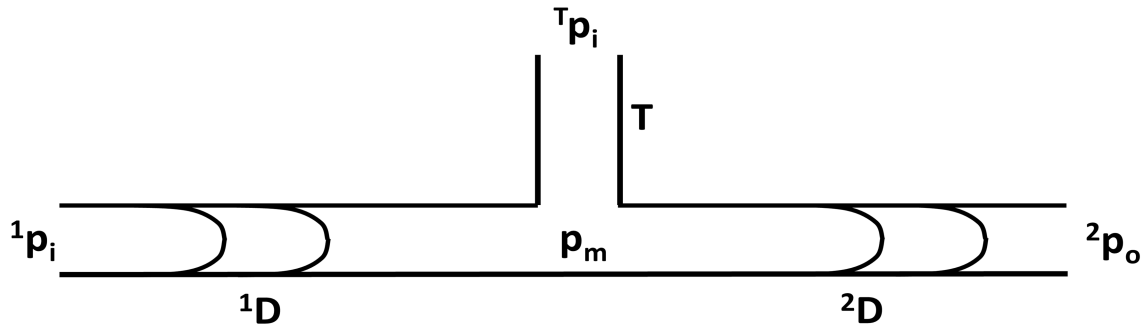

Figure 5.1 The coupling of the three columns in a T style orientation where ^{1}D is the primary separation channel, ^{2}D the secondary channel, T the uncoated tubing, $^{1}p_i$ the ^{1}D inlet pressure, $^{T}p_i$ the tube inlet pressure, $^{2}p_o$ the ^{2}D inlet pressure, and p_m the midpoint pressure.

5.3.1.2 Locking the ^{1}D Separation

To RTL a single column GC analysis, 5 sequential injections containing a reference compound are performed using the method intended to be locked. All 5 experiments are identical except for the column head pressure which is adjusted to -20, -10, 0, 10 and 20% of the original reference method that the analyst wishes to lock to. Depicted in **Figure 5.2**, the changes in the retention time of the reference compound between the 5 pressure settings, enables the analyst to map the relationship between the

column head pressure and retention. The pressure required to lock the reference compound to the proper retention time of the RTL library (for the same compound) is then determined and used in the method.

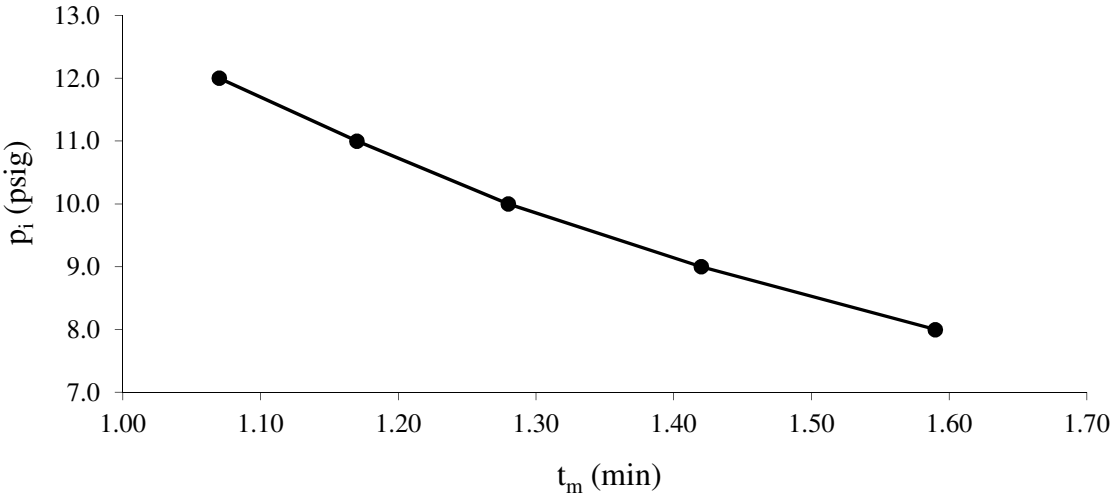

Figure 5.2 Relationship between column head pressure and column void time for a single column GC system. The values were calculated using the FlowCalc (Hewlett-Packard, Version A.02.07) software for a 30 m × 0.25 mm capillary column at 100 °C, H_2 carrier gas and atmospheric outlet pressure.

To lock the ^{1}D of the MDGC setup described here, a similar approach to the RTL of a single column GC system is taken. The ^1p_i is adjusted to -20, -10, 0, 10 and 20% of its original value and held constant for each experiment. While the ^1p_i is held constant the ^Tp_i is varied over a defined range with an injection being made at each adjustment. **Table 5.1** lists the ^1p_i pressures to be used in this study and their corresponding ^Tp_i pressures. The ^Tp_i adjustments are simply determined by adjusting the corresponding ^1p_i by the Δ pressure value found in the left column of **Table 5.1**.

Table 5.1 The ^1p_i pressures to be held constant while an injection is made for each of their corresponding ^Tp_i pressures presented directly below.

	^1p_i Values (psi)				
	36	33	30	27	24
Δ Pressure	**^Tp_i Values (psi)**				
-15.00	21.00	18.00	15.00	12.00	9.00
-12.00	24.00	21.00	18.00	15.00	12.00
-9.00	27.00	24.00	21.00	18.00	15.00

-6.00	30.00	27.00	24.00	21.00	18.00
-4.00	32.00	29.00	26.00	23.00	20.00
-3.00	33.00	30.00	27.00	24.00	21.00
-2.25	33.75	30.75	27.75	24.75	21.75
-1.75	34.25	31.25	28.25	25.25	22.25
-1.35	34.65	31.65	28.65	25.65	22.65

Employing the data from the 45 calculated void times arising from the settings in **Table 5.1**, the ${}^{T}p_i$ pressure needed to deliver the locked ${}^{1}D$ retention time (${}^{1}t_R$) for the reference compound is calculated for each of the five ${}^{1}p_i$ constant settings. The ${}^{1}p_i$ and ${}^{T}p_i$ pairs can then be used to define the relationship between ${}^{1}p_i$ and ${}^{T}p_i$ for a constant ${}^{1}t_R$.

5.3.1.3 Locking the ${}^{2}D$

The ${}^{2}D$ RTL process of a MDGC system is more similar to the locking of a single column GC system than it is for the ${}^{1}D$ RTL. Five injections containing a reference compound (can be the same compound as for the ${}^{1}D$ or different) on the ${}^{2}D$ are required. Each injection made will employ the values from the five pairs of ${}^{1}p_i$ and ${}^{T}p_i$ that resulted in the desired ${}^{1}t_R$. This is almost identical to the locking of a single GC system except rather than defining the relationship between the column head pressure and retention it defines the relationship between the ${}^{1}p_i$ and ${}^{T}p_i$ for a constant ${}^{1}t_R$, and the ${}^{2}t_R$. Importantly, for all five injections the ${}^{1}D$ remains locked at the required ${}^{1}t_R$ allowing the determination of the ${}^{1}p_i$ and ${}^{T}p_i$ pair that will lock the ${}^{2}D$ at the required ${}^{2}t_R$.

5.3.2 RTL-MDGC Poiseuille Model

5.3.2.1 The Poiseuille Gas Equation

To assess the effect of altering the pressure drop across a capillary column the average linear velocity (μ) can be determined using the Poiseuille equation expressed below as.

$$\bar{u} = \left[\frac{3r^2}{32\eta L}\right]\left[\frac{\left(p_i^2 - p_o^2\right)^2}{\left(p_i^3 - p_o^3\right)^3}\right]$$

Equation 5.1

Where r is the column radius, η is the dynamic viscosity of the carrier gas at the operating temperature, L is the column length, p_i is the inlet pressure and p_o is the outlet pressure [133].

Equation 5.1 can be used to model each of the three columns depicted in **Figure 5.1** therefore resulting in **Equation 5.2**, **Equation 5.3** and **Equation 5.4** shown below. Note that the variables have a superscript 1, 2 or T to indicate that they are from the ^{1}D, ^{2}D or transfer line respectfully.

$$^1\bar{u} = \left[\frac{3\ {}^1r^2}{32\ \eta\ {}^1L}\right]\left[\frac{\left({}^1p_i{}^2 - p_m{}^2\right)^2}{\left({}^1p_i{}^3 - p_m{}^3\right)^3}\right]$$

Equation 5.2

$$^T\bar{u} = \left[\frac{3\ {}^Tr^2}{32\ \eta\ {}^TL}\right]\left[\frac{\left({}^Tp_i{}^2 - p_m{}^2\right)^2}{\left({}^Tp_i{}^3 - p_m{}^3\right)^3}\right]$$

Equation 5.3

$$^2\bar{u} = \left[\frac{3\ {}^2r^2}{32\ \eta\ {}^2L}\right]\left[\frac{\left({}^2p_i{}^2 - p_m{}^2\right)^2}{\left({}^2p_i{}^3 - p_m{}^3\right)^3}\right]$$

Equation 5.4

To solve the average linear velocity for any of the three columns, their respective pressure drops must be known. For the hypothetical MDGC system described here ^1p_i and ^Tp_i will be defined by the analyst, while ^2p_o is determined by the type of detector used (an FID in this case, assumed to be atmospheric pressure 14.69 psi). The p_m (^1p_o, ^2p_i and ^Tp_o) however, is not a predefined value set by the analyst and therefore requires calculation. **Equation 5.5** expresses the p_m (^1p_o, ^2p_i and ^Tp_o) as a function of ^1p_i, ^Tp_i and ^2p_o enabling the determination of p_m and ultimately the $^1\bar{u}$, $^T\bar{u}$ and $^2\bar{u}$ values. Note that **Equation 5.5** was derived by solving **Equation 5.2**, **Equation 5.3**

and **Equation 5.4** for a shared pressure. The author makes no claim to this formula as it is simply the expression of three independent Poiseuille equations with respect to the pressure at their shared junction.

$$p_m = \sqrt{\frac{\frac{{}^1r^4}{{}^1L} \times {}^1p_i{}^2 + \frac{{}^2r^4}{{}^2L} \times {}^2p_o{}^2 + \frac{{}^Tr^4}{{}^TL} \times {}^Tp_i{}^2}{\frac{{}^1r^4}{{}^1L} + \frac{{}^2r^4}{{}^2L} + \frac{{}^Tr^4}{{}^TL}}}$$

Equation 5.5

A simplification can be made if the ${}^Tr$ is large enough (or ${}^TL$ short enough) to cause the pressure drop across T to become insignificant (${}^Tp_i \approx p_m$). The p_m would then assume the value of ${}^Tp_i$ therefore removing the need for **Equation 5.3** and **Equation 5.5**. As the ${}^1p_i$, p_m and ${}^2p_o$ are preset experimental variables, only **Equation 5.2** and **Equation 5.4** are required to effectively model the carrier gas flow through both the ${}^1D$ and ${}^2D$.

5.3.2.2 RTL Using ${}^1D$ and ${}^2D$ Void Times

$${}^1t_M = \frac{{}^1L}{{}^1\bar{u}}$$

Equation 5.6

$${}^2t_M = \frac{{}^2L}{{}^2\bar{u}}$$

Equation 5.7

In RTL a single peak must be chosen as a reference point to which all other experiments are required to lock/align to. The reference peak can be any peak within the chromatogram including the capillary column void time (t_m) usually determined *via* methane injection. Using **Equation 5.6** and **Equation 5.7** it is possible to calculate the ${}^1D$ column void time (${}^1t_m$) and ${}^2D$ column void time (${}^2t_m$) from their respective average linear velocities [133]. The theoretical void times of both the ${}^1D$ and ${}^2D$ can be used as the RTL reference peak to assess the effectiveness of the RTL-MDGC approach investigated here.

For this body of work all calculations were based on a hypothetical MDGC system with a ^{1}D of 15 m × 0.25 mm and a ^{2}D of 15 m × 0.25 mm. The columns are held at a constant temperature of 100 °C, and hydrogen was used as the carrier gas.

5.4 RESULTS & DISCUSSION

The approach investigated here revolves around the ability to adjust the p_m pressure with the addition of a supplementary supply of pressurised carrier gas. Illustrated in **Figure 5.1**, this is achieved by introducing a 3 way T-piece at the union between the ^{1}D and ^{2}D. A length of capillary tubing denoted as transfer line T delivers the additional carrier gas to the column union and in turn elevates p_m. As p_m is increased it begins to restrict the flow approaching the column union from ^{1}D while augmenting the carrier flow passing through ^{2}D. Specifically, an increase in p_m will result in a decrease in the ^{1}D pressure drop/carrier gas velocity and an increase of the ^{2}D pressure drop/carrier gas velocity. In this manner, ^Tp_i through its effect on p_m acts as an adjustable restrictor enabling the precise tuning of the ^{1}D and ^{2}D carrier gas velocities and retention.

With a precisely regulated p_m it is relatively straightforward to apply RTL to either of the columns *via* adjustment of their respective head pressures. However to lock both the ^{1}D and ^{2}D simultaneously and independently is a more challenging feat. The relationship between pressure drop and retention must be established for both columns and solved simultaneously to yield a set of ^1p_i and ^Tp_i values that result in the desired retention times. The methodology discussed previously, outlines a procedure to determine the ^1p_i and ^Tp_i values required to achieve a specified ^{1}D and ^{2}D retention thus achieve RTL-MDGC.

Calculated void times of 0.70 min and 0.40 min were chosen as the target locking times for the ^{1}D and ^{2}D respectively. The optimal average linear velocity was taken into consideration when selecting the RTL target. For the MDGC system described here a ^{1}D void time of 0.7 min requires an average linear velocity of 35.7 cm s^{-1} while a ^{2}D void time of 0.4 min requires 62.5 cm s^{-1} (optimal linear velocity range of H_2 is 30 to 55 cm s^{-1}). Ideally, both columns working within the optimal linear velocity range is prefered in order to maximise resolution. Therefore, a ^{1}D void time of 0.70 min with a linear velocity of 35 cm s^{-1} was deemed appropriate. The ^{2}D column however, is now fed by the carrier gas exiting ^{1}D plus the supplementry supply at the T-piece. This in turn will cause the linear velocity in ^{2}D to be elevated. For this

reason, a faster, yet somewhat below optimal ^{2}D void time of 0.04 min with a linear velocity of of 62.5 cm s^{-1} was chosen.

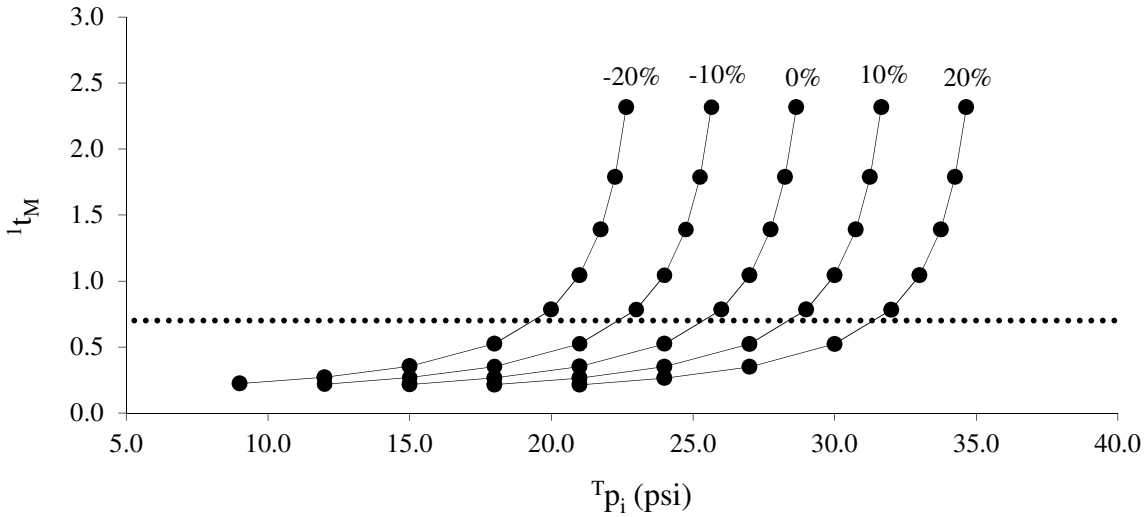

Figure 5.3 The calculated void times for the $^{1}p_i$ and $^{T}p_i$ settings reported in Table 1.

Figure 5.3 depicts the void times calculated when employing the $^{1}p_i$ and $^{T}p_i$ values in **Table 5.1**. As expected the lines are evenly spaced and the superimposed horizontal dotted line intersects all 5 of the curves at the target $^{1}t_M$ of 0.7 min. Using the MS Excel equation solver application the $^{T}p_i$ values were determined for all five curves at 0.7 min and are listed in **Table 2**. Viewed in graphical format of $^{1}p_i$ versus $^{T}p_i$ in **Figure 5.4**, it is possible to see the relationship between $^{1}p_i$ and $^{T}p_i$ while maintaining a constant $^{1}t_R$.

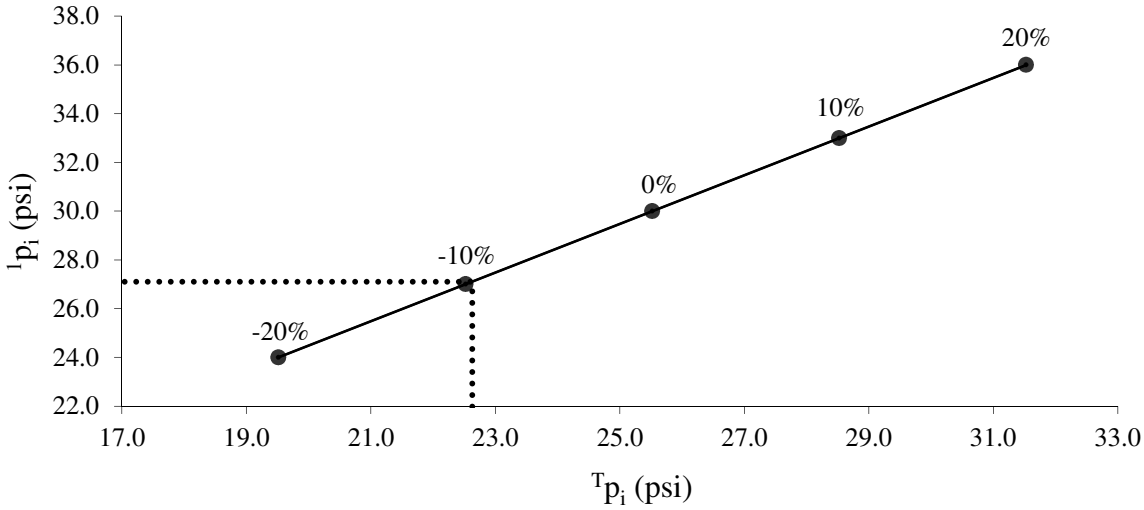

Figure 5.4 A plot of the ^1p_i against the ^Tp_i for a constant calculated void time of 0.70 min.

At any point along the straight line, the ^1p_i and ^Tp_i coordinates will return a ^1t_R of 0.7 min. As ^1p_i is increased at each setpoint from -20 to 20% of the original starting ^1p_i, ^Tp_i is adjusted appropriately. This change in ^Tp_i not only serves to maintain a constant ^1t_R but to also alter the pressure drop and carrier gas velocity across ^{2}D. **Figure 5.5** plots the resulting calculated ^{2}D void time as ^Tp_i is incremented in unison with ^1p_i to preserve the 0.7 min ^1t_R. The superimposed horizontal dotted line represents the ^{2}D target calculated void time of 0.4 min. At the point where the dotted line intersects the curve, it is extended to the horizontal axis of ^Tp_i where it gives an intercept of 22.63 psi. It is at this pressure the ^{2}D will generate the target calculated void time of 0.4 min. To determine the ^1p_i that pairs with a ^Tp_i of 22.63 psi to deliver a ^{1}D calculated void time of 0.7 min the straight line generated in **Figure 5.4** is required. Represented by the dotted lines in Figure 4, the ^1p_i was solved using a ^Tp_i of 22.63 psi to yield a value of 27.11 psi. Therefore, to successfully retention time lock the ^{1}D and ^{2}D columns at calculated void times of 0.7 and 0.4 min respectively, ^1p_i and ^Tp_i pressures of 22.63 and 27.11 psi are required respectively.

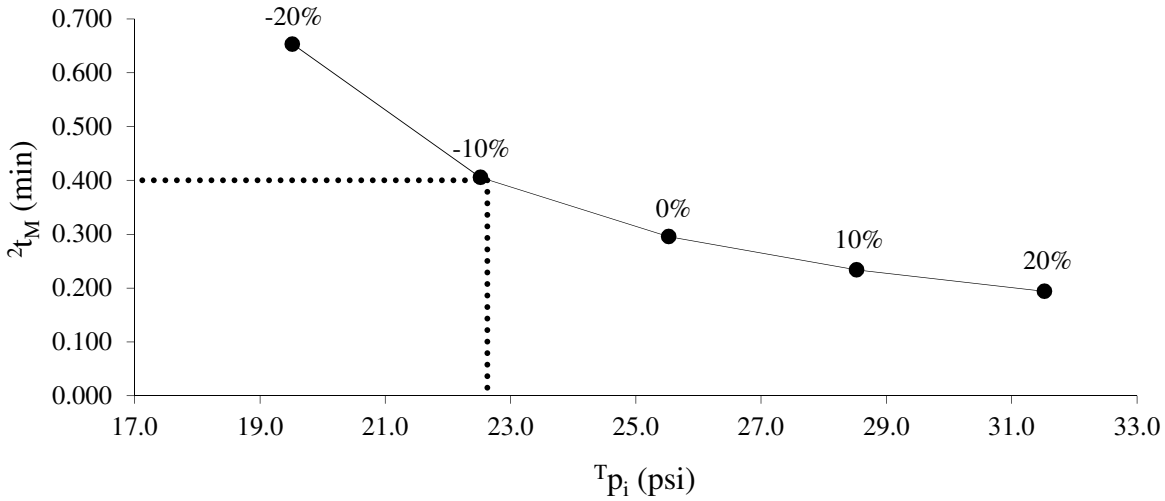

Figure 5.5 ^{2}D void times calculated using the ^Tp_i values in Table 2.

As discussed above, **Figure 5.5** closely resembles the locking of a single column GC system in **Figure 5.2**. Functionally there is no fundamental difference between the two figures except for the swapping of the vertical and horizontal axis. The supply of additional carrier gas at the union of ^{1}D and ^{2}D has allowed for the full control of both the ^{1}D outlet and ^{2}D inlet pressures. As illustrated in **Figure 5.5**, altering ^Tp_i in this manner enables the ^{2}D inlet pressure to be adjusted as if it was a single column installed into a GC system on its own. The respective pressure drops of ^{1}D and ^{2}D however, cannot be managed independently because for the MDGC system described, the ^{1}D outlet and ^{2}D inlet pressures are not controlled separately but together *via* the p_m setting. **Figure 5.4** provides a means by which the pressure drop in both ^{1}D and ^{2}D can be controlled to achieve unique target retentions. The relationship of ^1p_i and ^Tp_i for a constant ^{1}D calculated void time is the key in this approach to independently lock both ^{1}D and ^{2}D.

Table 5.2 Combinations of $^{1}p_i$ and $^{T}p_i$ for a target $^{1}t_R$ of 0.70 min, and the resulting ^{2}D criteria or data for elution of the compound.

	20%	**10%**	**0%**	**-10%**	**-20%**
$^{1}p_i$ (psi)	36	33	30	27	24
$^{T}p_i$ (psi)	31.53	28.52	25.52	22.52	19.52
$^{1}t_R$ (min)	0.700	0.700	0.700	0.700	0.700
^{1}u (cm s^{-1})	35.7	35.7	35.7	35.7	35.7
$^{2}t_R$ (min)	0.194	0.234	0.296	0.406	0.653
^{2}u(cm s^{-1})	128.8	106.9	84.5	61.6	38.3

Table 5.2 lists the calculated void times and linear velocities for the original five values of $^{1}p_i$ and the corresponding $^{T}p_i$ to yield a constant $^{1}t_R$ of 0.7 min. The approach described here need not be used solely for the purpose of retention time adjustment in a MDGC system. Due to the physical arrangement and installation of a MDGC system, the ability to control the linear velocity is limited. In most cases one or both of the separations are performed in less than ideal linear velocities. By using the procedure outlined here it is possible to negotiate such limitations and ensure that both columns are operating at optimal efficiency. The ultimate reason for adopting a MDGC approach is for more separation. It therefore begs the question; could one efficient column perform better than two inefficient columns? In short, it depends on many factors but by adopting the technique discussed here it should be possible to obtain a separation performance that exceeds that of a single column, and interpret the results based on the respective performance that can be achieved on each dimension.

There are some foreseen limitations with the technique investigated here. When coupling two columns together and applying head pressure at the ^{1}D inlet, the second column acts as a restrictor to the movement of carrier gas flow through ^{1}D. Termed as

the natural pressure restriction, p_m (^{1}D outlet and ^{2}D inlet pressure) is completely dependent on the extent to which ^{2}D restricts the flow. The greater the restriction of ^{2}D the greater the increase in p_m to provide flow through ^{2}D This affects the ability to RTL a MDGC system using the method described here because p_m cannot be lowered below the natural pressure. **Figure 5.6** illustrates the natural pressure restriction for a hypothetical MDGC system (line B). The natural pressure restriction was determined using **Equation 5.8** which calculates the pressure at any distance (Z) along a capillary column, where p is the head pressure and L is the column length [132].

$$p_Z = \sqrt{p^2 - \left(\frac{Z}{L}\right)\left(p^2 - 1\right)}$$

Equation 5.8

Located at line (A) is another limit termed the backflushing limit. This occurs when the pressure at the p_m exceeds that at the ^1p_i, thus reversing the pressure gradient and the carrier gas flow. Backflushing is by no means a new concept in MDGC, in fact it has been utilised in many MDGC and GC systems to remove unwanted high boiling compounds out through the column inlet (vent) to preserve column life [21]. Therefore, p_m is confined between two boundaries. It cannot be greater than ^1p_i nor can it be lower than the natural back pressure.

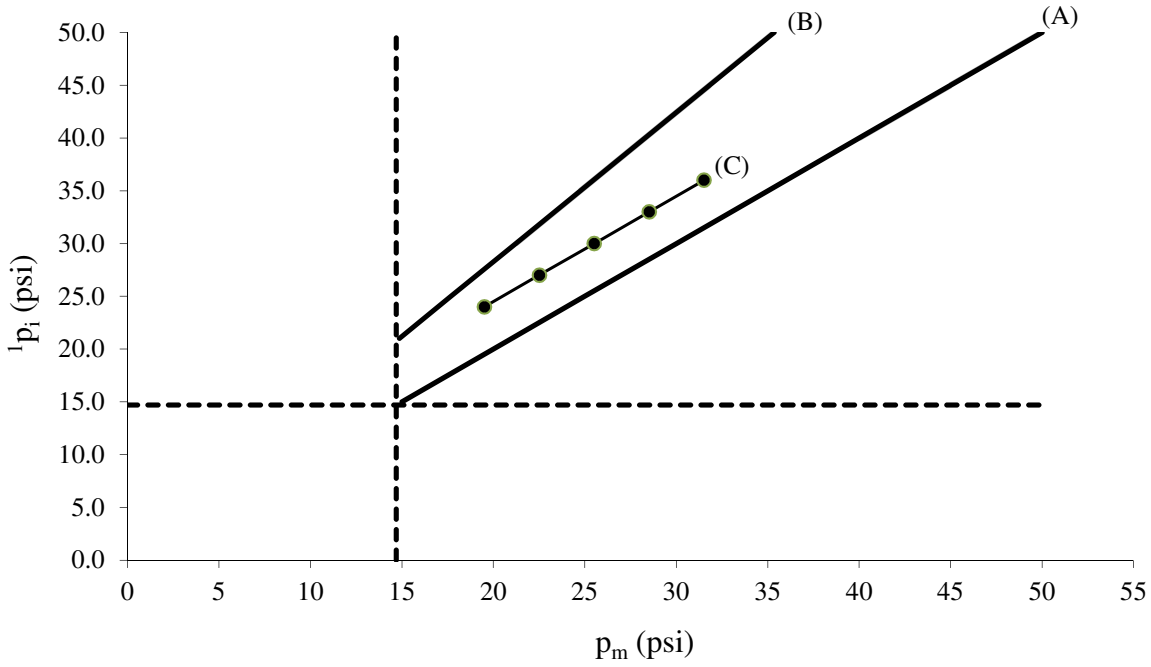

Figure 5.6 Settings of $^{1}p_i$ against p_m for a constant void time of 0.70 min (C) with pressure boundaries for backflushing (A) and the natural pressure restriction (B).

Another boundary is the atmospheric pressure represented by dashed lines in **Figure 5.6** at 14.69 psi; neither $^{1}p_i$ nor $^{T}p_i$ can be equal to or less than the atmospheric pressure (unless vacuum operation is provided at the midpoint). Taken from **Figure 5.4** the straight line representing $^{1}p_i$ and $^{T}p_i$ for a $^{1}t_R$ of 0.7 min is plotted as line (C). **Figure 5.6** shows that line (C) remains well within the boundaries of operation. However, the natural back pressure is not permanently fixed like the other pressure boundaries and can be either widened or restricted, as described below.

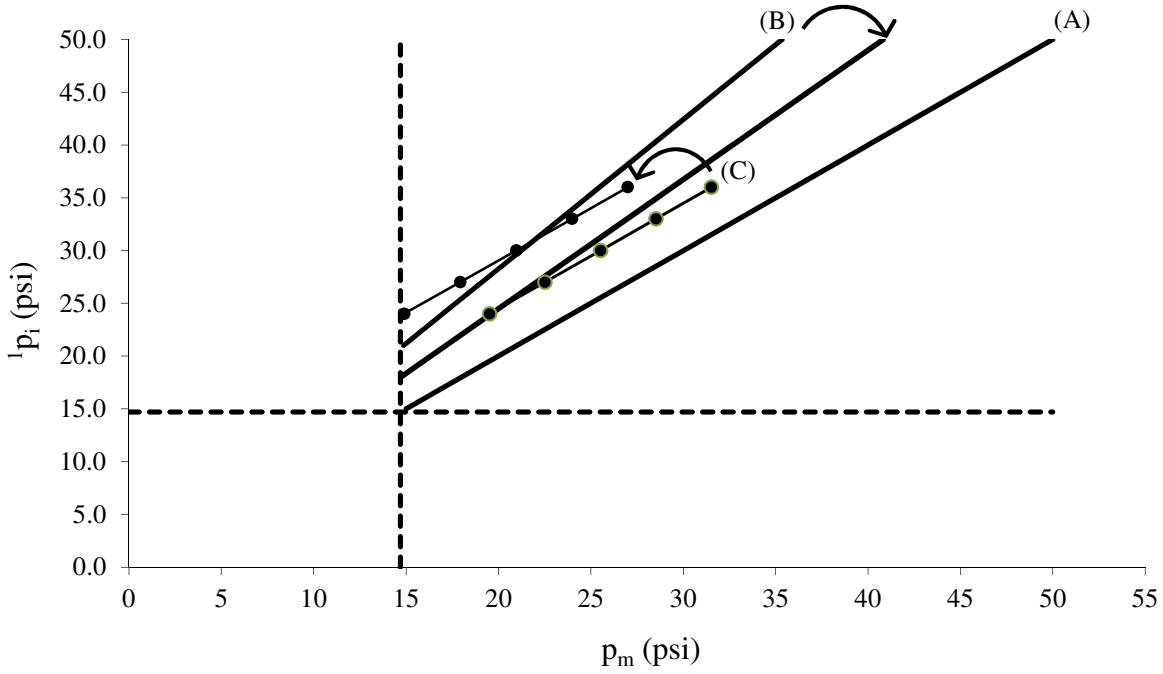

Figure 5.7 Settings of ^1p_i against p_m for a constant void time of 0.70 min (C) superimposed over the pressure boundaries for backflushing (A) and natural pressure restriction (B).

Figure 5.7 illustrates the effect of increasing the restriction of ^{1}D and ^{2}D with respect to the pressure boundaries presented in **Figure 5.6**. By increasing the ^{2}D length to 30 m the restriction to flow is increased and the natural back pressure (B) is bought closer to the back flushing limit. This has drastically reduced the workable area and intercepted the line of ^1p_i and ^Tp_i for a ^1t_R of 0.7 min (C). Any part of line (C) that crosses line (B) is unusable as the p_m pressure cannot be physically achieved. Consequently, only the upper region of line (C) can be used to lock the ^{2}D thus preventing the ability to slow the linear carrier gas velocity and generate longer calculated retention times.

By increasing ^{1}D to a length of 30 m the restriction to flow is increased and p_m required for a constant ^1t_R of 1.4 min is reduced. Note that ^1t_R has been adjusted to 1.4 min from the 0.7 min used in previous examples in order to maintain a ^{1}D linear velocity of 35.7 cm s^{-1}. The lower values of p_m have caused line (C) to shift left as indicated by the arrows in **Figure 5.7**. The increased ^{1}D restriction shifts the natural back pressure to the left and opens its angle, creating more usable space to RTL both columns. This suggest that when attempting to apply RTL to a MDGC system using the approach outlined, it is slightly advantageous to have the ^{1}D column as the source

of the greatest flow restriction. Note that normally the RTL approach is used for a system that is only marginally different to the initial system, so closely similar dimensions of columns are used.

For a tMDGC system, the analyst is somewhat free when it comes to column selection. tMDGC by nature has no practical limitations when it comes to the geometry of a column set. For the majority of applications a tMDGC column set should be able to provide both the ability to be locked at optimal conditions, and also to give the extent of separation required. By contrast, a GC×GC system is quite the opposite with very specific functions that each column in the column set must perform to achieve an optimal or desirable GC×GC separation. A GC×GC system works by utilising a modulator device at the union of the ^{1}D and ^{2}D columns the role of which is too continually sample and transfer small portions of the exiting ^{1}D effluent and reinject it to ^{2}D. To achieve this the ^{1}D column must provide peaks that are wide enough for the modulator to sample a number of times (typically 3-4) [134]. A longer and wider bore ^{1}D column will encourage peak broadening and increase the modulations across the peak.. The ^{2}D column requirements on the other hand demand a very fast separation so that each modualted ^{2}D chromatogram is completed before the next sampling event. To achieve this a very short ^{2}D column for with narrow internal diameter is used. The contradiction however is that the flow in the narrow ^{2}D column tends to be very high and consquently non-optimal.

With such restrictions in GC×GC column set geometry, it is predicted that the pressure restictions outlined in **Figure 5.7** will drastically limit the application of RTL to GC×GC using the approach described. To overcome this the T-piece located at the union between the ^{1}D and ^{2}D needs the ability to either subtract (*via* splitting) or add carrier gas. This will physically allow the the p_m to approach atmospheric pressure and hence eliminate the natural back pressure completely. To theoreticaly lock such a system, the assumption made earlier that $^{T}p_i$ approximates p_m if column segment T has a negligable pressure drop can no longer be made. To effectively split the exiting ^{1}D column effluent, T must possess restriction to the flow and hence maintain a pressure drop. **Equation 5.5** is now required to calculate the p_m which is then substituted into **Equation 5.2**, **Equation 5.3** and **Equation 5.4** to determine the linear velocities for ^{1}D, ^{2}D and T. An obvious concern with such a system would be the loss

of sample entering p_m, *via* the T column, and also possible non-linearity of splitting, though the former can be remedied by injecting more sample onto the ^{1}D. The GC×GC column set geometry lends itself to this solution in that the wide internal diameter of the ^{1}D resists overloading while the removal of the excess sample at the p_m protects the narrow ^{2}D from overloading. Regardless of the changes, the procedure investigated to independently lock both columns in the modified GC×GC system remains unchanged.

For a system where ^Tp_i is assumed to equal p_m, the RTL procedure presented here may be somewhat excessive. If ^1p_i (and ^2p_o) has no influence over p_m it is possible to simply apply a single column RTL approach to ^{2}D, followed by ^{1}D. This is of course, if the ^Tp_i value used to initially lock the ^{2}D falls under the limit of natural back pressure for the ^1p_i at the desired ^{1}D locking time. If ^Tp_i equalled p_m and the natural back pressure did not restrict the locking procedure this simplified approach would be ideal. However, **Equation 5.6 and Equation 5.7** imply that for a large majority of MDGC column sets the pressure limits imposed by the natural back pressure would severely hinder the ability to lock ^{1}D and ^{2}D at optimal or near optimal conditions. For this reason the removal of carrier gas at the T-piece may be required to eliminate the natural back pressure and lock the column set at the desired conditions. By removing carrier gas at the T-piece and diverting it along column T, the ^Tp_i no longer approximates p_m. Therefore, the single column RTL approach applied to both columns is no longer practical and the technique investigated here must be used.

5.5 CONCLUSION

Using a combination of Poiseuille equations to theoretically model a MDGC system, this chapter investigates a procedure for the independent retention time locking of both columns in a MDGC column set i.e. RTL-MDGC. This investigation proposes placement of a T-piece fitting at the union between the ^{1}D and ^{2}D of a MDGC column set; the addition of supplementary carrier gas at the T-piece was initially studied because of its inherent simplicity. However, the Poiseuille models reveals that such a MDGC system can become limited by the natural back pressure established at the column union. As the natural back pressure at the column union is strongly linked to the restriction of carrier gas flow through ^{2}D, it appears that MDGC systems with narrow or long ^{2}D will be most affected.

By extending the role of the T-piece to remove (split) as well as add carrier gas at the union between the ^{1}D and ^{2}D columns, it is possible to avoid any physical restrictions imposed by the presence of a natural back pressure. Although the RTL-MDGC procedure presented in this study refers to a MDGC system with supplemented carrier gas, no basic changes are required if the MDGC system is extended to the case of removal of carrier gas at the union. Though a slightly different approach was employed to model such a MDGC system, the results were largely similar.

The work presented in this chapter will be extended to the practical investigation of application of RTL to GC×GC and tMDGC systems.

CHAPTER 6

APPLICATION OF RETENTION TIME LOCKING TO TARGETED MULTIDIMENSIONAL GAS CHROMATOGRAPHY

6.1 SUMMARY

Retention time locking (RTL) is a gas chromatographic technique that enables the analyst to precisely reproduce the retention times of a separation between different instruments, column i.d./length and detectors. For a "locked" separation, peak identifications determined using a retention time library are just as valuable as when retention indexes (RI) are employed. Application of RTL to both columns in a multidimensional gas chromatographic system (RTL-MDGC) can provide enhanced separations (MDGC advantage with a greater degree of reproducibility) and identification (RTL advantage) never achieved before. By supplementing the column flow with additional carrier gas at or near the coupling of the columns, RTL-MDGC was successfully achieved for both targeted MDGC (tMDGC) and comprehensive MDGC (GC×GC) systems.

6.2 INTRODUCTION

The fundamental unit of measurement for chromatography, the retention time, provides invaluable evidence for the identification of known or unknown chromatographic peaks. Unfortunately the retention time of a compound is dependent on many individual and unique factors which cause the unit to vary thus making peak identification difficult if not impossible. Changes in instrument conditions (temperature, pressure), differences in columns (length, internal diameter, film thickness), and routine maintenance (column trimming) can lead to significant changes in retention times. In fact, it would not be uncommon for two identical gas chromatographic systems with identical columns from the same supplier to deliver very different retention times.

One approach to overcome the inconsistencies of retention times is to apply reference peaks to an analysis. An unknown peak may be identified by its position with respect to one or two bracketing reference peaks. In 1958 Kováts introduced the retention index (RI) concept by demonstrating that under isothermal conditions the logarithm of the adjusted retention times for a homologues series would generate a uniform reference scale [122]. van den Dool and Kratz further extended the Kováts approach by demonstrating the use of linear temperature programmed retention indexes [135]. Exclusively dependent upon the chromatographic phenomenon, the retention index approach requires precise control of the experimental conditions to preserve the accuracy of the index data. Small differences in thermal/pneumatic control or between columns of different suppliers could lead to significant changes in retention index.

When a suitable retention index library is available the analyst has a 65% chance of identifying an unknown peak using retention indexes on a single stationary phase. This increases to approximately 80% for two columns of differing polarity, and above 90% for three columns [128]. When two or more columns of different stationary phase are employed the result becomes comparable to that of mass spectrometry (MS) which has a ≈90% chance of successfully identifying an unknown peak. This does however demand more time than MS as a separation must be run for every unique column employed. To achieve successful identification within the time frame of a single analysis many dual column systems have been developed [136-139]. Following

injection the flow would be split between the two differing columns and detected. In this manner two successful matches could be obtained from the one experiment. Regardless, in the presence of MS many analysts have come to believe that the retention index methodology is approaching obsolescence. There are however, specific areas of analysis such as essential oils and flavours that still heavily depend on RI for identification. Typically for such analysis RI are not used alone but complemented with MS to achieve an almost unequivocal identification.

Targeted multidimensional gas chromatography (tMDGC) also utilises two or more columns in a single analysis. Unlike a dual column system the two columns are coupled in series using a flow switching device. At specified times the switching device diverts targeted portions of the primary column separation to the secondary column for further separation, a process termed "heart-cutting". For the primary column, RI have been employed to determine the identity of unknown peaks and in some cases the calculation of heart-cutting times. A literature search reveals no evidence that an investigation has been carried out where RI have been determined for both the primary and secondary columns simultaneously. In the authors' opinion this is almost certainly due to difficulties in the introduction of a homologous series to the secondary column. A tMDGC separation process that can be successfully complemented with RI for both columns would provide enhanced separation capabilities with an identification success rate comparable to MS. One can imagine the potential of such a system if hyphenated with MS detection.

Comprehensive two dimensional gas chromatography (GC×GC) is similar to tMDGC in that two columns of differing stationary phase are coupled in series. However, rather than a flow switching device located between the two columns they are instead joined in succession. This interface via a device called a modulator located at or near the union of the two columns to repeatedly trap and reinject the primary separated compounds throughout the entire experiment. Following reinjection the secondary separation must be completed within the cycle time of the modulator (3-8 sec) hence, before another secondary separation commences. This means that the secondary column must remain short in length to allow for such a fast separation. The end product is many fast second column separations resulting from the reoccurring current fractionation of the primary column separation.

For the determination of RIs for both separations in a GC×GC experiment Western assumed that the temperature is effectively isothermal for the fast second column separation and constructed isovolatility curves for members of a homologous series [129, 130]. The isovolatility curves were used as reference map for the two dimensional separation space from where pseudo isothermal retention indexes could be determined. Bieri further extended the approach by employing dual secondary columns and solid phase micro extraction (SPME) injection [131]. By splitting the primary column flow between dual secondary columns of different phases two GC×GC chromatograms were generated from the one experiment. Three independent RIs were successfully obtained in the one experiment, one for the primary column and two for the dual secondary columns.

A major limitation of the technique is the non-constant space between neighbouring isovolatility curves. Towards the later stages of a separation the space between two neighbouring isovolatility curves is barely the width of a second column peak. Together with the length restriction of the second column the generation of two and possibly three independent RIs may not substantially increase the probability of a successful identification as expected. An investigation into capabilities of such an approach for the identification of unknown peaks would be of importance.

To overcome the inconsistencies of retention times is to employ the method translation technique between two mutually translatable methods [124, 140]. Method translation views the void time as a universal time unit of a separation process. The translation of a method is simply the scaling of the void time whilst stretching or compressing of the temperature program in time. By adopting method translation it is possible to reduce the analysis time, improve resolution, change carrier gas or outlet pressures (vacuum for MS) all while maintaining a scaled peak elution pattern. Using method translation it is possible to maintain the elution order between two mutually translatable methods with no change in speed and hence retention time lock (RTL) the two methods. Therefore, two mutually translatable methods can be RTL when equal void times are obtained using identical temperature programs. With modern state of the art pneumatic and temperature control capabilities, precise adjustment in the void time of a method can be easily achieved by appropriate adjustment of the column

head pressure whilst the oven temperature program remains identical for all methods [126].

RTL relies upon reproduction of precise chromatograms to within hundredths of a minute when applying the same method from one GC to another [141, 142]. With such precision and reproducibility the retention time of any eluting compound now becomes a very powerful asset to support the identification of unknown peaks. Even between different detectors such as MS, NPD, FID, and AED, RTL still maintains strict control over retention times [143]. RTL has been successfully used to develop unified separations for the analysis of pollutants, [144, 145] drugs, [146-148] pesticides [149-153] and petroleum products [154].

Using RTL and an adequate "locked" library, a locked retention time now provides the same level of identification as RIs. The RI approach references the resulting separations, while method translation with RTL goes beyond this by providing identical chromatograms between instruments with different carrier gases or detectors, therefore, removing the need for any reference. Essentially RTL and RI are two very different approaches to achieve the same objective. Therefore, as with RI, peak identifications using locked retention times can only be considered significant when successful matches are obtained on two or more columns of different polarity. When two matches are obtained using locked retention times then the probability of a successful identification would be analogous to that provided by MS detection.

The ability to RTL all columns in a multidimensional GC system such as tMDGC/GC×GC would be highly advantageous. Such a technique if possible would avoid the difficulties and limitations of RIs for multidimensional GC systems whilst still delivering an enhanced level of identification comparable to MS. The application of RTL to multidimensional gas chromatography (RTL-MDGC) is not a novel concept [155]. By providing a supplementary gas supply to the outlet of a GC×GC column set Shellie adjusted the pressure drop for a separation and generated matched retention times between experiments utilising time-of-flight MS and flame ionisation detection [132]. Although successful, this approach can only translate and lock methods that differ in inlet and outlet pressures and does not independently adjust the pressure drop for both columns. As a consequence, the full capabilities of method

translation and RTL could not be obtained. By providing a supplementary carrier gas supply at, or close to the union of the primary and secondary columns it is possible to independently control the pressure drop of both the primary and secondary columns. This Chapter will discuss the investigation of such an approach towards the development of method translation and RTL for multidimensional gas chromatography.

6.3 EXPERIMENTAL

6.3.1 Gas Chromatography System

All analyses were performed using an Agilent Technologies 6890 model gas chromatograph equipped with two flame ionization detectors (FID 1 and 2) (detector rate 100 Hz), 7683 series auto sampler, two electronic pressure control modules (EPC) and two split/splitless inlets. The GC system was retrofitted with an Everest model longitudinally modulated cryogenic system (LMCS, Chromatography Concepts, Doncaster, Australia) and a pneumatic Deans switching system (model G2855B, Agilent Technologies, Burwood, Australia). The entire system was controlled using GC Chemstation software (revision A.09.01) by Agilent Technologies.

6.3.2 Separation Columns

The MDGC column set comprised of a ^{1}D fused silica capillary column of 95% methyl–5% phenyl polysilphenylene-siloxane (BPX5) phase (0.25 µm df) with dimensions 30 m × 0.25 mm i.d., a ^{2}D separation column of polyethylene glycol (BP20) phase (0.10 µm df) with dimensions 5 m × 0.10 mm i.d. and a Uncoated Tubing (UT) line of deactivated capillary tubing (5 m × 0.10 mm). The ^{1}D column was positioned between the injector and the Deans switch with the ^{2}D and UT columns located between the Deans switch and their corresponding FID. All columns were sourced from SGE International (Ringwood, Australia). An illustration of the chromatographic system with column installations is provided in a previous study [156].

6.3.3 System Settings

Unless specified elsewhere the following GC system settings were employed throughout this chapter.

Oven temperature	130 ˚C
Injector temperature	250 ˚C
Detector Temperature	300 ˚C
Injection Volume	1µl
Pneumatic Control	Constant pressure

6.3.4 The Pneumatic Deans Switch

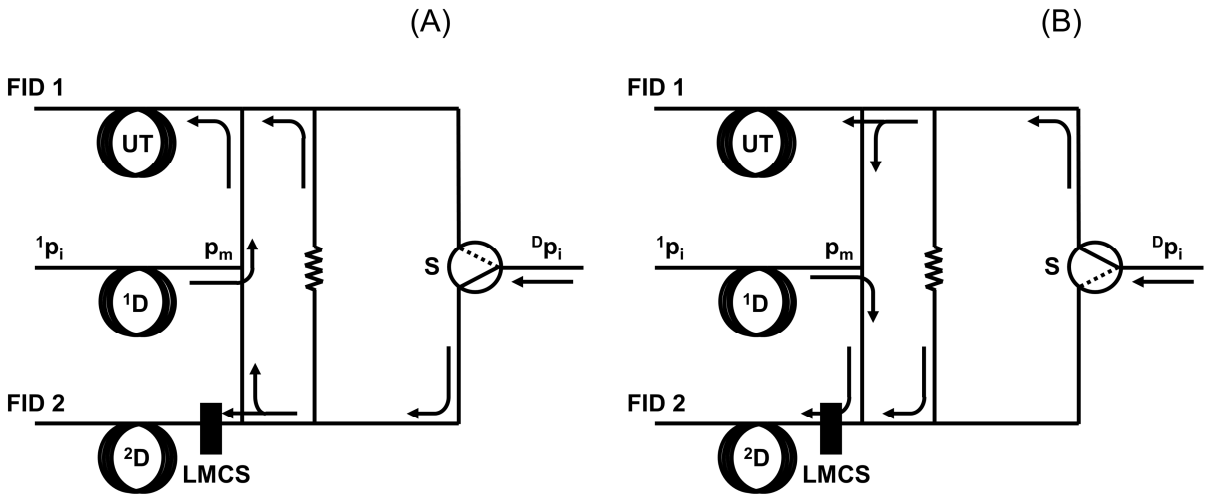

Figure 6.1 The inner workings of a pneumatic Deans Switch by Agilent Technologies. The exiting ^1D eluent can be transferred between the UT in position (A) for monitoring the ^1D or the ^2D in position (B) for transferring heart-cuts for further separation.

Figure 6.1 depicts the Deans switch with the capillary column and auxiliary carrier gas flow connections in both the monitoring and heart-cutting positions. The position of the DS is determined by a switch (S) that controls the direction of the ^Dp_i flow through the DS. The eluent exiting the ^1D is swept by the ^Dp_i flow and guided to the intended path (UT or ^2D). Due to the arrangement of the columns in **Figure 6.1** the ^1D outlet pressure (^1p_o), UT inlet pressure (^Up_i), ^2D inlet pressure (^Dp_i) and the DS outlet pressure (^Dp_o) all converge to the same physical point with the same pressure referred to as the mid-point pressure (p_m).

6.3.5 Samples

Heptanol >99.8% (Sigma & Aldrich) was diluted with hexane (Merck) to achieve a final concentration of 50 ppm. 2 ml GC vials were purged with methane (Sigma & Aldrich) and capped.

6.4 RESULTS AND DISCUSSION

6.4.1 Deans Switch as a Supplementary Source of Carrier Gas

The theoretical Poiseuille models in Chapter 5 suggest that RTL can be achieved for a MDGC system by making precise adjustments in p_m. In practice, the simplest and most effective way of adjusting p_m is by the addition and removal (if required) of carrier gas at the union between the ^{1}D and ^{2}D. This can be achieved by installing a T piece type device at or near the union of the ^{1}D and ^{2}D capillary columns of a MDGC system, thus allowing the ^{1}D eluent to be supplemented or split. Conveniently, there is such a MDGC device that does just this but for an entirely different purpose. Called a Deans switch, it is used to transfer select/targeted portions of a primary separation between two secondary separations (termed heart-cutting).

To successfully install and operate a Deans type switch the user must determine the correct pressure that is to be provided at the $^D p_i$. It is the $^D p_i$ pressure that provides the flow that meets the exiting ^{1}D eluent and guides it to the desired path. Therefore the $^D p_i$ pressure must provide the p_m with a pressure that equals the ^{1}D outlet pressure provided by the $^1 p_i$. To determine the appropriate switching $^D p_i$ pressure to be applied the user would inject a simple sample (typically methane) onto the ^{1}D and would adjust the $^D p_i$ to the point where the peak/s could only be recorded on only one of the two possible paths. This process of pressure tuning a DS is illustrated in

Figure 6.2 plots the resulting peak area from a series of heptanol injections against the $^D p_i$ as it is adjusted from 50 to 56 psig. Throughout the pressure tuning exercise the Deans switch is held in position (B) (see **Figure 6.1**), where the ^{1}D eluent is being swept towards the UT and FID 2.

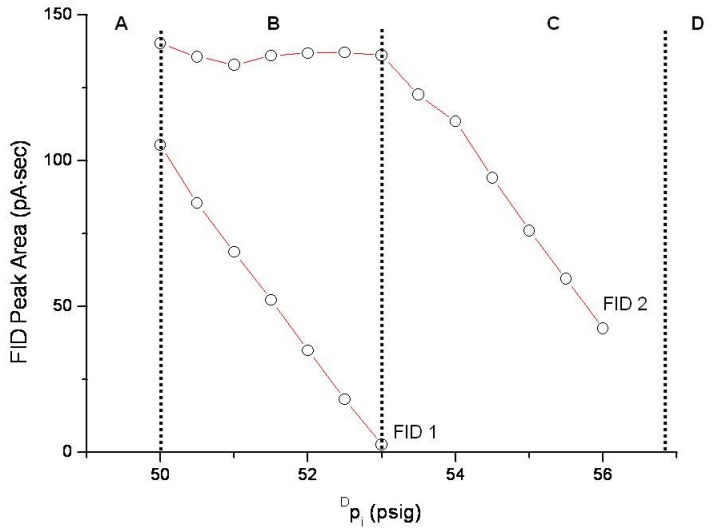

Figure 6.2 The Deans switch was held in position (B) from **Figure 6.1** and the $^{D}p_i$ increased as injections of heptanol (100 ppm) were made.

Figure 6.2 has been divided into four different sections denoted as A, B, C, and D. In section A, the $^{D}p_i$ is > 50 psig and does not generate enough pressure at the p_m to have any great affect on the ^{1}D eluent. Instead the ^{1}D eluent provides the dominant pressure and simply splits at the Deans switch interface yielding heptanol peaks on both FID 1 and FID 2. For section B, the $^{D}p_i$ is increased from 50 to 53 psig and begins to impact the p_m. As the $^{D}p_i$ is increased, so too is the resulting pressure at the p_m which meets the ^{1}D eluent. This results in a gradual decrease in the heptanol peak area being seen on FID 1 while the heptanol peak area seen on FID 2 remains relatively constant. Effectively, as the $^{D}p_i$ was increased and in turn increased the p_m, the split of the ^{1}D eluent seen in section A has been lowered. It is interesting to note that as the $^{D}p_i$ is increased, the heptanol peak area decreases from FID 1, but does not increase in FID 2. A possible explanation for this is that the increase in p_m does in fact increase the $^{1}p_o$ and the restriction to flow of the ^{1}D i.e. decreased pressure drop. It appears that as the experiments are being performed with a split inlet, the increased resistance to flow through the column is not accounted for by the GC system and causes the inlet split ratio to climb accordingly.

It is at 53 psig, the border between section B and C, that the split no longer exists and 100% of the heptanol peak is transferred to FID 2. Here, the p_m has been increased to such an extent that it equals the pressure of the inbound ^{1}D eluent and guides it to the ^{2}D and FID 2. At this point the $^D p_i$ carrier flow can be envisioned as a pseudo barrier to the ^{1}D eluent, blocking the path from which it travelled. In section C the $^D p_i$ has been increased beyond 53 psig and continues to increase the p_m and the resistance to flow through the ^{1}D. As with the heptanol peak area detected by FID 1 in section B, the heptanol peak area detected by FID 2 is gradually decreasing at an identical rate. The loss of heptanol peak area between FID 1 and 2 at the same rate over sections B and C is further evidence that the inlet split ratio is the cause. If the $^D p_i$ is pushed beyond 57 psig into section D of the p_m has increased to such an extent that it has become greater than the $^1 p_i$. This has ultimately caused the pressure drop from the $^1 p_i$ to the p_m to become negative and bring about a reversal in the direction of flow. Any sample being injected under these conditions would not enter the capillary column but be swept away out the inlet split vent i.e. a 100% inlet split ratio. Such a situation is commonly referred to as back flushing and is used in practice to prolong instrument maintenance and to preserve costly capillary columns.

For the sole purpose of heart-cutting, any $^D p_i$ value within the section C pressure range will ensure a 100% transfer of the ^{1}D eluent to either the UT or ^{2}D. It is commonly thought that it is best to operate a Deans switch at the $^D p_i$ marked by the boundary of section B and C to maximise the amount of sample entering the ^{1}D and hence the signal to noise ratio. However, it is actually far better to operate at a $^D p_i$ in the middle of section C, as this accounts for any slight difference in the resistance to flow between the UT and ^{2}D. If the UT and ^{2}D are not precisely pressure balanced (which is most likely) then the $^D p_i$ pressure boundary between sections B and C will differ slightly between positions (a) and (b) in **Figure 6.1**. This can be overcome by simply operating the $^D p_i$ in the middle of section C and adjusting the inlet split ratio to account for any losses of sample.

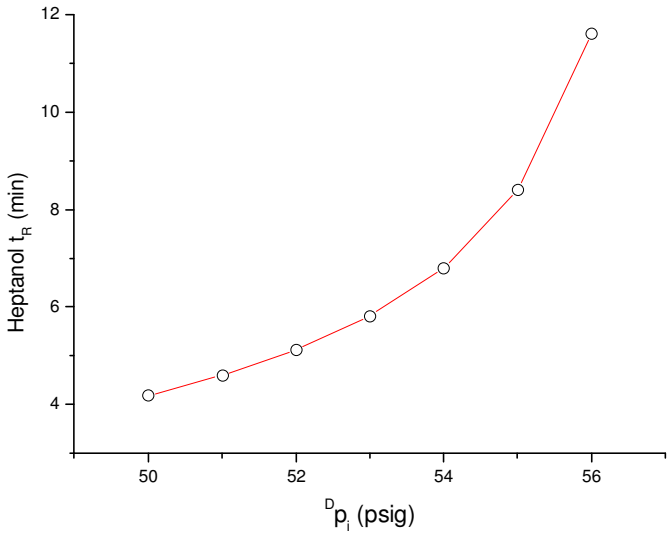

Figure 6.3 The $^{D}p_i$ is plotted against the retention time of heptanol to reveal a familiar relationship modelled in Chapter 4. This confirms that a Deans switch can act as a supplementary source of carrier gas at the union of the ^{1}D and ^{2}D.

Figure 6.3 illustrates the same set of experiments depicted in

Figure 6.2 but instead, the $^{D}p_i$ is plotted against the heptanol retention time. The relationship between the $^{D}p_i$ and the heptanol t_R appears to be very similar to the Poiseuille models studied in Chapter 4. This suggests that a DS can act as a supplementary source of carrier gas between the ^{1}D and ^{2}D columns like that described in the RTL-MDGC procedure in Chapter 4. An interesting point to note is that if by chance the $^{D}p_i$ required to lock the system falls within section C of

Figure 6.2, than the Deans switch should be able to perform both heart-cutting and RTL simultaneously.

The RTL-MDGC approach defined in Chapter 4 requires a device that can supplement and remove carrier gas at the ^{1}D and ^{2}D union of a MDGC system. By supplementing or removing carrier gas at the ^{1}D and ^{2}D union, the p_m will change and so to the pressure drop across the ^{1}D and ^{2}D. However, for the tMDGC system employed here the removal of carrier gas is not required, as the problem of a high ^{2}D natural back pressure (as discussed in Chapter 4), is not a concern. For a tMDGC

system a short narrow ^{2}D column is not essential and a wider, longer column with a much smaller back pressure can be used.

Figure 6.2 and **Figure 6.3** suggest that the DS is more than capable of supplementing the ^{1}D and ^{2}D union with additional carrier gas and even has the potential of performing its intended heart-cutting role while RTL.

6.4.2 Obtaining the ^{1}D Retention Times

Each heptanol $^{1}t_R$ in **Figure 6.3** is not the actual $^{1}t_R$ but the accumulation of two individual heptanol retention times from both the ^{1}D and ^{2}D. This is because the tMDGC system employed for this study has no means to directly measure a peak as it leaves the ^{1}D. As discussed above when the p_m changes *via* the $^{D}p_i$ in **Figure 6.3**, it not only alters the $^{1}\bar{u}$ but also the $^{2}\bar{u}$. Therefore, the curve in **Figure 6.3** represents the sum of the $^{1}t_R$ and $^{2}t_R$ rather than just the $^{1}t_R$ itself.

Ideally, for a pneumatic/retention curve that is to be used for RTL, the true $^{1}t_R$ must be used rather than the sum of the $^{1}t_R$ and $^{2}t_R$. If the $^{1}t_R$ and $^{2}t_R$ sum is used instead of the $^{1}t_R$ then the determination of the $^{1}p_i$ $^{D}p_i$ relationship for a constant $^{1}t_R$ will be askew. To overcome this it is assumed that the effect the ^{2}D has on the heptanol retention times in **Figure 6.3** is minimal due to its smaller length and internal diameter when compared to the ^{1}D. Differences in the $^{1}t_R$ caused by an increase in p_m *via* the $^{D}p_i$ will be in the order of minutes while differences in the $^{2}t_R$ will be in the order of seconds. Therefore, the $^{1}p_i$ $^{D}p_i$ relationship for a constant $^{1}t_R$ may be askew, but it should not amount to much in the scheme of the experiment and will remain within acceptable tolerances.

To minimise the effect of using the sum of the $^{1}t_R$ and $^{2}t_R$ instead of the $^{1}t_R$ and to keep the experimental time small, methane was used as the reference compound on the ^{1}D. Any difference in the $^{2}\bar{u}$ will be enhanced if the reference compound exhibits any retention.

6.4.3 Obtaining the ^{2}D Retention Times

Obtaining the $^{2}t_R$ is a much easier affair in comparison to the $^{1}t_R$. A cryogenic trapping and reinjection device called an LMCS is positioned at the front of the ^{2}D. By

reinjecting the ^{2}D reference peak at a defined time the ^2t_R can be easily deduced by subtracting the time of reinjection from the sum of the ^1t_R and ^2t_R.

For the ^{2}D, heptanol was chosen as the reference compound as it can be easily trapped and reinjected using an LMCS. Methane could not be used as a suitable reference compound for the ^{2}D reference compound as the LMCS trap would not trap it.

6.4.4 Locking the ^{1}D

Ideally, in a "real world" scenario a user would be locking the reference compounds to a set of "standard retention times" for the ^{1}D and ^{2}D. The "standard retention times" would be the result of an optimised method that has been used to create a RTL-MDGC library that the user wishes to utilise. As no such RTL library exists, retention times of 2.00 (^{1}D) and 0.08 min (^{2}D) will be viewed as the standard retention times for the reference compounds methane and heptanol respectfully. These target retention times of methane and heptanol were chosen for no apparent reason except that they were reasonable targets. As with single column RTL, initial pressure settings are required as a reference point to vary from. Normally these values would be provided with the tMDGC system and method settings used to generate a RTL library. Instead values of 63.00 and 55.50 psi were chosen as the p_i and p_m respectfully. The initial pressure settings were selected as they resulted in realistic differences that were to be expected in the retention times of methane and heptanol compared to the standard retention times.

Using the pressures stated above as a starting point, p_i (63.00 psi) was adjusted by 20%, 10%, 0%, -10% and -20%. At each adjustment, p_i was held constant while p_m (55.5 psi) was adjusted by the corresponding percentage increase or decrease in p_i and varied by increments of -2.0, -1.0, 0.0, 0.5, 1.0, 1.5, 2.0 and 2.5 psi. **Table 6.1** displays the calculated p_i and p_m values to be employed. For each pairing of p_i and p_m in **Table 6.1**, an injection of methane was made and recorded on the UT FID. As explained previously and illustrated in **Figure 6.3** the adjustment of p_m influences the pressure drop across the ^{1}D which in turn affects the $^1\bar{u}$ and peak elution. An increase in p_m with respect to p_i would increase the ^{1}D column outlet pressure and lessen the pressure drop across the ^{1}D. This would cause a slowing of the $^1\bar{u}$ and an increase to the ^1t_R, and vice versa. **Figure 6.4** illustrates the effect on the ^1t_R of methane measured

at the end of the UT, as p_m is increased against a constant p_i. The results are displayed as five data sets in **Figure 6.4**, one data set for each of the values of p_i in **Table 6.1**.

Table 6.1 $^{1}p_i$ and $^{D}p_i$ pressure coordinates (psig) used to generate poly-pneumatic curves. Methane was injected and used to define the void time of ^{1}D ($^{1}t_m$). * denotes the original values of $^{1}p_i$ and $^{D}p_i$.

$^{1}p_i$	**20%**	**10%**	**0%**	**-10%**	**-20%**
	75.60	69.30	*63.00	56.70	50.40
$^{D}p_i$	**20%**	**15%**	**0%**	**5%**	**10%**
-2.0	67.1	61.4	55.6	49.8	44.1
-1.0	68.1	62.4	56.6	50.8	45.1
0.0	69.1	63.4	*57.6	51.8	46.1
0.5	69.6	63.9	58.1	52.3	46.6
1.0	70.1	64.4	58.6	52.8	47.1
1.5	70.6	64.9	59.1	53.3	47.6
2.0	71.1	65.4	59.6	53.8	48.1
2.5	71.6	65.9	60.1	54.3	48.6

Using LAB Fit (Paraiba, Brazil, Version 7.2.29) a modified Bleasdale equation (**Equation 6.1**) was found to be a suitable model for each of the five data sets in Figure 4.

$$^{1}t_R = \left(A + B \times \sqrt{^{D}p_i}\right)^{C}$$

Equation 6.1

Through **Equation 6.1**, lines of best fit were determined for all five data sets and superimposed over the data in **Figure 6.1**. For each of the five lines of best fit, the variables A, B and C and there corresponding R^2 value were calculated using the LAB Fit software and displayed in **Table 6.2**. With all R^2 values greater than 0.9999, this approach using **Equation 6.1** proved to be very successful in modelling the results in **Figure 6.4**. To simplify future discussion, the curves generated in **Figure 6.4** will be referred to as pneumatic curves from here forth.

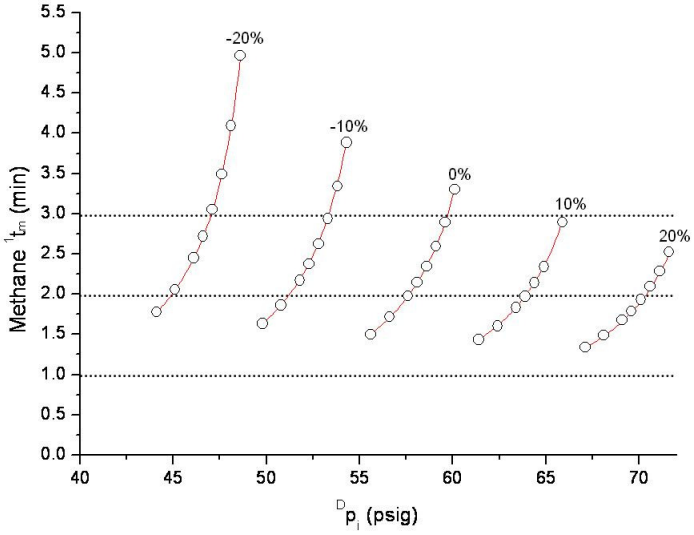

Figure 6.4 Poly-pneumatic curves for 20%, 10%, 0%, -10% and -20% adjustments of the reference p_i value.

Table 6.2 The modified Bleasdale equation used to map the pneumatic curves has 3 constants denoted A, B and C. The values of the constants and the resulting R^2 value were determined using LAB Fit (Version 7.2.29) for each of the pneumatic curves at 20%, 10%, 0%, -10% and -20% of the original p_i setting.

Initial p_i %	**p_i**	**A**	**B**	**C**	**R^2**
20 %	50.40	7.674	-1.079	-0.8471	0.9999
10 %	56.70	8.700	-1.154	-0.8411	0.9999
0 %	63.00	9.949	-1.250	-0.8833	0.9999
-10 %	69.30	10.940	-1.313	-0.8439	0.9999
-20 %	75.60	12.17	-1.400	-0.8092	0.9999

Using **Equation 6.1** and the constants presented in **Table 6.2**, the $^D p_i$ can be calculated for any given value of ^1t_m. It is therefore possible to solve each of the five pneumatic curves for a constant ^1t_R and examine the relationship of ^1p_i and $^D p_i$ for a constant ^1t_m. **Figure 6.5** depicts the ^1p_i and $^D p_i$ coordinates calculated when each of the five pneumatic curves are solved with a constant ^1t_R of 1.0, 2.0 and 3.0 min. Due to the observed linear nature of the 3 curves of constant ^1t_m in **Figure 6.5**, a straight line model (**Equation 6.2**) was fit to the data using Microsoft Excel (2003).

$$^{1}p_i = M \times {}^{D}p_i + C$$

Equation 6.2

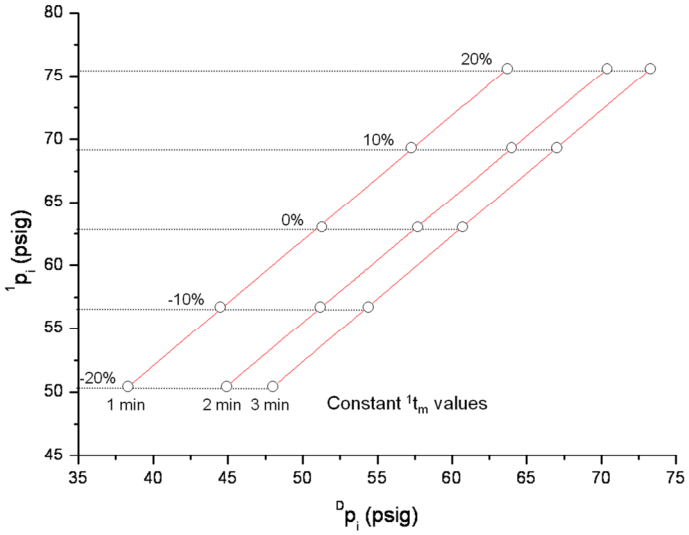

Figure 6.5 $^{D}p_i$ values calculated for 20%, 10%, 0%, -10% and -20% adjustments of the reference p_i to deliver a $^{1}t_m$ of 1.0, 2.0 and 3.0 min.

Table 6.3 contains the corresponding constants M and C and the R^2 values for each of the three fitted lines of constant $^{1}t_m$. With R^2 values greater than 0.999 for all three lines, the relationship of $^{1}p_i$ and $^{D}p_i$ for a constant value of $^{1}t_m$ is undoubtedly linear. Denoted as M in Equation 2, the slope of the all three straight lines for constant $^{1}t_m$ are identical to two decimal places and are thus parallel to one another. In fact, all that differs between the three lines in **Figure 6.5** is their interception of the $^{1}p_i$ axis. This implies that in maintaining a constant $^{1}t_m$, $^{1}p_i$ and $^{D}p_i$ are linearly related with a constant gradient for all values of $^{1}t_R$. Therefore, only two pneumatic curves are required to generate any straight line of constant $^{1}t_R$. Two pneumatic curves will result in two $^{1}p_i$ and $^{D}p_i$ coordinates that can be used to determine the gradient. Being that the gradient is constant for any $^{1}t_R$, once it is determined it can be applied to any $^{1}p_i$ and $^{D}p_i$ coordinates on **Figure 6.5** and extrapolated.

Table 6.3 The relationship of the $^{1}p_i$ and $^{D}p_i$ for a constant $^{1}t_m$ results in a straight line curve. Microsoft Excel was used to derive the constants M and C for a line of best fit and its corresponding R^2 value.

Const. $^{1}t_R$ (min)	M	C	R^2
1.00	0.991	12.482	0.9998
2.00	0.990	5.911	1.0000
3.00	0.994	3.654	1.0000

Table 6.4 contains the $^{1}p_i$ and $^{D}p_i$ values calculated from the five pneumatic curves for a constant $^{1}t_m$ of 2.00 min. For each $^{1}p_i$ and $^{D}p_i$ pair, an injection of methane was performed and transferred to the UT (DS position A) following elution from the ^{1}D. Column (A) in **Figure 6.6** depicts the results and shows the successful locking of the ^{1}D at 2.00 min. For all five experiments, the methane peak eluted within ±0.05 of 2.00 min showing both precision and accuracy in the technique.

Column (B) in **Figure 6.6** mirrors the same experiment described in column (A), apart from methane being substituted for heptanol. The experiments in column (B) were conducted to determine the $^{1}t_R$ of heptanol for the impending heart-cut of the heptanol peak to the ^{2}D. However, rather than a consistent heptanol $^{1}t_R$ as seen with methane, the precision over the five experiments is greatly reduced. This is because the eluting peaks are not detected at the point which additional carrier gas is provided i.e. at the end of the ^{1}D. To truly lock a column one must alter the pressure drop across the whole column from injection to detection. In the study presented here, peaks eluting from the ^{1}D are not detected directly at the DS but are passed to a length of uncoated tubing (UT) to be detected. The actual ^{1}D length is therefore a combination of the ^{1}D and the UT which cannot be successfully locked by precise pressure adjustments between the ^{1}D inlet and DS as presented here. Methane was successfully locked at 2.00 min for a number of calculated $^{1}p_i$ and $^{D}p_i$ combinations as seen in **Figure 6.6** (A), though this was only achieved since the ^{1}D target compound was in fact methane and the models generated in **Figure 6.4** are all based on its elution through the ^{1}D and UT. Therefore, the calculated ^{1}pi and $^{D}p_i$ combinations account for any such variance in the target compound (methane) $^{1}t_m$ that was introduced by the displacement of the ^{1}D pressure outlet control and detection. For compounds of differing retention to methane, precise locking cannot be achieved for

the $^{1}p_i$ and $^{D}p_i$ combinations in **Table 6.4**. **Figure 6.6** (B) shows the inability to precisely lock heptanol on the ^{1}D for the $^{1}p_i$ and $^{D}p_i$ combinations determined from the models in **Figure 6.4**. Over the five experiments the heptanol $^{1}t_R$ is seen to vary between 2.55 to 2.65 min, a total range of 0.1 min. It is expected that the extent of the $^{1}t_R$ variance will change with the retention of an eluting compound. The longer a compound spends in the ^{1}D column the greater is its $^{1}t_R$ variance when employing the calculated $^{1}p_i$ and $^{D}p_i$ values of constant $^{1}t_R$ retention and *vice versa*.

Table 6.4 The $^{1}p_i$ and $^{D}p_i$ values that result in a constant methane $^{1}t_m$ of 2.00 min and the corresponding heptanol $^{2}t_R$ values following heart-cutting, trapping and reinjection on the ^{2}D. The $^{2}t_R$ total time represents the ^{2}D elution of heptanol from initial injection while the $^{2}t_R$ is from the ^{2}D reinjection at 3.00 min.

Initial $^{1}p_i$ %	$^{1}p_i$ (psig)	$^{D}p_i$ (psig)	$^{2}t_R$ total (min)	$^{2}t_R$ (min)
-50%*	31.50	25.8	3.169	0.169
-40%*	37.80	32.2	3.126	0.126
-30%*	44.10	38.6	3.102	0.102
-20%	50.40	44.9	3.085	0.085
-10%	56.70	51.3	3.074	0.074
0%	63.00	57.6	3.067	0.067
10%	69.30	64.0	3.062	0.062
20%	75.60	70.4	3.058	0.058
30%*	81.90	76.7	3.052	0.052
40%*	88.20	83.1	3.048	0.048
50%*	94.50	89.4	3.046	0.046

* Values of $^{1}p_i$ and $^{D}p_i$ were calculated by extrapolating the line of best fit.

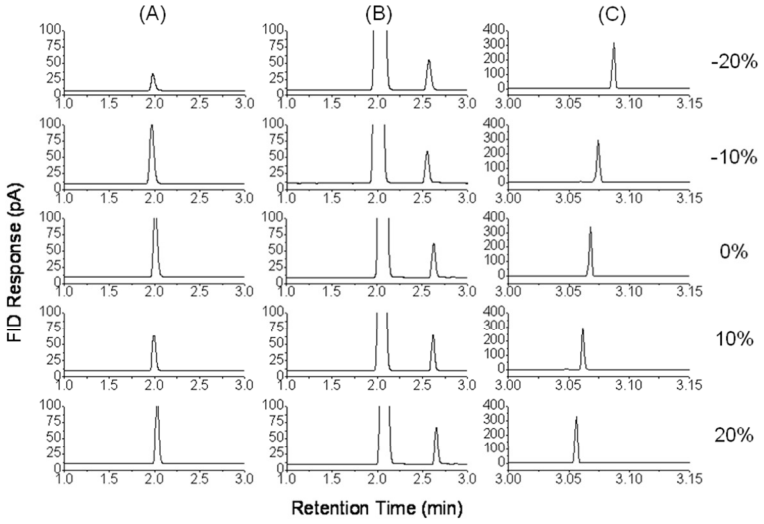

Figure 6.6 ^{2}D poly-pneumatic curve for the elution of heptanol for all $^{1}p_i$ and $^{D}p_i$ values that deliver a $^{1}t_m$ of 2.00 min.

Ideally one would prefer to detect eluting compounds directly at the point where the ^{1}D outlet pressure is adjusted (p_m) but this was not possible due to the installation requirements of the DS. One approach would be to calculate the void time of the UT for all experiments used to derive the pneumatic retention curves in **Figure 6.4** and subtract it from its corresponding experimental $^{1}t_m$. Assuming that the UT tubing does not retain the target compound this would provide a simple solution to determine the time at which the target compound reaches the p_m i.e. the DS. A GC×GC experiment may be exempt from such problems as the ^{1}D separation window is actually reconstructed by the aligning of the many ^{2}D separations in series at their respective ^{2}D separation start time. It would be highly unlikely that such small changes in the actual $^{1}t_R$ would result in any change at all for the reconstructed GC×GC $^{1}t_R$. Though some refinement is required, the results suggest that the approach taken in this study to independently retention time lock the ^{1}D in a tMDGC system is sound. Discussion hereafter will assume the approach undertaken in this study has achieved the absolute locking of the ^{1}D for all eluting compounds.

6.4.5 Locking the ^{2}D

Figure 6.5 illustrates that as $^{1}p_i$ is increased from -20% (50.40 psig) to 20% (75.60 psig) of its original setting (63.00 psig), the $^{D}p_i$ is altered in concert to maintain a constant average linear velocity across the ^{1}D and hence a constant $^{1}t_m$. As discussed

previously the $^{D}p_i$ pressure plays a dual role, where it not only provides restriction to the column outlet of the ^{1}D but also head pressure to the ^{2}D. So as the $^{1}p_i$ and $^{D}p_i$ move in unison to maintain a constant ^{1}D average linear velocity, the head pressure of the ^{2}D shall be inadvertently altered. In this manner the locking of the ^{2}D is now somewhat comparable to the locking of a single capillary column. Except that both the $^{1}p_i$ and $^{D}p_i$ are interrelated by **Equation 6.2** and move in unison to maintain a constant $^{1}t_m$ and make precise adjustments to the ^{2}D head pressure.

Table 6.5 The DS and LMCS were operated at precise times to successfully heart-cut, trap and reinject the heptanol peak.

Time (min)	Device	ON/OFF	Action
2.50	Deans Switch	ON	Begin heart-cut from ^{1}D to ^{2}D
2.80	Deans Switch	OFF	End heart-cut from ^{1}D to ^{2}D
3.00	LMCS	ON	LMCS re-injects the heart-cut on the ^{2}D
3.20	LMCS	OFF	LMCS returns to its trapping position

From **Figure 6.6** (B) it was determined that heptanol had a $^{1}t_R$ (^{1}D to UT) of 2.55 to 2.65 min. For the complete transfer of the eluting heptanol peak from the ^{1}D to the ^{2}D with precise reinjection the DS and LMCS were operated at the times listed in **Table 6.5**. A heart-cut between 2.50 – 2.80 min proved to envelop all of the heptanol peaks as they eluted from the ^{1}D and transfer them to the ^{2}D. Once transferred the heptanol peak then becomes cryogenically trapped by the LMCS at the front of the ^{2}D and is rapidly reinjected at precisely 3.00 min. **Figure 6.7** shows an example employing the event times listed in **Table 6.5** with the ^{1}D heptanol elution (A), the complete heptanol heart-cut to the ^{2}D (B) and the precise ^{2}D reinjection (C). **Figure 6.6** (C) illustrates the resulting ^{2}D chromatograms for the experiments at -20%, -10%, 0%, 10% and 20% of the initial $^{1}p_i$ starting point with the $^{D}p_i$ adjusted to deliver a constant methane $^{1}t_R$ of 2.00 min. As the $^{D}p_i$ was altered in unison with the $^{1}p_i$ for each of the five separations the $^{2}t_R$ of heptanol went from 0.085 to 0.058 min, a range 0.027 min (1.62 sec). Although, this range includes the locked ^{2}D target time of 0.08 min, it was hoped that the heptanol $^{2}t_R$ range was larger thus allowing for more flexibility in potential locking times.

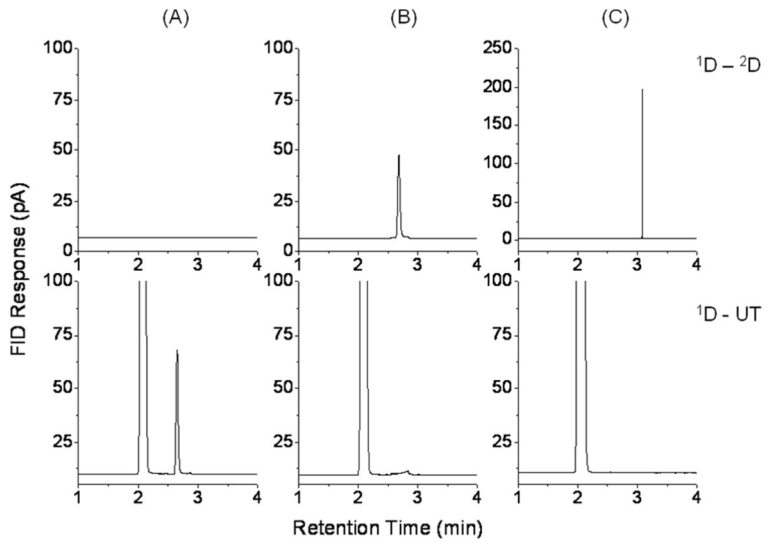

Figure 6.7 The successful heart-cut, cryofocusing and rapid reinjection of heptanol while the ^1t_m is locked at 2.0 min.

To further extend the heptanol ^2t_R window and widen the potential locking range, six more experiments were carried out at -50, -40, -30, 30, 40, and 50% of the initial ^1p_i. To maintain a methane ^1t_m of 2.00 min, the corresponding ^Dp_i values for the six injections were calculated by extrapolating the straight line of $^1t_R = 2.00$ min pictured in **Figure 6.5** and noted in

Table 6.3. For all 11 experiments the ^1p_i and ^Dp_i combinations the resulting ^2t_R times are listed in **Table 6.4**. It is observed that decreasing the ^Dp_i has a more profound effect in widening the heptanol ^2t_R locking range than by increasing the ^Dp_i. By increasing the ^1p_i to 50% of its original value the heptanol ^2t_R locking range gained 0.012 min (0.72 sec), compared to 0.085 min (5.1 sec) when decreasing the ^1p_i to -50% of its original value. The cause of this effect lies in the use of a ^2D of smaller internal diameter than the ^1D. The narrow ^2D column restricts the carrier flow and thus generates a high velocity. Because the velocity of the ^2D is naturally fast, any increases in ^Dp_i to speed the velocity and shorten the ^2t_R have little effect. A ^2D column of greater length or larger internal diameter would reduce the ^2D velocity and potentially allow for a greater ^2t_R range. It is predicted that this phenomenon will pose a more serious problem for the application of RTL to GC×GC where short narrow bore columns are commonly used for the ^2D.

The original 5 and additional 6 data points used to further extend the $^{2}t_{R}$ locking range are plotted together in **Figure 6.8** with a superimposed line of best fit derived using LAB Fit (Version 7.2.29). An inverse straight line equation (shown below) proved to be a successful match for the data with an R^2 value greater than 0.999. The determined constants A, B and C for the line of best fit are noted in **Table 6.6**.

$$^{2}t_{R} = \frac{1}{\left(A \times {}^{D}p_{i} + B\right)} + C$$

Equation 6.3

Superimposed over the data in **Figure 6.8**, the line of best fit provides a means to calculate and predict the relationship between $^{D}p_{i}$ and the heptanol $^{2}t_{R}$. Rearranging **Equation 6.3** to express $^{D}p_{i}$ as function of $^{2}t_{R}$ allows for the determination of $^{D}p_{i}$ for any specified $^{2}t_{R}$. It is therefore possible to precisely adjust the heptanol $^{2}t_{R}$ between 0.046 min (2.76 sec) and 0.170 min (10.2 sec), a range of 0.124 min (7.44 sec). The ability to adjust the heptanol $^{2}t_{R}$ within a range of 7.44 sec may not appear to be substantial, but when considering that the ^{2}D is a high resolution fast GC capillary column of only 5 meters in length with an internal diameter of 0.1 mm, 7.44 sec is a very generous window of time to lock within.

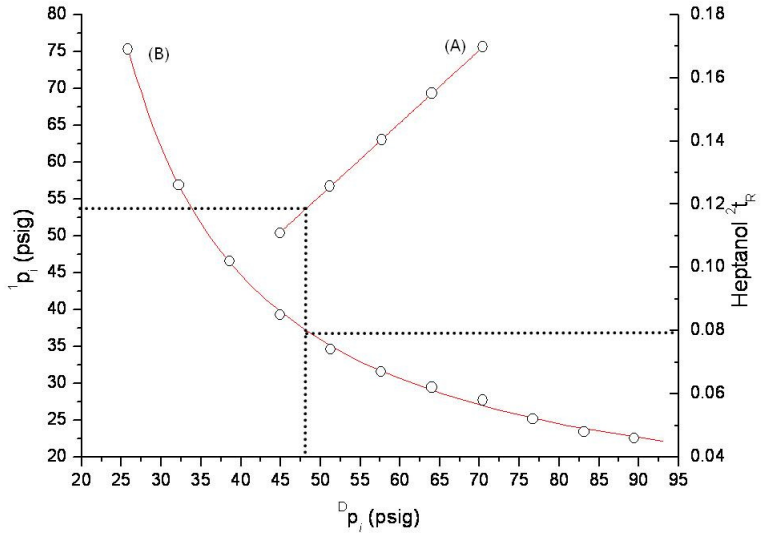

Figure 6.8 Line (A) is the pi and pm relationship for a constant 1tm of 2.00 min as found in **Figure 6.5**. Line (B) is the corresponding 2D poly-pneumatic curve of heptanol following heart-cut and reinjection.

The dotted lines in **Figure 6.8** clearly illustrate the procedure undertaken to determine the $^{1}p_i$ and $^{D}p_i$ values required to independently lock the tMDGC system at 2.00 and 0.08 min for the $^{1}t_m$ and $^{2}t_R$ respectively. Curve (A) represents the $^{1}p_i$ and $^{D}p_i$ relationship required to deliver a constant $^{1}t_m$ of 2.00 min, while curve (B) is the resulting $^{2}t_R$ of heptanol for the $^{1}p_i$ and $^{D}p_i$ coordinates of curve (A). To calculate the $^{1}p_i$ and $^{D}p_i$ values required to independently lock the tMDGC system at 2.00 and 0.08 min respectively, curves (A) and (B) must be solved simultaneously for a common value of $^{D}p_i$. Using **Equation 6.3**, it is determined that a $^{D}p_i$ pressure of 48.20 psig is required to generate a heptanol $^{2}t_R$ of 0.08 min. Substituting the $^{D}p_i$ value of 48.20 psig into **Equation 6.2** and solving for $^{1}p_i$ results in 53.66 psig. Therefore, $^{1}p_i$ and $^{D}p_i$ values of 53.66 and 48.20 psig should result in $^{1}t_m$ and $^{2}t_R$ times of 2.00 and 0.08 min respectively.

Table 6.6 The inverse straight line equation used to map the ^{2}D pneumatic curve has 3 constants denoted A, B and C. For a line of best fit the values of the constants and the resulting R^2 value were determined using LAB Fit (Version 7.2.29).

Const. $^{1}t_m$ (min)	A	B	C	R^2
2.00	0.39675	-3.78951	0.0148	0.9994

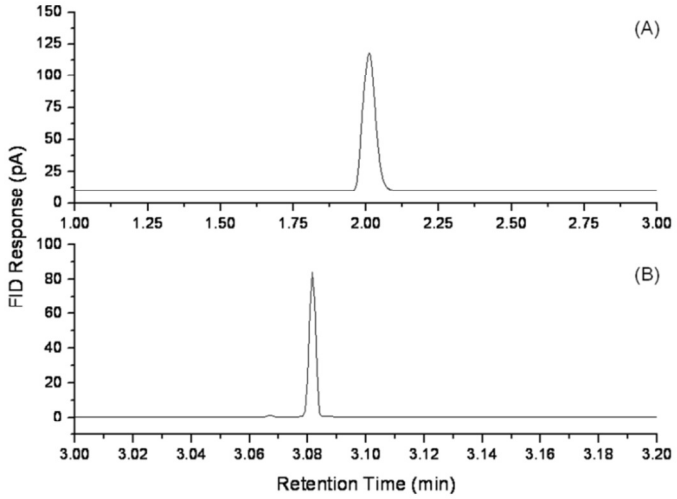

Figure 6.9 Chromatograms of methane (A) and heptanol (B) for the calculated ${}^{1}p_i$ and ${}^{D}p_i$ values of 53.66 and 48.20 psig.

Figure 6.9 shows the chromatograms of methane and heptanol on the ${}^{1}D$ and ${}^{2}D$ when applying the calculated ${}^{1}p_i$ and ${}^{D}p_i$ values of 53.66 and 48.20 psig, respectfully. For the calculated ${}^{1}p_i$ and ${}^{D}p_i$ pressures, methane gave a ${}^{1}t_m$ time of 2.01 min while heptanol gave a ${}^{2}t_R$ time of 3.081 min. The methane ${}^{1}t_m$ and heptanol ${}^{2}t_R$ determined experimentally differed from the ${}^{1}t_m$ and ${}^{2}t_R$ targets of 2.00 and 0.08 min by 0.01 and 0.001 min, respectfully. Though there are differences between the calculated t_R and the experimental t_R, they are diminutive from a GC standpoint. It must be noted that although the results are deemed accurate, the number of experiments is still relatively small and the precision of the technique still yet to be fully investigated. The results outlined and described here have provided considerable evidence for the successful locking of both the ${}^{1}D$ and ${}^{2}D$ in a tMDGC system i.e. RTL-tMDGC.

Although all experiments discussed in this study have been conducted under isothermal conditions, method translation theory suggests that if an identical temperature ramp was used throughout the study RTL-MDGC would be possible. Experimental work not presented in this study has demonstrated this, with no differences found in the retention time locking of temperature programmed and isothermal methods.

6.5 CONCLUSION

Using a combination of Poiseuille equations to theoretically model a MDGC system, this chapter investigates a procedure for the independent retention time locking of both columns in a MDGC column set i.e. RTL-MDGC. This investigation proposes placement of a T-piece fitting at the union between the ^{1}D and ^{2}D of a MDGC column set; the addition of supplementary carrier gas at the T-piece was initially studied because of its inherent simplicity. However, the Poiseuille models reveals that such a MDGC system can become limited by the natural back pressure established at the column union. As the natural back pressure at the column union is strongly linked to the restriction of carrier gas flow through ^{2}D, it appears that MDGC systems with narrow or long ^{2}D will be most affected.

By extending the role of the T-piece to remove (split) as well as add carrier gas at the union between the ^{1}D and ^{2}D columns, it is possible to avoid any physical restrictions imposed by the presence of a natural back pressure. Although the RTL-MDGC procedure presented in this study refers to a MDGC system with supplemented carrier gas, no basic changes are required if the MDGC system is extended to the case of removal of carrier gas at the union. Though a slightly different approach was employed to model such a MDGC system, the results were largely similar to warrant being presented.

The RTL-MDGC technique developed can be successfully applied to both tMDGC and GC×GC systems and only requires approximately 15 fast separations (10-20 min depending on reference compounds). As with ^{1}D RTL, RTL-MDGC can lock methods applied to different GC systems, columns of nominal length/i.d., and detectors. Because of its speed and simplicity, this approach has the potential to become fully automated within a GC software package allowing for a fast and user friendly technique. With the aid of adequate RTL-MDGC libraries for a preferred column arrangement the success rate of identifying unknown peaks with only one separation will be comparable to that of MS. In fact RTL-MDGC can be applied to any detection source including MS and can be combined (RTL-MDGC-MS) to deliver a very simple yet powerful tool for the separation and identification of compounds within a complex mixture. It is not hard to imagine the capabilities of a

fully integrated RTL-MDGC-MS software based library search engine that combines two independent retention times and the mass spectrum of a peak from a single experiment.

CHAPTER 7

THE APPLICATION OF RETENTION TIME LOCKING TO COMPREHENSIVE TWO DIMENSIONAL GAS CHROMATOGRAPHY

7.1 SUMMARY

This chapter documents the successful application of independent retention time locking (RTL) to each separation of a GC×GC system (RTL-GC×GC). The procedure is straightforward, with the potential of being included in a macro/software application for full automation. To achieve RTL-GC×GC, a typical GC×GC system is modified to include a T-piece fitting positioned at the union between the two capillary columns. A length of deactivated capillary tubing is installed between this T-piece and a second conventional split injector. This arrangement allows variation in pressure at the second split injector to directly alter the pressure at the T-piece/column union, which in turn simultaneously affects both the primary column (^{1}D) outlet pressure and the secondary column (^{2}D) inlet pressure. With precise control of the second split injector pressure, it becomes possible to regulate the pressure drop of both the ^{1}D and ^{2}D columns and ultimately to pressure-tune both columns. A procedure is outlined that accurately pressure-tunes both the ^{1}D and ^{2}D enabling the alignment/locking of their respective separations.

Using heptanol as the target component, relationships are established that define the change in retention on both the ^{1}D and ^{2}D columns according to the various pressure settings of the system. Target retentions of 5 min and 5.0 s were chosen as the locking times for the ^{1}D and ^{2}D respectively. The ^{1}D and ^{2}D lengths were altered and the relationship between pressure drop and retention were re-evaluated to allow the return of the target heptanol retention time.

After the heptanol target time was achieved a 9-compopnents mix was injected to demonstrate the reproducibility of the RTL-GC×GC approach.

7.2 INTRODUCTION

Retention time locking (RTL) is a technique that aligns the retention times of eluting compounds with that of a standard method [125, 126]. RTL achieves this by precisely adjusting the pressure drop of a separation column to compensate for any differences in retention which arise from e.g. column dimension changes or phase thickness (but not phase type). Through RTL, the retention time of an eluting compound is transformed into a unique value representing a compound's chromatographic interaction with the stationary and mobile phases (distribution constant K value). If a library of retention times is produced for a standard method, any method "locked" to the standard method can utilise the library for peak identification, and/or contribute to it.

Groups from both academe and industry adopt RTL as an effective means to identify or assist in the identification of unknown compounds, or to maintain the reliability of identification. The literature contains a number of innovative studies where RTL has been successfully employed in conjunction with hyphenated GC techniques such as GC-mass spectrometry (GC-MS), GC-atomic emission detection (GC-AED) and GC-olfactometry (GC-O) [145-147, 150, 157-163]. A unique study by Mac Namara et al generated an extensive RTL GC-MS library from complex essential oil mixtures by using the second column separations from a targeted multidimensional gas chromatography (tMDGC) system equipped with mass spectrometry [161]. The second column was then reinstalled directly into the GC-MS in a one-dimensional fashion and "locked" to its former tMDGC experiment. Unknown components in a complex mixture of gin essential oil could then be identified by a powerful combination of retention time and mass spectrometry with deconvolution.

A hyphenated GC technique that should benefit immensely from RTL is comprehensive two-dimensional gas chromatography (GC×GC) due to the pictorial representation of components in 2D space [155]. GC×GC provides enhanced separation by subjecting all components of an injected sample to two independent and orthogonal separations in one experiment [104]. The resulting chromatogram for a GC×GC analysis is a 3 dimensional surface plot with the retention of the first and second separations (^{1}D and ^{2}D) being plotted in the x and y dimensions respectively and the detector response in the z dimension. For all separated peaks in a GC×GC analysis, two unique retention times are generated for both separations allowing for a

greater level of identification. The application of RI or RTL to GC×GC would be most advantageous for the analysis of complex samples. Equipped with extensive libraries for both the ^{1}D and ^{2}D (RTL or RI), identifications can be made for two orthogonal separations with an 80% chance of success [128]. Furthermore, such approaches could be further extended to GC×GC with mass spectrometric detection (GC×GC-MS); a well-established three dimensional GC hyphenation technique. Armed with two RI or RTL values from two orthogonal separations and mass spectrometry, positive identification of a peak by such a technique would be highly likely.

Studies by Western et al.[129, 130] and more recently Bieri et al. [131] successfully developed a technique to obtain a RI map that could be superimposed over the separation space of the GC×GC 3 dimensional surface plot (RI-GC×GC). Although successful, the creation of a RI map is quite laborious requiring many experiments. The RI map is also limited to specific areas of the separation space, and assignment of index values for ^{2}D may be imprecise due to the small retention differences of reference compounds.

Theoretically, the RTL of a GC×GC system (RTL-GC×GC) would not be hindered by issues such as that found for RI as it is not dependent upon the elution of bracketing reference compounds. Shellie *et al.* showed that the addition of a supplementary supply of carrier gas at a union between the end of ^{2}D and detector had the potential to adjust the pressure drop across an entire GC×GC column set, and alter the retention times of eluting compounds [132]. This approach enabled the setting of equivalent retention times of two GC×GC systems, using an identical column set, and employing flame ionisation and mass spectral detection with H_2 and He carrier gas respectively. An identical column set must be used since if a column differs slightly in dimensions its pressure drop will be altered, and that of any column coupled to it. This implies independent control of the pressure drop for both ^{1}D and ^{2}D columns is required.

This chapter documents an approach to achieving RTL-GC×GC by means of addition or removal of carrier gas at the union between the ^{1}D and ^{2}D capillary columns.

7.3 EXPERIMENTAL

7.3.1 Gas Chromatography System:

All analyses were performed using an Agilent Technologies 6890 model gas chromatograph equipped with flame ionization detection, 7683 series auto sampler, two injection modules, and Chemstation software. The GC system was retrofitted with an Everest model longitudinally modulated cryogenic system (LMCS, Chromatography Concepts, Doncaster, Australia). The GC system was equipped with a two split/splitless injectors.

7.3.2 Separation Columns:

The GC×GC column set comprised of a ^{1}D fused silica capillary column of 95% methyl–5% phenyl polysilphenylene-siloxane (BPX5; SGE International, Ringwood, Australia) phase (0.25 µm d_f) with dimensions 30 m × 0.25 mm i.d., a ^{2}D separation column of polyethylene glycol (BP20; SGE) phase (0.10 µm d_f) with dimensions 1 m × 0.10 mm i.d. The column set was coupled using a Quick Swap capillary flow device that allowed for the simple addition of supplementary carrier gas at the union of the two columns. An illustration of the chromatographic system with column installations is provided in **Figure 7.1**.

7.3.3 Experimental Parameters:

Unless specified, all experiments discussed in this investigation employ the following settings. Injections of 1 µL were made using a 10 µL syringe installed into the 7683 series auto sampler/injector. The oven temperature was initially held at 80 °C and immediately increased by 5 °C/min to 130 °C. The FID was operated at 300 °C and acquired data at a rate of 100 Hz. Both the spilt/splitless injectors were held at a temperature of 250 °C and operated in constant pressure mode.

7.3.4 Samples:

Heptanol was used as the reference peak for all retention locking experiments. Once locked a 9 component mixture of octan-3-one, heptanol, 1, 8 cineole, γ terpinene, terpinolene, linalool, menthone, linalyl acetate and geraniol was prepared and used as a real sample.

7.4 RESULTS AND DISCUSSION

The advantage of RTL lies in its ability to assist the chromatographer in the rapid identification of unknown peaks. Once a GC method has been finalised, it can be used to collect the unique retention times of many known peaks and to build a retention time library. This is important for routine applications and therefore also for automated identification. If the GC system is unchanged, and the same GC method performed, the library can be used as a means of peak identification. Any change in the GC system that impacts the retention of eluting compounds will negate the link between the GC method and the library thus making any identification void. A different GC instrument, new column, column maintenance and column deterioration are all very common causes that directly influence a solute's retention. For this reason, a solute's retention time alone has never been widely accepted as a means to identify peaks over an extended period of time. With RTL however, it is possible to compensate for such changes in retention times and re-establish the viability between the GC method and the library. By realigning a GC method back to its initial performance the analyst can continue to use and contribute to the retention time library.

Whether attempting to reproduce a former GC method or realign a current GC method, the RTL procedure remains the same. Precise adjustment to the column pressure of the GC method is employed to re-align/lock the retention time of a chosen solute to that initially achieved. Starting with the original GC method settings, the column head pressure is varied while injections containing a chosen solute are made. This enables the relationship between the column head pressure and the solute retention time to be established. The column head pressure that realigns the solute retention time can be determined and adopted into the GC method. The GC method is now locked to its original state and can accurately reproduce previous separations.

Chapter 5 describes in detail a technique that allows both capillary columns of a GC×GC system to be independently pressure tuned and locked i.e. RTL-GC×GC. The technique requires that a tee piece fitting be installed between the ^{1}D and ^{2}D allowing for the removal or addition of carrier gas. **Figure 7.1** illustrates the modified GC×GC

system for implementing the RTL-GC×GC technique. A commercially available Y press-fit capillary splitter has been used as the tee piece fitting between the ^{1}D and ^{2}D columns. A length of deactivated fused silica capillary is installed into the secondary split injector and attached to the third position of the Y press-fit.

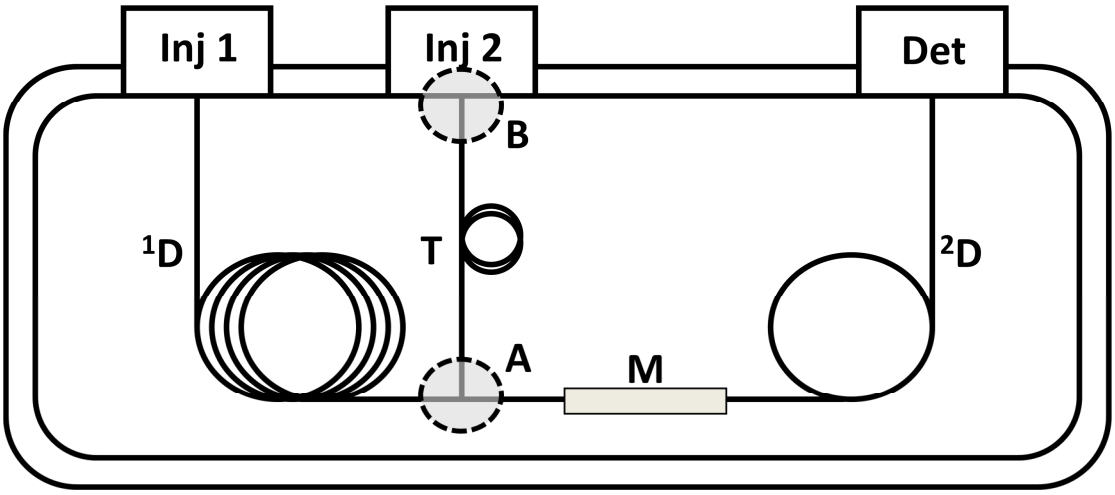

Figure 7.1 Illustration of the modified GC×GC system used to apply the RTL-GC×GC technique. ^{1}D is the primary column, ^{2}D is the second column, T is the transfer line, M is the modulator, Inj 1 is the primary split injector, Inj 2 is the second split injector, and Det is the FID detector. A and B are insets that are expanded for more detail in **Figure 7.2**.

Figure 7.2, Inset A illustrates the Y press-fit arrangement in more detail. The coupling of ^{1}D, ^{2}D and T in such an arrangement results in equivalency of ^{1}D outlet ($^{1}p_o$), T outlet ($^{T}p_o$) and ^{2}D inlet ($^{2}p_i$) pressures, assuming the same value known henceforth as the midpoint pressure (p_m). The ^{1}D pressure drop is between the ^{1}D head pressure ($^{1}p_i$) and p_m while the ^{2}D pressure drop is between p_m and $^{2}p_o$. Any change in p_m will simultaneously alter the pneumatics of both the ^{1}D and ^{2}D. Indicated by the arrows in **Figure 7.2** Inset A, an increase in p_m will restrict the flow of carrier gas through ^{1}D while increasing the flow of carrier gas through ^{2}D and *vice versa*. With control over p_m (eg. provided by $^{T}p_i$) it becomes possible to adjust the pneumatics of ^{1}D or ^{2}D to compensate for any changes in retention, and effect RTL as described above.

Figure 7.2, Inset B depicts the installation of T into the secondary split injector in greater detail. By positioning a split injector at the end of T, the $^{T}p_i$ can be varied

below the p_m or above. If ${}^{T}p_i > p_m$ then the carrier gas will flow from the secondary split injector to the Y press-fit and along the ${}^{2}D$. If $p_m > {}^{T}p_i$, the carrier gas will flow from the Y press-fit to the split injector and out the split line. The ability to split away carrier gas that enters the transfer line is most advantageous as it varies the natural pressure that occurs when ${}^{2}D$ restricts the carrier flow provided by the ${}^{1}p_i$ setting which in the absence of the T-piece creates a natural pressure p_m. Without diverting the carrier gas entering the transfer line, it would not be possible to lower the ${}^{T}p_i$ beyond the natural back pressure of column arrangement.

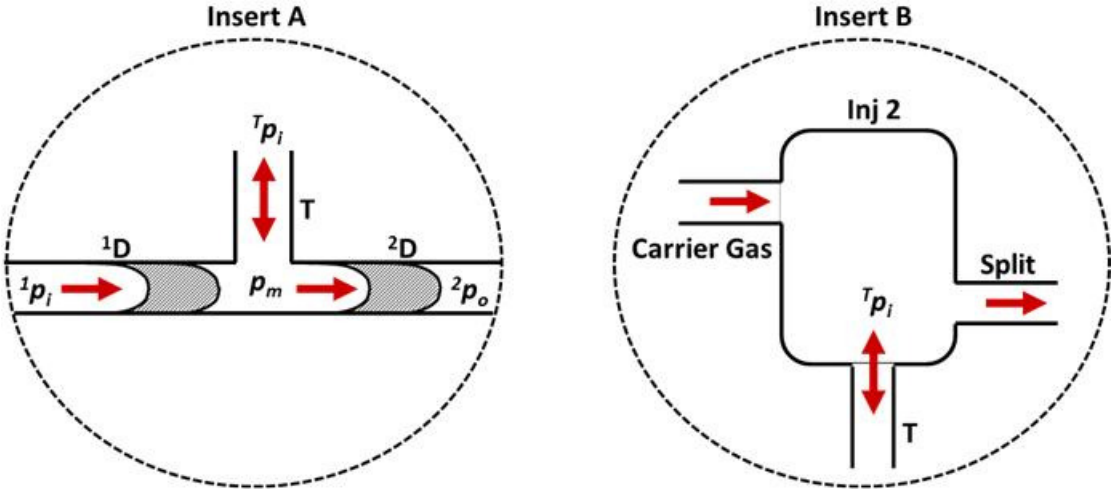

Figure 7.2 Enlargements of sections A and B from Figure 1. Inset A depicts the connection between ${}^{1}D$, ${}^{2}D$ and T. Inset B depicts the second split injector.

The p_m cannot be independently controlled in this GC×GC system as it is a consequential value resulting from the combination of ${}^{1}p_i$, ${}^{T}p_i$ and ${}^{2}p_o$. A single adjustment in either one of ${}^{1}p_i$, ${}^{T}p_i$ or ${}^{2}p_o$ is all that is required to simultaneously alter the pressure drops of ${}^{1}D$, T or ${}^{2}D$. For example, if ${}^{T}p_i$ is altered, it directly impacts the pressure drop across T and causes p_m to change, which then impacts the pressure drop for ${}^{1}D$ and ${}^{2}D$. It is therefore possible to indirectly control p_m and ${}^{1}D$ and ${}^{2}D$ pressure drops by modifying ${}^{T}p_i$. As discussed earlier the second split injector allows ${}^{T}p_i$ to move above and below p_m the system natural back pressure. This enables the controlled splitting ($p_m > {}^{T}p_i$) or supplementation (${}^{T}p_i > p_m$) of carrier gas exiting ${}^{1}D$. Whether splitting or supplementing flow at the Y press-fit, the electronic pressure control module for the second split injector will ensure that ${}^{T}p_i$ will always remain

constant (if operated in constant pressure mode). In this sense, the second split injector becomes a device for the precise control of ${}^{T}p_i$ and ${}^{1}D$ and ${}^{2}D$ pressure drops.

For RTL-GC×GC to be achieved, independent adjustment of both ${}^{1}D$ and ${}^{2}D$ separations to their respective targets is required. For the purpose of this investigation ${}^{1}D$ and ${}^{2}D$ of the GC×GC system described will be locked to a heptanol retention time of 5 min and 5 sec respectively. Heptanol was chosen as the target compound because of its low boiling point and polarity thus enabling a short ${}^{1}D$ retention time and its ability to be cryofocused and reinjected on the ${}^{2}D$ polar stationary phase.

Utilising the successful approach to RTL-MDGC outlined in prior research ${}^{1}p_i$ is held constant while ${}^{T}p_i$ is varied. **Table 7.1** lists three values of ${}^{1}p_i$ each of which remains constant while ${}^{T}p_i$ is adjusted to the values indicated for each ${}^{1}p_i$ setting. At each ${}^{1}p_i$, ${}^{T}p_i$ combination in **Table 7.1** an injection of heptanol was made and a GC×GC separation performed.

Table 7.1 ${}^{1}p_i$ pressure settings (varying from 25 psig) that are held constant while injections of heptanol are made for each of the corresponding ${}^{T}p_i$ pressures.

${}^{1}p_i$ Values (psig)		
15	25	35
${}^{T}p_i$ Values (psig)		
0	4.95	9.9
1.3	6.69	12.08
3.3	9.37	15.43
5.3	12.04	18.77
7.3	14.71	22.12
9.3	17.39	25.47
11.3	20.06	28.81
13.3	22.73	32.16
14.3	24.07	33.84

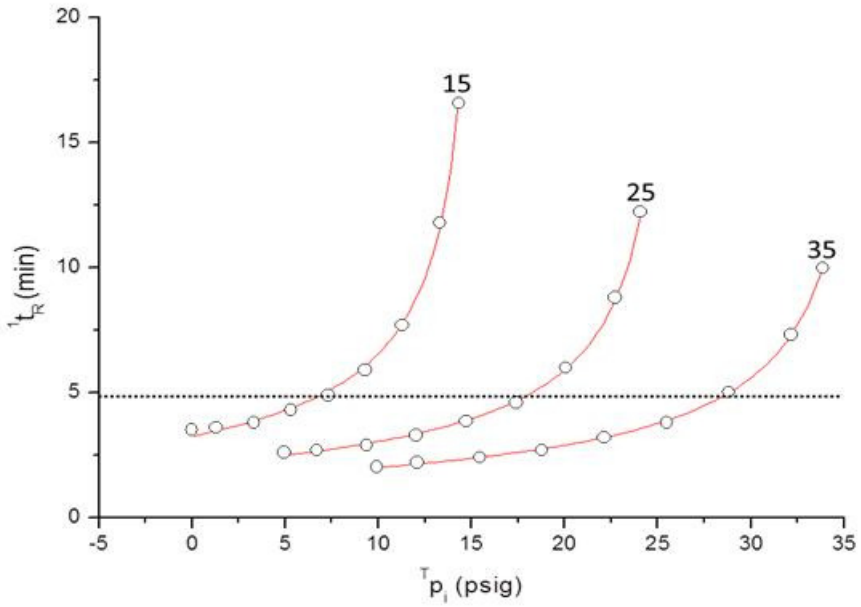

Figure 7.3 Heptanol ^1t_R values for GC×GC separations performed using the ^1p_i and ^Tp_i combinations listed in **Table 7.1**.

Figure 7.3 plots the resulting heptanol ^{1}D t_R (^1t_R) against the ^Tp_i for the GC×GC separations using the ^1p_i, ^Tp_i combinations listed in **Table 7.1**. The data are grouped into three separate curves, each representing the three constant values of ^1p_i. in **Table 7.1**. For each of the three data sets, lines of best fit were determined using LAB Fit curve fitting software (Version 7.2.47) and superimposed in **Figure 7.3**. The modified Bleasdale equation shown in **Equation 7.1** was found to accurately map the relationship between the heptanol ^1t_R and ^Tp_i (for a constant ^1p_i) with **Table 7.2** listing the variables A, B, C and the resulting R^2 values.

$$^1t_R = \left(A + B \times \sqrt{^Tp_i}\right)^C$$

Equation 7.1

A dotted horizontal line has been superimposed on **Figure 7.3** at a heptanol ^1t_R of 5.0 min. The point at which the dotted line intercepts the curves of constant ^1p_i, determines the ^Tp_i value required to achieve the desired heptanol ^1t_R of 5.0 min. By rearranging **Equation 7.1** so that the ^Tp_i becomes a function of ^1t_R, the ^Tp_i for a ^1t_R of

5 min can be determined. The far right column of **Table 7.2** displays the $^{T}p_i$ values for a heptanol $^{1}t_R$ of 5.0 min for all three curves, at constant $^{1}p_i$.

					$^{T}p_i$ (psig)
$^{1}p_i$ (psig)	**A**	**B**	**C**	**R^2**	**5.0 min**
15	0.486079	-0.08835	-0.61501	0.9988	7.16
25	0.7732	-0.12110	-0.6309	0.9996	18.26
35	1.164	-0.16230	-0.6777	0.9997	28.85

Table 7.2 Constants A, B and C estimated for **Equation 7.1** when lines of best fit are determined for the three curves of $^{1}t_R$ against $^{T}p_i$ for a constant $^{1}p_i$ of 25, 30 and 35 psig. The $^{T}p_i$ values have been solved using **Equation 7.1** with a heptanol $^{1}t_R$ of 5.0 min

Line (A) in **Figure 7.4** shows the relationship between $^{1}p_i$ and $^{T}p_i$ for a constant heptanol $^{1}t_R$ of 5.0 min. The three open circle points in line (A) are $^{1}p_i$ and $^{T}p_i$ values determined above for a constant heptanol $^{1}t_R$ of 5.0 min. Using MS Excel (Microsoft Office 2007) a straight line of best fit was determined for the three points and superimposed on **Figure 7.4**. The linear equation is shown in **Equation 7.2** and the values of the constants are M; 0.92218, C; -5.23437, with R^2 of 0.999816. $^{T}p_i$ values that result in a heptanol $^{1}t_R$ of 5.00 min corresponding to $^{1}p_i$ of 20 and 30 psi are 12.67 and 23.51 psig respectively.

$$^{1}p_i = \mathrm{M} \times {}^{T}p_i + \mathrm{C}$$

Equation 7.2

Defining the relationship between the $^{1}p_i$ and $^{T}p_i$ for a constant $^{1}t_R$ (i.e. the target $^{1}t_R$) is the foundation to the RTL-GC×GC technique employed. This enables p_m to be varied via $^{T}p_i$ without any change in $^{1}t_R$. Essentially, $^{1}p_i$ moves in concert with $^{T}p_i$ to compensate for any changes in $^{1}t_R$. Adjustments can be made to p_m with the intention to alter $^{2}t_R$ without affecting the already locked ^{1}D. The locking of ^{2}D will not disturb the pressure tuned ^{1}D and can therefore be achieved using the conventional single column technique discussed above.

Progressing along line (A) in **Figure 7.4** from $^{1}p_i$ of 15 to 25 psig, $^{T}p_i$ increases by an amount defined by **Equation 7.2** and the values reported above. This increase in $^{T}p_i$ causes p_m ($^{1}p_o$) to increase thus compensating for the increase in $^{1}p_i$ and maintaining a heptanol $^{1}t_R$ of 5 min. As discussed above p_m represents all the values $^{1}p_o$, $^{T}p_o$ and $^{2}p_i$, therefore as p_m is adjusted it alters both $^{1}p_o$ and $^{2}p_i$ simultaneously. Moving along line (A) from $^{1}p_i$ of 15 to 35 psig, $^{2}p_i$ increases (via the ^{T}pi setting) and changes the pressure drop of ^{2}D. Through the use of line (A) it is possible to RTL the ^{2}D, in the same manner as a single column GC system where the relationship between the head pressure and retention time are used. To determine the relationship between $^{T}p_i$ and $^{2}t_R$, GC×GC separations of heptanol with $^{1}p_i$, $^{T}p_i$ values from line (A) are required. However, because there are only three curves of $^{1}t_R$ *vs*. $^{T}p_i$ in **Figure 7.3** only three $^{1}p_i$, $^{T}p_i$ combinations of line (A) are available. This is insufficient to plot the heptanol $^{2}t_R$ against $^{T}p_i$ and apply a line of best fit to model the relationship. Using **Equation 7.2** with the values determined for this, it is possible to determine any number of $^{1}p_i$, $^{T}p_i$ coordinates for line (A). $^{T}p_i$ values determined for $^{1}p_i$ of 20 and 30 psig (12.67 and 23.51 psig) are added to line (A) in **Figure 7.4** as solid circles.

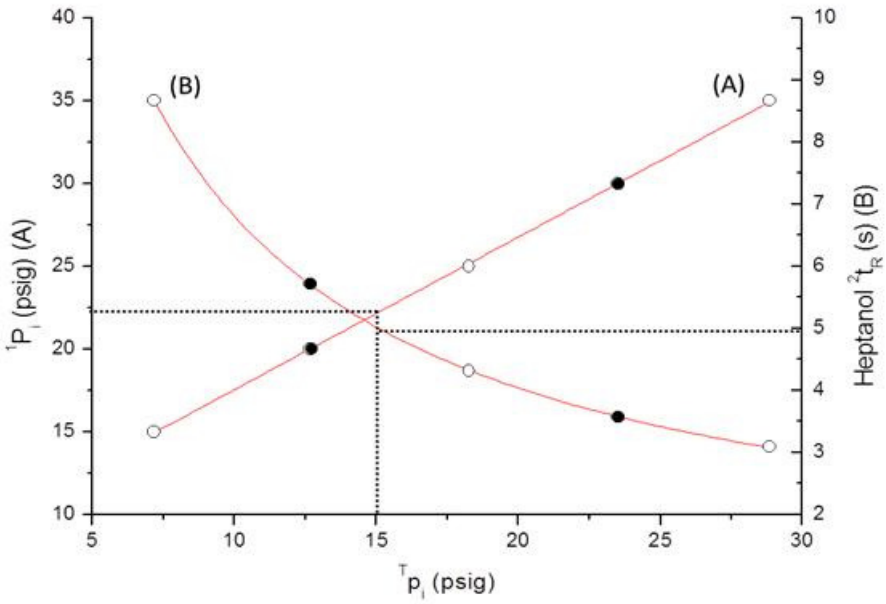

Figure 7.4 Line A is the relationship of the $^{1}p_i$ and $^{T}p_i$ for a constant heptanol $^{1}t_R$ of 5.0 min. Line B is the heptanol $^{2}t_R$ resulting from the $^{1}p_i$ and $^{T}p_i$ coordinates in line A.

At each of the five $^{1}p_i$ and $^{T}p_i$ settings found in **Table 7.2**, an injection of heptanol was made and the $^{2}t_R$ noted. Line (B) in **Figure 7.4** illustrates the relationship found for the heptanol $^{2}t_R$ and the $^{T}p_i$. As with Line (A) the two solid points on line (B) represent the heptanol $^{2}t_R$ where the $^{1}p_i$ and $^{T}p_i$ values were determined using **Equation 7.2**. Using LAB Fit curve fitting software a line of best fit was determined using **Equation 7.3** and superimposed on **Figure 7.4**. Variables in this equation are A; 0.01345, B; -0.1688, and C; 0.6899, and the corresponding R^2 value of 0.9997. To lock $^{1}t_R$ to 5.00 min, and $^{2}t_R$ to 5.00 s, $^{T}p_i$ and $^{1}p_i$ settings of 15.07 and 22.21 psi are required. The inclusion of the two extra points at $^{1}p_i$ 20 and 30 psi allowed a good mathematical fit which would not be possible with only the original three points.

$$p_m = \frac{\sqrt{(^{2}t_R - C)} - B}{A}$$

Equation 7.3

Figure 7.5, (A) is a GC×GC plot of the five heptanol injections made for the five $^{1}p_i$, $^{T}p_i$ combinations in Line (A). All five of the GC×GC 3D heptanol peaks can be seen to elute from ^{1}D at ~5.0 min. This proves the effectiveness of establishing the relationship between the $^{1}p_i$ and $^{T}p_i$ for a constant $^{1}t_R$. As shown here, $^{2}t_R$ can be adjusted while ^{1}D is firmly locked at the desired $^{1}t_R$. The relationship of $^{1}p_i$ and $^{T}p_i$ to generate a constant $^{1}t_R$ must be disconnected from the ^{2}D column, through the intermediate pressure control provided by the Y-piece. **Figure 7.4**, line (B) and **Figure 7.5** (A) illustrate the ability to adjust heptanol $^{2}t_R$ while having no effect on the locked ^{1}D.

Though they are both presenting the same experiments, the five heptanol $^{2}t_R$ values in **Figure 7.4** line (B) and **Figure 7.5** (A) do not match. For example the fastest heptanol $^{2}t_R$ in **Figure 7.4** line (B) was 3.1 min while in **Figure 7.5** (A) it appeared to be 2.7 min. This is because of the wrap around effect where a components $^{2}t_R$ is greater than the modulation cycle. The component elutes after the following injection and as such is interpreted by the software as being part of the following modulation cycle. For this reason what seems to be the fastest heptanol $^{2}t_R$ in **Figure 7.5** (A) at 2.7 s is in fact the longest at 8.7 s. For this point the true $^{2}t_R$ = apparent $^{2}t_R$ + P_M (6.00 s) = 8.7 s, as suggested in **Figure 7.4**.

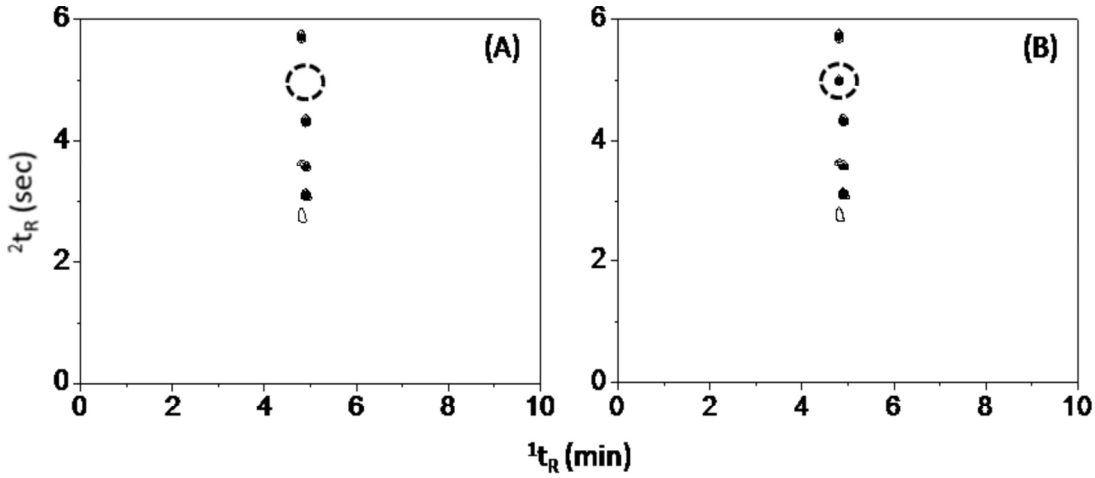

Figure 7.5 GC×GC chromatograms for (A) five heptanol separations made with the ^1p_i and ^Tp_i pairs listed in **Table 7.2** and derived from **Equation 7.2**, and (B) mirrors (A) except for the inclusion an extra heptanol separation using the ^1p_i and ^Tp_i values calculated to lock the heptanol ^1t_R and ^2t_R at 5.0 min and 5.0 sec.

Using **Equation 7.3**, ^Tp_i can be calculated for any heptanol ^2t_R within 3.1 to 8.7 s. Though not investigated here, it may be possible to extrapolate line (B) **Figure 7.4** beyond the experimental boundary of the 3.1 to 8.7 s heptanol ^2t_R and still successfully solve ^Tp_i with respect to the ^2t_R. The dotted lines in **Figure 7.4** depict the procedure taken to calculate the ^Tp_i required to lock ^{2}D whilst still maintaining a locked ^{1}D. Beginning at the heptanol ^2t_R axis, a dotted line extends from the desired heptanol ^2t_R time of 5 s. The line extends left to intercept line B. This intercept represents the ^Tp_i required to yield a 5 s heptanol ^2t_R with respect to the ^1p_i, ^Tp_i relationship for a constant heptanol ^1t_R of 5.0 min. The ^Tp_i value is calculated using **Equation 7.3**, giving 15.07 psig, which is depicted by the second dotted line extended to the ^Tp_i axis in **Figure 7.4**. This determines the ^1p_i value that, combined with ^Tp_i of 15.07 psig yields a heptanol ^1t_R and ^2t_R of 5.0 min and 5.0 s respectively (also determined by rearranging **Equation 7.2** to express ^1p_i as a function of ^Tp_i). Substituting in a ^Tp_i value of 15.07 psig and solving **Equation 7.2** gives ^1p_i of 22.21 psig, also shown in **Figure 7.4** by extending the vertical dotted line to intercept line (A), at which point the ^1p_i value 22.21 is found.

Figure 7.5 (A) and (B) have a superimposed dotted circle positioned at the $^{1}t_{R}$ and $^{2}t_{R}$ desired locking coordinates of 5.0 min and 5.0 s. These figures are identical except that (B) includes the peak resulting from a GC×GC experiment employing the calculated $^{1}p_{i}$ and $^{T}p_{i}$ values of 22.21 and 15.07 psig respectively – the locked separation. The resulting $^{1}t_{R}$ and $^{2}t_{R}$ values are found to be 4.83 min and 5.0 sec, respectively. While the locking of ^{2}D was successful to reproduce the desired time, locking of ^{1}D was slightly lower than the anticipated time. None of the GC×GC heptanol peaks in **Figure 7.5** (B) have a $^{1}t_{R}$ of exactly 5.0 min; all are consistently slightly short of 5.0 min. Line (A) in **Figure 7.4** is the most likely cause for the low heptanol $^{1}t_{R}$, being slightly imprecise so as not to reflect the relationship of $^{1}p_{i}$ and $^{T}p_{i}$ for a 5.0 min heptanol $^{1}t_{R}$, but giving ~4.8 min instead. However the RTL-GC×GC approach is still considered a success, with precise locking of ^{2}D and the relationship of $^{1}p_{i}$ and $^{T}p_{i}$ for a constant $^{1}t_{R}$ being achieved.

Figure 7.6 illustrates the individual modulated GC×GC heptanol separations. Presenting the GC×GC separation in this manner gives the true experimental output for each modulation event, displaying the successive 6 s fractionations of heptanol into the many fast ^{2}D separations. Each 6 s sampled ^{1}D separation is compressed and reinjected into the ^{2}D column. The contour plot presentation of **Figure 7.5** is a familiar format for GC×GC, but may not allow exact extraction of retentions Modulated ^{2}D separations in **Figure 7.6** indicate the heptanol peak has $^{1}t_{R}$ values ranging from 4.8 to 5.4 min (48^{th} to the 54^{th} modulation – noting that there is some tailing on the ^{1}D column). Details such as ^{1}D peak start time, peak stop time, peak width and retention time cannot be reliably determined directly from the GC×GC contour chromatogram. This raises the question on how to determine the $^{1}t_{R}$ of GC×GC peaks. Three possible approaches may be used; the middle of a contour peak, the modulation time of the ^{2}D separation containing the greatest peak area, or the apex from a Gaussian fit of the data. Estimating $^{1}t_{R}$ by selecting the middle of a peak in a contour plot may not be the best approach, although this was used to create **Figure 7.3** and **Figure 7.4**. If contour lines are made at an FID response of <20 pA then the peak would span from 4.8 to 5.2 min (**Figure 7.6**), giving an average $^{1}t_{R}$ of 5.0 min. If the contour lines are made at an FID response of >20 pA then the heptanol peak would span from 4.8 to 4.9 min, giving a $^{1}t_{R}$ of 4.85 min. The relationships and mathematical models in **Figure 7.3** and **Figure 7.4** have been determined by taking

$^{1}t_R$ as the middle of the GC×GC contour peak and this may cause ^{1}D to be locked at 4.8 min instead of 5.0 min.

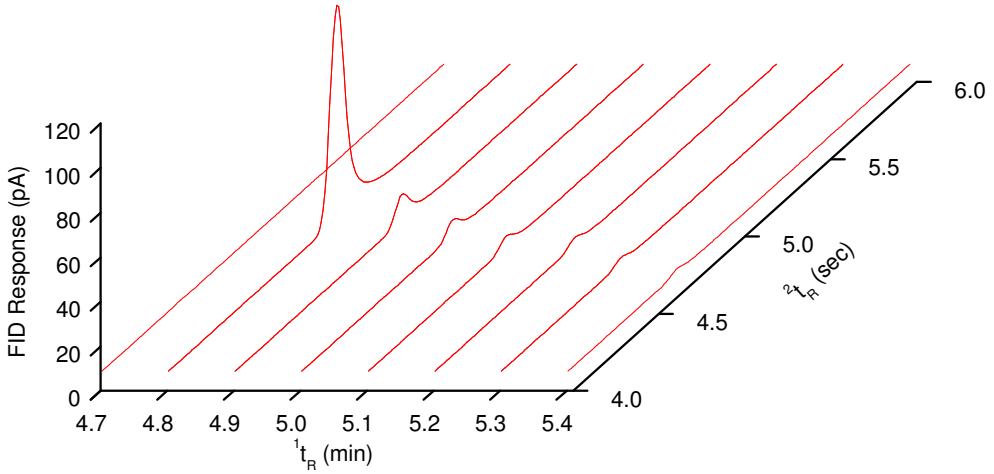

Figure 7.6 A 3 dimensional illustration showing individual ^{2}D chromatograms arising from modulation of a heptanol, employing $^{1}p_i$ and $^{T}p_i$ of 22.21 and 15.07 psig respectively.

Figure 7.7 displays 6 GC×GC 3D contour chromatograms of heptanol (upper plots) and a 9 component mix also containing heptanol (lower plots). The chromatograms in Figure 7A are performed with a $^{1}p_i$ and $^{T}p_i$ of 22.21 and 15.07 psig respectively i.e. the pressures determined above for heptanol (5.0 min $^{1}t_R$ and 5.0 s $^{2}t_R$). The chromatograms in **Figure 7.7** (B) duplicate the GC×GC separations in **Figure 7.7** (A) except for a 10% reduction in the capillary column length of both the ^{1}D and ^{2}D. The shortening of the ^{1}D and ^{2}D columns has disturbed the net pressure balance achieved in **Figure 7.7** (A) thus resulting in the heptanol retention shifting from 4.8 min and 5.0 s to 3.7 min and 4.5 s, respectively. The effect of shortening the columns is clearly seen in the 9 component mix between **Figure 7.7** (A) and (B) where the two dimensional separation pattern in (A) is barely recognisable in (B).

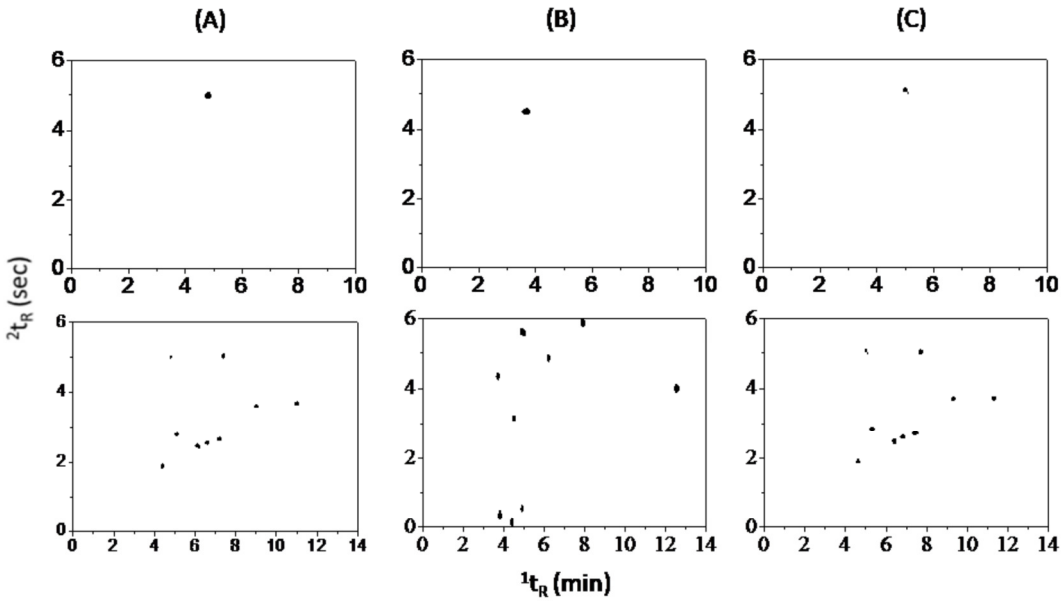

Figure 7.7 The top row displays GC×GC separations of heptanol while the lower shows GC×GC separations of a 9 component mix (including heptanol). Column A is the GC×GC separations when using ^1p_i, ^Tp_i of 22.21 and 15.07 psig respectively. Column B is the resulting GC×GC separations when using ^1p_i, ^Tp_i of 22.21 and 15.07 psig respectively but with both columns shortened by 10%. Column C is the GC × GC separations after the $^1D/^2D$ shortening, using locked ^1p_i and ^Tp_i pressures of 17.97 and 11.75 psig respectively.

Shortening of ^1D and ^2D by 10% has a considerable effect on the retention time of eluting peaks, thus illustrating the problem of reproducible separations for GC×GC if the exact geometry of both the ^1D and ^2D is not precisely matched; it is near impossible to duplicate a previous GC×GC separation in the absence of 'locking'. In practice, matching the geometry of GC×GC column sets to obtain identical separations is impractical. This inability to consistently reproduce GC×GC separations is a critical limitation in the technique and may be a reason for the slow adoption of GC×GC technology for routine applications. Many analytical methods and techniques used in industry must be validated and qualified to satisfy the requirements of a governing/regulatory body such as the Therapeutic Goods Administration (TGA) or Food and Drug Administration (FDA). Regardless of superior separation, if a GC×GC method cannot consistently reproduce separations then it is highly unlikely that it can be validated and used as an analytical tool for regulatory conformance. Precise reproduction of GC×GC separations has the potential to boost the development of validated methods within industry.

Table 7.3 $^{1}t_R$ and $^{2}t_R$ of the 9 components in the test mix before and after the reduction in the ^{1}D and ^{2}D length. Times were taken by measuring the middle of a peak on a GC×GC contour plot.

	Locking Pre-Cut		Locking Post-Cut	
Compound	**$^{1}t_R$ (min)**	**$^{2}t_R$ (sec)**	**$^{1}t_R$ (min)**	**$^{2}t_R$ (sec)**
Octan-3-one	4.42	1.87	4.63	1.89
Heptanol	4.82	4.98	5.02	5.02
1,8 Cineole	5.11	2.78	5.32	2.85
γ Terpinene	6.13	2.45	6.43	2.48
Terpinolene	6.64	2.53	6.84	2.60
Linalool	7.24	2.64	7.45	2.72
Menthone	7.43	5.01	7.74	5.01
Linalyl Acetate	9.04	3.60	9.35	3.70
Geraniol	11.04	3.66	11.37	3.70

The RTL result shown for the reduced length column in **Figure 7.7** (C) is determined as described below. **Figure 7.8** illustrates the $^{1}p_i$, $^{T}p_i$ relationship for a constant heptanol $^{1}t_R$ of 5.0 min when the RTL procedure is applied. A heptanol $^{1}t_R$ of 5.0 min and $^{2}t_R$ of 5.0 sec requires $^{1}p_i$ and $^{T}p_i$ values of 17.97 and 11.75 psig respectively. **Figure 7.7** (C) shows two GC×GC separations of heptanol and a 9 component test mix following the 10% reduction in column length and the locked pressures $^{1}p_i$ and $^{T}p_i$ of 17.97 and 11.75 psig. Visually, the RTL-GC×GC procedure appears to be an outstanding success with the GC×GC separation pattern of **Figure 7.7** (A) returned.

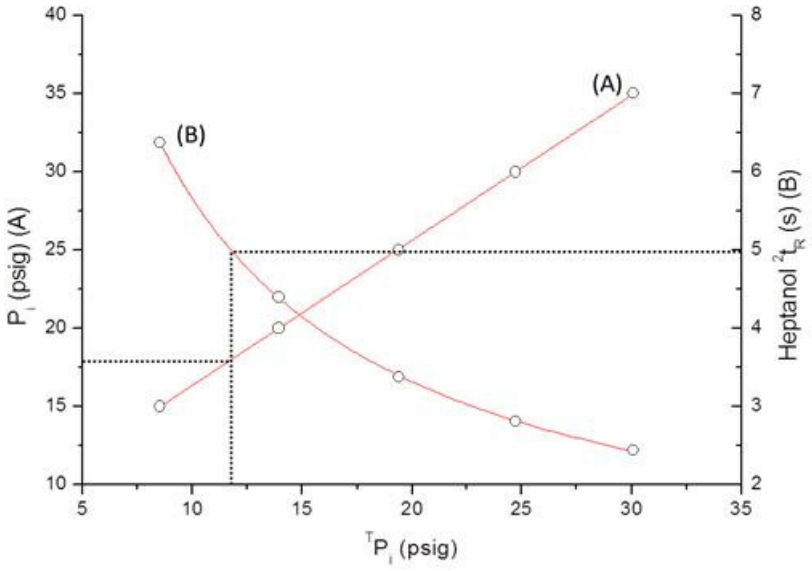

Figure 7.8 After shortening ^{1}D and ^{2}D by 10%, the relationship of ^1p_i and ^Tp_i for a constant heptanol ^1t_R of 5.0 min and the resulting heptanol ^2t_R was re-established.

Figure 7.3 and **Figure 7.4** were created using ^1t_R data that was estimated by determining the middle of a GC×GC contour peak. Errors that may be introduced by such an approach may have led to the imprecision of line (A) in **Figure 7.4**.. This approach proves to be more successful than that used before, with Figure 7.9 showing the largest portion of the fractionated ^{1}D heptanol peak eluting in the 50th modulation cycle, beginning at 5.0 min.

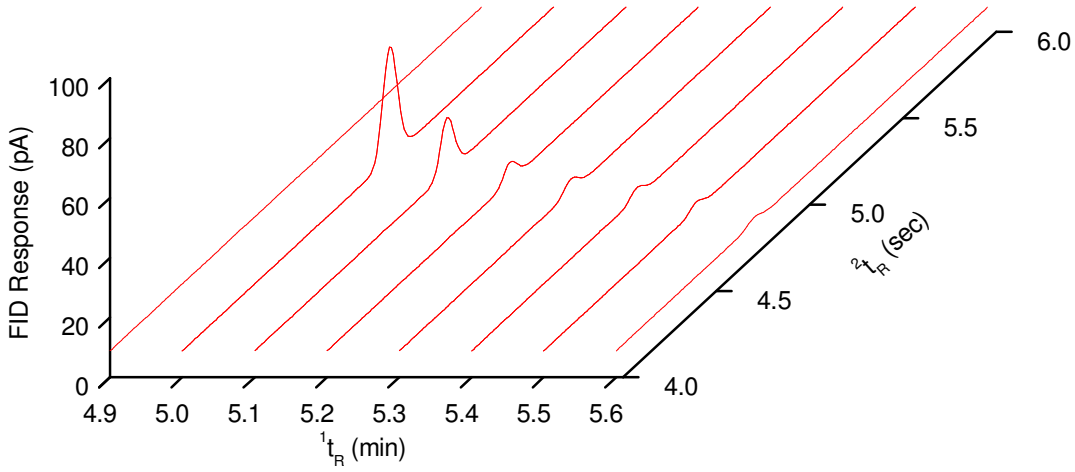

Figure 7.9 A 3 dimensional illustration showing the individual 2D chromatograms from a heptanol GC×GC separation employing a 1pi and Tpi of 17.97 and 11.75 psig

This implies that the second attempt at locking the GC×GC system after shortening the ^{1}D and ^{2}D length is a more successful with a ^1t_R and ^2t_R of 5.0 min and 5.0 sec respectively.

7.5 CONCLUSION

By coupling the ^{1}D and ^{2}D with a commercially available Y-press fit capillary column connector, a three way T-piece arrangement is achieved. Connecting the third line from the T-piece arrangement to a second split injector makes it possible to split away or add carrier gas with precision at the midpoint of the two columns, and adjust the pressure drops in both ^{1}D and ^{2}D to achieve RTL.

Relationships between $^{1}p_i$ and $^{T}p_i$ for a constant $^{1}t_R$ can be established, so that a range of settings of the input pressures will give a specific value of $^{1}t_R$ – here shown for heptanol solute. The $^{2}t_R$ value of heptanol can be set by suitable adjustment of $^{T}p_i$, since this alters the midpoint pressure (p_m) to ensure that the second column heptanol retention is reproduced. This strategy was followed for both the original column set, and a column set where each column length was reduced to 90% of its original length.

It was found that some measure of imprecision arises according to how accurately the ^{1}D retention is measured, and using the contour plot to predict this value is not as precise as studying the individual ^{2}D chromatographic traces.

A 9-component mixture was analysed under conditions of the original column set and pressures, then using a column set shortened by 10% length but using the same pressures as above, and finally with the locked pressures find for the new column dimensions. The locked condition GC×GC result very closely matched that of the original result, suggesting that the locking approach used here was sound. RTL results were within 0.2 min for ^{1}D and 0.1 s for ^{2}D.

CHAPTER 8

FINAL CONCLUSIONS & FURTHER WORK

8.1 CONCLUSIONS

8.1.1 Multidimensional Statistical Model of Overlap

Although many advancements of this early SMO approach have been made to help better model the chromatographic phenomenon, the original work by Davis and Giddings remains a popular tool for chromatographers to approximate the performance of a chromatographic system. By expanding the original SMO theory to a targeted multidimensional system an equivalent tool has been developed to approximate the performance and understand the advantages of multidimensional separation systems.

In this work the SMO theory has been expanded but not refined and still fails to account for the many factors that would affect a separation or the apparent quality of a separation such as varying peak heights, column overloading, column bleed, tailing and varying distributions of peaks within a separation space. In fact, this work is primarily based on the combination of two independent SMO predictions that are linked by a heart-cut mechanism. It is assumed that the number of peaks being analysed on the ^{1}D are evenly distributed and a heart-cut of given length would transfer a proportional amount of peaks to the ^{2}D. Therefore the multidimensional SMO theory presented here must contend with the imprecision of two SMO predictions and the added assumption regarding the number of peaks contained within a heart-cut. For these reasons this adaption of SMO to multidimensional separations cannot be viewed as more than a simple tool for the generation of numerical values relating to the probable separating power of a multidimensional system.

8.1.2 tMDGC or GC×GC

Since its invention GC×GC has quickly dominated the scientific literature regarding MDGC separations. The ability to subject the entire sample to two unique separations in the one experiment and represent the data in 3D surface plots has provided the GC×GC technique with a large amount of interest. While in contrast, interest in tMDGC has fallen by the wayside, making way for its more modern and sophisticated successor. Comparisons made between the two techniques using the multidimensional SMO predictions developed in Chapter 3 and the complex fragrance analysis in Chapter 4 suggest that tMDGC is by no means a lesser technique and is very much underutilised.

Unlike GC×GC where the whole sample is subjected to a short length of ^{2}D, tMDGC only exposes selected portions of the ^{1}D to a length of ^{2}D column that can be considerably longer. By exploiting this, and adopting a longer, fast ^{2}D column, the targeted regions may be analysed on a column of much greater peak capacity than that available to a GC×GC experiment. Though GC×GC provides a greater separation space then tMDGC, it is spread over the entire separation. Complex regions of the ^{1}D separation containing a high peak density may suffer from the lack of separation provided by the short ^{2}D, while areas of low peak density may have too much. Therefore it is recommended that if performing a qualitative analysis such as a chromatographic profile or chemical fingerprint on a sample than GC×GC is the most suitable option. Conversely, if quantitation of one or more components is required then tMDGC is the better option. tMDGC is not restricted in optimising the ^{1}D separation to achieve better separations and can selectively apply more separating power via its ^{2}D where necessary.

8.1.3 Developing a RTL-MDGC Technique

When setting up and installing the pneumatic Deans switching device for the tMDGC analysis of allergens in Chapter 4, it was noted how the retention of a peak could be altered on both dimensions simultaneously. An increase in the carrier gas supply of the Deans switch (located between the ^{1}D and ^{2}D) would restrict the incoming ^{1}D flow while feeding the departing ^{2}D flow and *vice versa*. This then led to the realisation that there would be a specific combination of ^{1}D head and Deans switching pressures that would result in the precise delivery of retention times i.e. retention time locking. Chapter 5 further investigates this concept by developing a pressure balancing procedure and assessing it with a theoretical model based on a combination of Poiseuille equations.

The Poiseuille model aided in the development and refinement of a pressure tuning procedure, that would theoretically determine the pressures to independently retention time lock the void times of both the ^{1}D and ^{2}D. The investigation originally focused on the hypothetical placement of a T-piece type fitting between the ^{1}D and ^{2}D that would supply carrier gas through an auxiliary type controller. Though the models suggested that such an arrangement would be successful they did indicate some potential limitations regarding the natural back pressure at the ^{1}D and ^{2}D union. A natural pressure already exists at the ^{1}D and ^{2}D union that

arises from the ^{1}D head pressure. The ^{1}D and ^{2}D union pressure cannot be lowered further then this value and as such limits the ability to reduce the union pressure i.e. increase the ^{1}D flow while slowing the ^{2}D flow. This is of little consequence if the ^{2}D column provides little or no restriction to the passing carrier gas. However, for short and narrow (fast GC) ^{2}D columns that are typically used in GC×GC, the natural pressure can become so high that carrier gas velocities of around 300 cm s^{-1} are achieved. A T-piece fitting that can only supplement this already very high pressure will have cause problems for the pressure tuning procedure developed.

To overcome the issue of natural back pressure the Poiseuille model was modified to extend the role of the T-piece to not only supply carrier gas but remove it (split). This then allowed for the controlled increase or reduction of the ^{1}D and ^{2}D union and the hypothetical independent retention time locking of both tMDGC and GC×GC systems.

8.1.4 RTL-tMDGC

In Chapter 6 the pressure tuning procedure was applied to a tMDGC system equipped with a Deans pneumatic switch. For this investigation the Deans switch played a dual role, while it would operate as a switching device and enable the transfer of heart-cuts from one column to another, it also acted as a supplementary pressure supply to perform the pressure tuning procedure. It should be noted that if the pressure required at the Deans switch for retention time locking is lower the switching pressure then the Deans switch can only perform the heart-cutting role. The switching pressure represents the precise pressure required for the auxiliary flow of carrier gas to equal that of the ^{1}D column flow inside the Deans switch. This then causes the ^{1}D column flow to alter its path towards the desired ^{2}D. If the switching pressure is lowered beyond the balanced point then it cannot block and guide the path of the ^{1}D flow. Instead the ^{1}D flow is split between the two paths and no heart-cutting can be performed. If no heart-cutting can be performed then the system ceases to be multidimensional and the task of applying retention time locking made redundant.

For the purpose of the investigation the desired retention times were deliberately chosen as to ensure the pressure required for retention time locking was greater than that needed for operating the Deans switch. Following the application of the pressure tuning procedure it was

determined that to achieve a ^{1}D methane retention time of 2.00 min and ^{2}D heptanol retention time of 0.08 min, a ^{1}D head pressure of 53.66 psig needed to be combined with a switching pressure of 48.2 psig. Following the application of the determined pressures, injections of methane and heptanol were performed with retention times of 2.01 min (^{1}D) and 0.081 min (^{2}D) respectively. With differences of 0.01 min and 0.001 min between target and experiment for the ^{1}D and ^{2}D respectively, the multidimensional retention time locking concept is well and truly proven beyond a doubt.

It should also be stated that the entire locking procedure can be performed with 15 injections and take no more than 20 min (pending on the reference compounds chosen). It is possible that a simple yet fast experimental procedure such as this could be automated within the instruments software thus potentially allowing the tMDGC system to be routinely locked.

8.1.5 RTL-GC×GC

For a GC×GC system the ^{1}D and ^{2}D are directly coupled to form one combined length of the two. This coupled length of capillary column is then installed into a GC injector (^{1}D end) and detector (^{2}D end) as if it was a single capillary column, bearing in mind different ferrules may be required if the ^{1}D and ^{2}D internal diameters differ greatly. If an injection and subsequent separation on the combined ^{1}D and ^{2}D column was performed by such a system it would not be considered multidimensional. Instead the resulting separation would simply be the combination of two columns. The installation of a modulator at the ^{1}D and ^{2}D union effectively splits the combined column back into its original components. The time a peak enters and leaves the ^{1}D and ^{2}D can be precisely monitored, that is if the modulation cycle is fast enough and allows for the reconstruction of the destroyed ^{1}D. Unlike a tMDGC system there is no need to interrupt the path of the carrier gas with one or more flow switching devices attaching to numerous columns and detectors.

As described, the only source of carrier gas supplied to a GC×GC system is by the injector inlet where the ^{1}D column end is installed. This enables precise control of the pressure drop over the entire combined column but not over the individual ^{1}D and ^{2}D columns. To control the pressure drop across both the ^{1}D and ^{2}D would require the ability to control the pressure at the ^{1}D and ^{2}D union i.e. the combined ^{1}D outlet and ^{2}D head pressures. A GC×GC system

allows for no such control at the ^{1}D and ^{2}D union, it instead adopts the residual pressure from the ^{1}D head pressure as the flow makes its way to the ^{2}D outlet. In Chapter 5 this residual pressure at the union was termed as the natural back pressure as it is directly related to the restriction of flow for the ^{2}D column. For a GC×GC system the restriction of the ^{2}D is typically large due to the use of short capillary columns with narrow internal diameters. This causes the natural back pressure (the pressure at the ^{1}D and ^{2}D union) to increase dramatically and cause the carrier gas to slow through the ^{1}D and speed up through the ^{2}D.

The Poiseuille models in Chapter 5 illustrate the issues in applying the pressure tuning procedure used in Chapter 6 to a GC×GC system, or for that matter a MDGC system with a large natural back pressure. The models suggest that in GC×GC the natural back pressure becomes so high and the ^{2}D carrier gas velocity so fast that the ability to tune the pressure and potentially slow the ^{2}D is compromised. To overcome this, the pressure tuning procedure is modified to not only supplement the carrier gas and increase the pressure at the ^{1}D and ^{2}D union but to also split it and reduce the pressure. To achieve this a T-piece arrangement was created at the ^{1}D and ^{2}D union by linking the two capillary columns with a Y-press fit. A length of deactivated capillary column was then installed between a second split/splitless injector and the third attachment on the Y-press fit. Operated in split mode, the injector could then control the pressure at the ^{1}D and ^{2}D union. If the second injector pressure was below the natural back pressure a split to the second injector and out the split valve would result thus lowering the ^{1}D and ^{2}D union pressure. Conversely, if the second injector pressure was greater than the natural back pressure it would supplement the ^{1}D and ^{2}D union with additional carrier gas and increase the pressure.

The pressure tuning procedure was then applied to a modified GC×GC system to achieve heptanol ^{1}D and ^{2}D retention times of 5 min and 5 sec respectively. Unfortunately, the procedure proved to be less accurate than when applied to a tMDGC system in Chapter 5 with the calculated pressures returning ^{1}D and ^{2}D retention times of 4.8 min and 5.0 sec respectively. The inaccuracy in the ^{1}D retention time is thought to arise from the determination of the ^{1}D retention times during the pressure tuning. As the ^{1}D is destroyed in a GC×GC experiment it must be reconstructed from the many ^{2}D separations. For the pressure tuning procedure the ^{1}D retention time was obtained by visually selecting the middle of a 2D peak from a suitable contour plot. It now seems necessary to view the individual ^{2}D

chromatograms that span a ^{1}D peak to determine a far more accurate view of the ^{1}D retention time.

Following the shortening of the ^{1}D and ^{2}D capillary columns by 10%, the pressure tuning procedure was repeated with the new approach to ^{1}D retention time determination. When applied the calculated pressure returned heptanol ^{1}D and ^{2}D retention times of 5.0 min and 5.0 sec respectively. Suggesting that the inaccuracy found for the first pressure tuning attempt was due to the poor collection of ^{1}D retention data. A 9 component mix was analysed using the calculated pressures both before and after the shortening of the columns. Considering the stated issues with the first attempt, all peaks within the chromatograms have good alignment. This investigation is therefore considered a successful "proof of concept" for the independent retention time locking of both the ^{1}D and ^{2}D in a GC×GC separation.

8.1.6 Final Conclusion

This body of work used statistical models and experimental results to assess the benefits, problems and boundaries of MDGC. Comparisons between the two MDGC techniques of tMDGC and GC×GC were performed to determine their comparative strengths and weaknesses. The results suggested that although modern MDGC provided enhanced separations with little drawbacks, the choice of whether to apply tMDGC or GC×GC to a specific analysis was critical. The application of tMDGC proved to be more suited to the need for quantification while GC×GC proved more suitable for qualification. This assessment goes against the current trends in the scientific literature which suggests that GC×GC is the successor of tMDGC. This seems partly due to the fact that GC×GC is the more modern technique and that it can be represented by a 3D contour plot chromatogram that gives the appearance of providing more separation than it actually is. The investigation found that if a ^{1}D separation has areas of high and low peak density and overlap (as is the case with most complex samples), that a GC×GC ^{2}D is not necessary in the areas of low density but can easily fall short in areas of high density. With tMDGC it is possible to further optimise the ^{1}D to separate the areas of low peak density and apply a ^{2}D of greater separating power to the select ^{1}D regions of high peak density.

In performing the experimental comparisons between tMDGC and GC×GC it was noted how a Deans switching device could alter the retention times of both the ^{1}D and ^{2}D dimensions simultaneously. This led to the development of a pressure adjustment procedure that would enable the independent retention time locking of both separations within a MDGC system. As the potential impact of such a technique was thought to be of great significance in the improvement and commercialisation of MDGC, investigations into its development and application became the focus of this work. In relation to the stated objectives, an investigation into retention time locked multidimensional gas chromatography is more than fitting due to its commercial implications for MDGC. In assessing the limitations of MDGC, a critical flaw was the ability to reproduce retention times and to find a means to identify peaks according to their retentions on both columns. Initially the pressure tuning procedure was assessed and refined using Poiseuille based models. Theoretically modelling the procedure provided an element of hind sight, enabling the identification of a number of potential issues and allowing for the necessary refinements prior to conducting any experiments. With little difficulty the pressure tuning technique was then successfully applied to achieve retention time locking for both separations of a tMDGC and GC×GC system. This technique has the capacity to deliver consistent ^{1}D and ^{2}D retention times between laboratories, analysts, instruments and columns, thus allowing for the creation of retention time libraries for identification. Though further studies are still required this achievement is considered to be an outstanding success and a significant contribution to the development of MDGC.

8.2 FURTHER WORK

8.2.1 Acceptance of MDGC

Being that the majority of industrial laboratories seek the approval of a regulatory body such as the Therapeutic Goods Administration (TGA) or Food and Drug Administration (FDA) to conduct business within their respective markets, it is important to understand what implications this may have on the uptake of technology for the sector. For the analytical testing of therapeutics and pharmaceuticals each piece of analytical instrumentation must go through a stringent and lengthy approval procedure to ensure it is qualified for the assigned tasks. Once installed the instrument must undergo qualification and performance checks that prove the installed system can perform as specified. Then on a yearly basis (pending the instrument) further qualification and performance maintenance checks are required to ensure qualification is always met. Furthermore, when a test method is developed that specifies the use of an analytical instrument it must undergo a series of tests to determine that its accuracy, precision and robustness can meet defined specifications. It is no surprise that compliance to these measures comes at a very high price. Over the lifetime of a typical instrument (approx. 10 – 15 years) its purchase price will be only a small fraction of its total cost. It is therefore the cost of compliance that holds back the acceptance of new technology by industry.

The majority of literature on MDGC is centred on its theory, techniques and application to samples, with very little regarding its compliance to industry regulations. Scientists in industry view MDGC as an impressive trick but nothing more. Just because you can now isolate a critical compound that you couldn't before is no justification for upgrading, as procedures must always be followed. The analytical advantages of such a powerful separation are clearly understood by industry but so too are the compliance related disadvantages and the associated costs. For these reasons an investigation into the potential qualification of MDGC instrumentation and the application and development of validated methods is recommended. Such a study would determine the potential of MDGC in its current commercial state, to be adopted by industry and become a common feature of most analytical laboratories.

8.2.2 RTL-MDGC

The application of retention time locking to multidimensional gas chromatography has many benefits. The ability to increase the precision and accuracy of retention times in both

separations will greatly assist in the acceptance of the technology. As discussed section 8.2.1, compliance is a major hurdle for any new technology. If consistent retention times cannot be achieved then the technology would likely fail the qualification and validation elements of instrumental compliance. Retention time locking also enables the direct comparison of retention times for the identification of unknown peaks. For MDGC it is either impossible or impractical to apply retention indices to both separations for identification. For an unknown peak to be identified using a MDGC separation either a mass spectrometric detector is required or a known standard must be analysed alongside the sample and the chromatograms compared. Consistent retention times will enable chromatographers to utilise MDGC as it was originally envisioned and allow the identification of a single peak across the two separations. For these reasons it is central to the development of MDGC technology that research in the field of retention time locking continue. Further studies in the assessment and refinement of the approach, real world application, hyphenation with mass spectrometric detection and method validation are necessary in continuing this body of work and it objectives. To do so would strengthen the application of retention time locking to MDGC and in turn strengthen the MDGC techniques.

CHAPTER 9

REFERENCES

[1] M. Tswett, Biochem Z, 5 (1907) 6-32.

[2] L.S. Ettre, Lc Gc N Am, 19 (2001) 506-+.

[3] A.J.P. Martin, R.L.M. Synge, Biochem J, 35 (1941) 1358-1368.

[4] A.T. James, A.J.P. Martin, Biochem J, 48 (1951) R7-R7.

[5] L.S. Ettre, Lc Gc N Am, 19 (2001) 120-+.

[6] M.J.E. Golay, Anal Chem, 29 (1957) 928-932.

[7] R.D. Dandeneau, E.H. Zerenner, J. High Res. Chromatog., 2 (1979) 351-356.

[8] H.M. McNair, J.M. Miller, Basic Gas Chromatography, Wiley-Interscience, 1997.

[9] W. Bertsch, Journal of High Resolution Chromatography, 22 (1999) 647-665.

[10] A.C. Lewis, Multidimensional high resolution gas chromatography., in: L. Mondello, A.C. Lewis, K.D. Bartle (Eds.) Multidimensional Chromatography, John Wiley & Sons, Chichester, 2001.

[11] T.A. Berger, Chromatographia, 42 (1996) 63-71.

[12] J.M. Davis, J.C. Giddings, Anal.Chem., 55 (1983) 418-424.

[13] J.C. Giddings, Use of multiple dimensions in analytical separations, in: H.J. Cortes (Ed.) Multidimensional chromatography, Marcel Dekker, New York, 1990, pp. 1-27.

[14] J.C. Giddings, Anal. Chem., 56 (1984) 1259A-1270A.

[15] W. Bertsch, J. High Res. Chromatogr., (1978) 85-90.

[16] D.R. Deans, J. Chromatogr., 203 (1981) 19-28.

[17] J.F. Elder, B.M. Gordon, M.S. Uhrig, J. Chromatogr. Sci., 24 (1986) 26-33.

[18] G. Schomburg, H. Husmann, E. Hübinger, W.A. König, J. High Resolut. Chromatogr., 7 (1984) 404-410.

[19] D.R. Deans, I. Scott, Anal. Chem., 45 (1973) 1137-1141.

[20] G. Schomburg, J. Chromatogr. A., 703 (1995) 309-325.

[21] D.J. McEwen, Anal. Chem., 36 (1964) 279.

[22] D.J. McEwen, Anal. Chem., 38 (1966) 1047-1053.

[23] G. Schomburg, H. Kotter, F. Hack, Anal. Chem., 45 (1973) 1236-1240.

[24] W. Jennings, J. Chromatogr. Sci., 22 (1984) 129-135.

[25] D.R. Deans, Chromatographia, 1 (1968) 19-22.

[26] A. Hagman, S. Jacobsson, J. High Resolut. Chromatogr. Chromatogr. Commun., 8 (1985) 332-336.

[27] E.L. Anderson, M.M. Thomason, H.T. Mayfield, W. Bertsch, HRC & CC, 2 (1979) 335-342.

[28] B.M. Gordon, C.E. Rix, M.F. Borgerding, J. Chromatogr. Sci., 23 (1985) 1-10.

[29] G. Schomburg, F. Weeke, F. Muller, M. Oreans, Chromatographia, 16 (1982) 87-91.

[30] D.C. Fenimore, R.R. Freeman, P.R. Loy, Anal. Chem., 45 (1973) 2331-2335.

[31] G. Schomburg, H. Husmann, F. Weeke, J. Chromatogr., 112 (1975) 205-217.

[32] Z. Liu, J.B. Phillips, J. Chromatogr. Sci., 29 (1991) 227-231.

[33] P. Schoenmakers, P. Marriott, J. Beens, LC-GC Europe, June (2003) 1-4.

[34] P.J. Marriott, Orthogonal GC-GC, in: L. Mondello, A.C. Lewis, K.D. Bartle (Eds.) Multidimensional Chromatography, John Wiley & Sons, Chichester, 2001.

[35] W. Bertsch, J. High Resol. Chromatogr., 23 (2000) 167 - 181.

[36] D. Ryan, P. Marriott, Anal. Biochem., 379 (2003) 295-297.

[37] P. Marriott, R. Ong, R. Shellie, R. Western, Y. Shao, R. Perera, L. Xie, A.J. Kueh, P.D. Morrison, Aust. J. Chem., 56 (2003) 187-191.

[38] P. Marriott, R. Shellie, Trends Anal. Chem., 21 (2002) 573-583.

[39] L.M. Blumberg, J. Chromatogr. A, 985 (2003) 29-38.

[40] J. Dalluge, J. Beens, U.A.T. Brinkman, J. Chromatogr. A., 1000 (2003) 69-108.

[41] P.Q. Tranchida, D. Sciarrone, P. Dugo, L. Mondello, Anal Chim Acta, 716 (2012) 66-75.

[42] P.Q. Tranchida, D. Sciarrone, L. Mondello, Multidimensional Gas Chromatography, in: E.G.N. Grushka (Ed.) Advances in Chromatography, Vol 48, 2010, pp. 289-328.

[43] M. Herrero, E. Ibanez, A. Cifuentes, J. Bernal, J Chromatogr A, 1216 (2009) 7110-7129.

[44] H.J. Cortes, B. Winniford, J. Luong, M. Pursch, Journal of Separation Science, 32 (2009) 883-904.

[45] M.P. Pedroso, L.A. Fonseca de Godoy, C.H. de Vasconcellos Fidelis, E.C. Ferreira, R.J. Poppi, F. Augusto, Quimica Nova, 32 (2009) 421-430.

[46] P. Schoenmakers, Chromatography in Industry, in: Annual Review of Analytical Chemistry, 2009, pp. 333-357.

[47] P.J. Marriott, R.M. Kinghorn, Anal. Chem., 69 (1997) 2582-2588.

[48] R.M. Kinghorn, P.J. Marriott, J. High Resol. Chromatogr, 21 (1998) 620-622.

[49] K.A. Krock, N. Ragunathan, C.L. Wilkins, J. Chromatogr., 645 (1993) 153-159.

[50] P. Marriott, M. Dunn, R. Shellie, P. Morrison, Anal. Chem., 75 (2003) 5532-5538.

[51] B.M. Gordon, M.S. Uhrig, M.F. Borgerding, H.L. Chung, W.M. Coleman, J. Elder Jr. III, F.J.A. Giles, D.S. Moore, C.E. Rix, E.L. White, J. Chromatogr. Sci., 25 (1988) 174-180.

[52] C.P.G. Ruehle, J. Niere, P.D. Morrison, R.C. Jones, T. Caradoc-Davies, A.J. Canty, M.G. Gardiner, V.-A. Tolhurst, P.J. Marriott, Anal Chem, 82 (2010) 4501-4509.

[53] C. Ruehle, G.T. Eyres, S. Urban, J.P. Dufour, P.D. Morrison, P.J. Marriott, J Chromatogr A, 1216 (2009) 5740-5747.

[54] M. Heil, F. Podebrad, T. Beck, A. Mosandl, A.C. Sewell, H. Bohles, Journal of Chromatography B, 714 (1998) 119-126.

[55] J. Dallüge, L.L.P.v. Stee, X. Xu, J. Williams, J. Beens, R.J.J. Vreuls, U.A.T. Brinkman, J. Chromatogr., A, 974 (2002) 169-184.

[56] J.B. Phillips, J. Beens, J Chromatogr A, 856 (1999) 331-347.

[57] J. Shi, B. Liu, W. Xie, Se pu = Chinese journal of chromatography / Zhongguo hua xue hui, 28 (2010) 623-627.

[58] Y. Takanami, M. Chida, H. Hasebe, Y. Sone, S. Suhara, Journal of Chromatographic Science, 41 (2003) 317-322.

[59] J. Blomberg, P.J. Schoenmakers, J. Beens, R. Tijssen, Hrc-Journal of High Resolution Chromatography, 20 (1997) 539-544.

[60] G.S. Frysinger, R.B. Gaines, E.B. Ledford, Hrc-Journal of High Resolution Chromatography, 22 (1999) 195-200.

[61] F. Adam, D. Thiebaut, F. Bertoncini, M. Courtiade, M.-C. Hennion, J Chromatogr A, 1217 (2010) 1386-1394.

[62] F. Bertoncini, C. Vendeuvre, D. Thiebaut, Oil & Gas Science and Technology-Revue De L Institut Francais Du Petrole, 60 (2005) 937-950.

[63] R. Edam, J. Blomberg, H.G. Janssen, P.J. Schoenmakers, J Chromatogr A, 1086 (2005) 12-20.

[64] C. Vendeuvre, R. Ruiz-Guerrero, F. Bertoncini, L. Duval, D. Thiebaut, Oil & Gas Science and Technology-Revue De L Institut Francais Du Petrole, 62 (2007) 43-55.

[65] R. Shellie, P. Marriott, Flavour Frag. J., 18 (2003) 179-191.

[66] R. Costa, P. Dugo, L. Santi, G. Dugo, L. Mondello, Current Organic Chemistry, 14 (2010) 1752-1768.

[67] D. Sciarrone, R. Costa, C. Ragonese, P.Q. Tranchida, L. Tedone, L. Santi, P. Dugo, G. Dugo, D. Joulain, L. Mondello, J Chromatogr A, 1218 (2011) 137-142.

[68] D. Sciarrone, C. Ragonese, C. Carnovale, A. Piperno, P. Dugo, G. Dugo, L. Mondello, J Chromatogr A, 1217 (2010) 6422-6427.

[69] Y. Seung-Ok, K. Yujin, K. Hee-su, H. Sun-Hee, K. So-Hyun, C. Hyung-Kyoon, P.J. Marriott, J Chromatogr A, 1218 (2011) 2626-2634.

[70] S.-O. Yang, Y. Kim, H.-s. Kim, S.-H. Hyun, S.-H. Kim, H.-K. Choi, P.J. Marriott, J Chromatogr A, 1218 (2011) 2626-2634.

[71] A.C. Lewis, N. Carslaw, P.J. Marriott, R.M. Kinghorn, P. Morrison, A.L. Lee, K.D. Bartle, M.J. Pilling, Nature, 405 (2000) 778-781.

[72] T. Larson, C. Ostman, A. Colmsjo, Analytical and Bioanalytical Chemistry, 400 (2011) 449-458.

[73] S. Zhang, L. Cai, J.A. Koziel, S.J. Hoff, D.R. Schmidt, C.J. Clanton, L.D. Jacobson, D.B. Parker, A.J. Heber, Sensors and Actuators B-Chemical, 146 (2010) 427-432.

[74] P.J. Marriott, P.D. Morrison, R.A. Shellie, M.S. Dunn, E. Sari, D. Ryan, Lc Gc Europe, 16 (2003) 23-31.

[75] P.D. Klein, S.A. Tyler, Anal. Chem., 37 (1965) 1280.

[76] M. Martin, D.P. Herman, G. Guiochon, Anal. Chem., 58 (1986) 2200-2207.

[77] J.M. Davis, J.C. Giddings, Anal. Chem., 57 (1985) 2168-2177.

[78] J.M. Davis, J.C. Giddings, J. Chromatogr., 289 (1984) 277.

[79] F. Dondi, Y.D. Kahle, G. Lodl, M. Remell, P. Reschigllan, C. Bighl, Anal. Chim. Acta, 191 (1986) 261.

[80] D. Rosenthal, Anal. Chem., 54 (1982) 63-66.

[81] L.J. Nagals, W.L. Creten, P.M. Vanpeperstraete, Anal. Chem., 55 (1983) 216.

[82] D.P. Herman, M.-F. Gonnord, G. Guiochon, Anal. Chem., 56 (1984) 994.

[83] J.M. Davis, J.C. Giddings, Anal. Chem., 57 (1985) 2178.

[84] S. Coppi, A. Betti, F. Dondi, Anal. Chim. Acta, 212 (1988) 165.

[85] J.M. Davis, J. Chromatogr., 449 (1988) 41.

[86] S.L. Delinger, J.M. Davis, Anal. Chem., 62 (1990) 436-443.

[87] J.M. Davis, J. Microcol. Sep., 7 (1995) 3-15.

[88] J.M. Davis, Anal. Chem., 69 (1997) 3796-3805.

[89] J.M. Davis, Anal. Chem., 66 (1994) 735-746.

[90] A. Felinger, L. Pasti, F. Dondi, Anal. Chem., 62 (1990) 1846-1853.

[91] A. Felinger, L. Pasti, P. Reschiglian, F. Dondi, Anal. Chem., 62 (1990) 1854-1860.

[92] A. Felinger, L. Pasti, F. Dondi, Anal. Chem., 63 (1991) 2627-2633.

[93] J.M. Davis, Statistical theories of peak overlap in chromatography, in: Advances in chromatography, Marcel Dekker, New York 1995, pp. 109-176.

[94] J.M. Davis, Anal. Chem., 63 (1991) 2141-2152.

[95] J.M. Davis, Anal. Chem., 65 (1993) 2014-2023.

[96] W. Shi, J.M. Davis, Anal. Chem., 65 (1993) 482-492.

[97] K. Rowe, D. Bowlin, M. Zou, J.M. Davis, Anal. Chem., 67 (1995) 2994-3003.

[98] K. Rowe, J.M. Davis, Anal. Chem., 67 (1995) 2981-2993.

[99] J.M. Davis, J. Sep. Sci., 28 (2005) 347-359.

[100] J.D. McCurry, B.D. Quimby, J. Chromatogr. Sci., 41 (2005) 524-527.

[101] L.R. Bordajandi, M.J. Gonzalez, Journal of Dairy Science, 91 (2008) 483-489.

[102] J. Munoz-Arnanz, C. Bosch, P. Fernandez, J.O. Grimalt, B. Jimenez, J Chromatogr A, 1216 (2009) 6141-6145.

[103] B. Mitrevski, R.L. Webster, P. Rawson, D.J. Evans, H.-K. Choi, P.J. Marriott, Journal of chromatography. A, 1224 (2012) 89-96.

[104] R.C.Y. Ong, P.J. Marriott, J. Chromatogr. Sci., 40 (2002) 276-291.

[105] S.C. Rastogi, J.D. Johansen, P. Frosch, T. Menne, M. Bruze, J.P. Lepoittevin, B. Dreier, K.E. Andersen, I.R. White, Contact Dermatitis, 38 (1998) 29-35.

[106] S.C. Rastogi, J.D. Johansen, T. Menne, P. Frosch, M. Bruze, K.E. Andersen, J.P. Lepoittevin, S. Wakelin, I.R. White, Contact Dermatitis, 41 (1999) 84-88.

[107] S.C. Rastogi, S. Heydorn, J.D. Johansen, D.A. Basketter, Contact Dermatitis, 45 (2001) 221-225.

[108] A. Chaintreau, D. Joulain, C. Marin, C.-O. Schmidt, M. Vey, J. Agric. Food Chem., 51 (2003) 6398-6403.

[109] S.C. Rastogi, J. High Res. Chromatog., 18 (1995) 653-658.

[110] K. Ellendt, G. Hempel, H. Kobler, SÖFW-J., 127 (2001) 29-.

[111] R. Shellie, P. Marriott, A. Chaintreau, Flavour Frag. J., 19 (2004) 91-98.

[112] H. Leijs, J. Broekhans, L.v. Pelt, C. Mussinan, J. Agric. Food Chem., 53 (2005) 5487-5491.

[113] H.-U. Baier, LC-GC Europe, (2005) 49-50.

[114] R. Shellie, P. Marriott, P. Morrison, Anal. Chem., 73 (2001) 1336-1344.

[115] R.A. Shellie, P.J. Marriott, Analyst, 128 (2003) 879-883.

[116] M. Adahchour, M. Brandt, H.-U. Baier, R.J.J. Vruels, A.M. Batenburg, U.A.T. Brinkman, J. Chromatogr. A.,, 1067 (2005) 245-254.

[117] M. Adahchour, J. Beens, R.J.J. Vreuls, A.M. Batenburg, U.A.T. Brinkman, J. Chromatogr., A, 1054 (2004) 47-55.

[118] D. Ryan, R. Shellie, P. Tranchida, A. Casilli, L. Mondello, P. Marriott, J. Chromatogr. A, 1054 (2004) 57-65.

[119] L. Mondello, M. Catalfamo, G. Dugo, J. Chromatogr. Sci., 36 (1998) 201-209.

[120] M.S. Dunn, R. Shellie, P. Morrison, P. Marriott, J. Chromatogr. A., 1056 (2004) 163-169.

[121] P.J. Marriott, R.C.Y. Ong, R.M. Kinghorn, P.D. Morrison, J. Chromatogr. A, 892 (2000) 15-28.

[122] E. Kováts, Helv. Chim. Acta, 41 (1958) 1951-1932.

[123] M.S. Klee, B.D. Quimby, L.M. Blumberg, in, Hewlett-Packard Company, U.S.A., 1999.

[124] L.M. Blumberg, M.S. Klee, Anal. Chem., 70 (1998) 3828-3893.

[125] L.M. Blumberg, A.D. Broske, in, Hewlett-Packard Company, U.S.A., 2000.

[126] V. Giarroocco, B. Quimby, M. Klee, in, Agilent Technologies, Inc., Wimington, 1997.

[127] K.R. Weiner, H.F. Prest, in, Agilent Technologies Inc., 1999.

[128] C. Bicchi, A. Binello, A. D'Amato, P. Rubiolo, J. Chromatogr. Sci., 37 (1999) 288-294.

[129] R.J. Western, P.J. Marriott, J. Sep. Sci., 25 (2002) 832-838.

[130] R.J. Western, P.J. Marriott, J. Chromatogr., A, 1019 (2003) 3-14.

[131] S. Bieri, P.J. Marriott, Analytical Chem, 78 (2006) 8089-8097.

[132] R. Shellie, P. Marriott, P. Morrison, L. Mondello, J. Sep. Sci., 27 (2004) 504-512.

[133] R.K. Bansal, A textbook of fluid mechanics, Laxmi Publications, New Delhi, 2005.

[134] W. Khummueng, J. Harynuk, P.J. Marriott, Anal Chem, 78 (2006) 4578-4587.

[135] H.V.D. Dool, P.D. Kratz, J. Chromatogr., 11 (1963) 463-471.

[136] T.A. Brettell, P.A. Moore, R.L. Grob, J. Chromatogr., 358 (1986) 423-428.

[137] C. Bicchi, C. Frattini, G.M. Nano, A. D'Amato, J. High Res. Chromatog., 11 (1988) 56-60.

[138] S.L. Kopczynski, J. Chromatogr., 463 (1989) 253-260.

[139] S. Alm, S. Jonson, H. Karlsson, E.G. Sundholm, J. Chromatogr., 254 (1983) 179-186.

[140] W.D. Snyder, L.M. Blumberg, in, Hewlett Packard Company, U.S.A., 1995.

[141] T. Sullivan, M. Klee, Am. Lab., 30 (1998) 20c, 22c, 24c.

[142] M. Klee, T. Sullivan, Enviromental Testing & Analysis, 7 (1998) 16-17, 44-45.

[143] P. Cormia, H. Prest, in, Agilent Technologies Inc., 1999.

[144] P. Sandra, F. David, J. Chromatogr. Sci., 40 (2002) 248-253.

[145] C. Almeida, P. Serodio, M.H. Florencio, J.M.F. Nogueira, Analytical And Bioanalytical Chemistry, 387 (2007) 2569-2583.

[146] I. Rasanen, I. Kontinen, J. Nokua, I. Ojanperä, E. Vuori, J. Chromatogr., B, 788 (2003) 243-250.

[147] S.A. Savchuk, E.A. Simonov, V.I. Sorokin, O.B. Dorogokupets, A.N. Vedenin, Journal Of Analytical Chemistry, 59 (2004) 954-964.

[148] T. Ishida, K. Kudo, H. Inoue, A. Tsuji, T. Kojima, N. Ikeda, J. Anal. Toxicol., 30 (2006) 468-477.

[149] A. Kende, Z. Csizmazia, T. Rikker, V. Angyal, K. Torkos, Microchem. J., 84 (2006) 63-69.

[150] J.A. Muñoz, E.F. González, L.E. García-Ayuso, A.G. Casado, L. Cuadros-Rodríguez, Talanta, 60 (2003) 433-447.

[151] N. Ochiai, K. Sasamoto, H. Kanda, T. Yamagami, F. David, B. Tienpont, P. Sandra, J. Sep. Sci., 28 (2005) 1083-1092.

[152] P. Sandra, B. Tienpont, F. David, J. Chromatogr., A, 1000 (2003) 299-309.

[153] J.-H. Wang, Y.-B. Zhang, X.-L. Wang, J. Sep. Sci., 29 (2006) 2330-2337.

[154] L. Bartolomé, M. Deusto, N. Etxebarria, P. Navarro, A. Usobiaga, O. Zuloaga, J. Chromatogr., A, 1157 (2007) 369-375.

[155] M.S. Klee, in, Agilent Technologies Inc., U.S.A., 2002.

[156] M.S. Dunn, N. Vulic, R.A. Shellie, S. Whitehead, P. Morrison, P.J. Marriott, J. Chromatogr., A, 1130 (2006) 122-129.

[157] K.M. Namara, J. Howell, Y. Huang, A.R. Jr., J. Chromatogr., A, 1164 (2007) 281-290.

[158] N. Etxebarria, O. Zuloaga, M. Olivares, L.J. Bartolome, P. Navarro, J Chromatogr A, 1216 (2009) 1624-1629.

[159] C. Hartig, J Chromatogr A, 1177 (2008) 159-169.

[160] C. Devos, M. Vliegen, B. Willaert, F. David, L. Moens, P. Sandra, J Chromatogr A, 1079 (2005) 408-414.

[161] K. Mac Namara, J. Howell, Y.L. Huang, A. Robbat, J Chromatogr A, 1164 (2007) 281-290.

[162] D. Baloga, J. Budin, Abstr Pap Am Chem S, 218 (1999) 87-AGFD.

[163] J. Cook, M. Engel, P. Wylie, B. Quimby, J Aoac Int, 82 (1999) 313-326.